Evaluating the involvement of mtDNA variants in patients diagnosed with myalgic encephalomyelitis

HC van Dyk

22135189

BSc (Honours) Biochemistry

Dissertation submitted in partial fulfilment of the requirements for the degree ***Magister Scientiae*** in ***Biochemistry*** at the Potchefstroom Campus of the North-West University

Supervisor: Prof FH van der Westhuizen

May 2016

ACKNOWLEDGEMENTS

I would firstly like to thank and acknowledge my supervisor, **Prof. Francois van der Westhuizen**, for his guidance, support and patience. His determination, wisdom and willingness to always go the extra mile, set the standard which I will always strive to attain.

I would also like to thank the following people and institutions whose vital contributions made this study possible:

- The financial assistance of the **National Research Foundation (NRF)** towards this research is hereby acknowledged. Opinions expressed and conclusions arrived at, are those of the author and are not necessarily to be attributed to the NRF.
- The financial assistance of the **North-West University.**
- **Prof. Joanna Elson** from Newcastle University (UK), for her enthusiasm and major involvement in this study as well as her invaluable assistance and guidance with regards to the statistics performed.
- **Prof. Lodovica Vergani** from the University of Padova (Italy), for her effort and generous donation of RD ρ^0 cells.
- **Marianne Pretorius**, for her support, advice, valued input and assistance with the next-generation sequencing.
- **Mari van Reenen**, for her assistance, advice and time regarding the statistics performed in this study.
- **Valerie Viljoen**, for her friendly service and thorough language editing.
- The staff and fellow post-graduate students at the **mitochondrial laboratory, NWU,** for their support, laughter and understanding.

I would like to thank my **Mom and Dad** for all the opportunities they have given me, their guidance, and for their unconditional love and support. It is a privilege to call myself their daughter. Thank you to my sisters, **Robin and Tessa,** for their love, support and for always knowing how to make me laugh (and for teasing the “nerdy baby sister”).

I would also like to thank my fiancé, **Hamish,** for putting up with me through all the ups and downs, for his constant support and understanding, for always being a shoulder that I can lean on, and for his unconditional love.

Lastly, but most importantly, I would like to thank the **Lord** for the privileges He has given me, the talents He has blessed me with, the people He has sent across my path and for His unwavering goodness.

ABSTRACT

In mitochondrial research, many investigators have examined the association between mitochondrial DNA (mtDNA) variants in rare as well as common complex diseases. Previous studies at the CHM (NWU) detected three known pathogenic mtDNA variants (m.7497G>A, m.9185T>C and m.10197G>A) at low allele frequencies in a number of patients diagnosed with myalgic encephalomyelitis (ME). Since no diagnostic examinations or conclusive treatments currently exist for ME, an association between ME and known pathogenic variants, or a cumulative effect of rare non-synonymous variants (pathogenicity score) on ME, could provide valuable insights into understanding the causes of ME. Literature shows contradicting data regarding the role of mitochondrial dysfunction in ME, and while uncommon mtDNA deletions have been reported, the three known pathogenic mtDNA variants introduced here have not previously been observed in ME patients (but were later identified as sequencing artefacts in the duration of this study), nor has the combined effect of numerous rare non-synonymous variants on the mitochondrial bioenergetics of ME patients been assessed. To do this, cytoplasmic hybrid (cybrid) cells were developed by fusing ρ^0 (mtDNA-depleted) cells with healthy control and ME patient's blood platelets (containing solely mtDNA). These cybrid cells were used for mitochondrial bioenergetic analyses, using a Seahorse XF^e96 analyser, and for determination of the relative mtDNA copy number (RMCN), using real-time PCR. In addition, conditions for analysing selected cell lines (including the cybrids) using the Seahorse XF^e96 analyser were optimized. While no apparent bioenergetic irregularities were observed in ME patient cybrids compared to healthy controls, an increased pathogenicity score appeared to be associated with a decrease in ATP production and a decreased electron transport system (ETS) capacity in ME patients. This new approach for investigating mtDNA variants and a common complex disease may provide new insights into the diagnostic and causative factors of ME.

Key words: bioenergetics, myalgic encephalomyelitis, mtDNA variants, Seahorse XF analyser, mutational load hypothesis, haplogroups, mtDNA copy number.

TABLE OF CONTENTS

TABLE OF CONTENTS continued…

TABLE OF CONTENTS continued…

TABLE OF CONTENTS continued…

TABLE OF CONTENTS continued…

LIST OF TABLES

APPENDIX

LIST OF FIGURES

CHAPTER 4

ABBREVIATIONS, SYMBOLS AND UNITS

°C	Degrees Celsius
143B	Human osteosarcoma cells
3’	Three prime end
5’	Five prime end
β-globin	Hemoglobin, beta
λ	Lambda
ρ^0	mtDNA depleted cells
ω3	Omega 3
A549	Human lung carcinoma cells
AC	Alternating current
ADP	Adenosine diphosphate
ANT	Adenine nucleotide translocator
ATCC	American Type Culture Collection
ATP	Adenosine triphosphate
BHI	Bioenergetic Health Index
bp	Base pairs
BrdU	5-bromo-2’-deoxyuridine
BSN	Bilateral striatal necrosis
C2C12	Mouse myoblast cells
Ca^{2+}	Calcium
CDC	Centers for Disease Control and Prevention
CFS	Chronic Fatigue Syndrome
CHM	Centre for Human Metabonomics
CO_2	Carbon dioxide
CV	Coefficient of variation
Cybrid	Cytoplasmic hybrid cell
DC	Direct current
ddH_2O	Distilled H_2O
df	Degrees of freedom
DH	Dehydrogenase
D-loop	Displacement loop
DMEM	Dulbecco’s Modified Eagle Medium
DMSO	Dimethyl sulfoxide
DNA	Deoxyribonucleic acid

e^-	Electron
ECAR	Extracellular Acidification Rate
EtBr	Ethidium bromide
ETF	Electron transfer flavoprotein
ETS	Electron transport system
$FADH_2$	1,5-dihydroflavin adenine dinucleotide
FAM	6-carboxyfluorescein
FBS	Fetal Bovine Serum
g/L	Gram per litre
H^+	Proton
HEPG2	Human hepatocellular carcinoma cells
HPA	Hypothalamic-pituitary-adrenal axis
HVR	Highly variable region
ICC	International Consensus Criteria
KSS	Kearns-Sayre syndrome
L	Litre
LHON	Leber's hereditary optic neuropathy
M	Molar
ME	Myalgic encephalomyelitis
MELAS	Mitochondrial encephalomyopathy, lactic acidosis and stroke-like episodes
MERRF	Myoclonic epilepsy with ragged red fibres
µg/mL	Microgram per milliliter
µL	Microliter
µM	Micromolar
µM	Micromolar
mg/L	Milligram per litre
MGB	Minor groove binder
min	Minutes
mL	Millilitre
mM	Millimolar
mpH/min	Milli pH per minute
mRNA	Messenger ribonucleic acid
MSQ	Medical symptom questionnaire
mtDNA	Mitochondrial DNA
MT-ND2	Mitochondrially encoded NADH dehydrogenase 2
NAD^+	Oxidized nicotinamide adenine dinucleotide
NADH	Reduced nicotinamide adenine dinucleotide

NARP	Neuropathy, ataxia, and retinitis pigmentosa
nDNA	Nuclear DNA
ng	Nanogram
ng/µL	Nanogram per microliter
NGS	Next-generation sequencing
nm	Nanometer
NWU	North-West University
O_2	Oxygen
O2k	OROBOROS Oxygraph-2k
OCR	Oxygen Consumption Rate
OXPHOS	Oxidative phosphorylation
PBS	Physiological Buffered Saline
PCR	Polymerase Chain Reaction
PEG	Polyethylene glycol
PEO	Progressive external ophthalmoplegia
PFS	Piper Fatigue Score
PGM	Personal genome sequencing
P_i	Inorganic phosphate
pmf	Proton motive force
pmol/min	Picomol per minute
POLG	mtDNA polymerase gamma
r	Pearson's correlation coefficient
RCR	Respiratory control ratio
rCRS	Revised Cambridge reference sequence
RD	Human rhabdomyosarcoma cells
RFLP	Restriction fragment length polymorphism
RMCN	Relative mtDNA copy number
RNA	Ribonucleic acid
RNS	Reactive nitrogen species
ROS	Reactive oxygen species
rRNA	Ribosomal ribonucleic acid
SEM	Standard error of the mean
SH-SY5Y	Human neuroblastoma cells
SIED	Systemic Exertion Intolerance Disease
SNHL	Non-syndromic and aminoglycoside-induced sensorineural hearing loss
SNP	Single nucleotide polymorphism
t	Test statistic

TAE	Buffer containing Tris base, acetic acid and EDTA
TBE	Buffer containing Tris base, boric acid and EDTA
TK^-	Thymidine kinase negative
tRNA	Transfer ribonucleic acid
UCP	Uncoupler
UK	United Kingdom
UQ	Ubiquinone
v/v	Volume per total volume
w/v	Weight per total volume
XF	Extracellular flux

CHAPTER 1: Introduction

Myalgic encephalomyelitis (ME) is a systemic disease known to cause unrelenting fatigue not caused by physical exertion, not relieved with rest, and which is known to cause neurological, immunological and cardiovascular irregularities, as well as ion transport and energy metabolism deficiencies (Carruthers *et al.*, 2011). Despite the contradicting results that can be seen in literature, numerous studies have found evidence of mitochondrial dysfunction and bioenergetic irregularities in patients diagnosed with ME.

Mitochondria are cellular organelles found in all mammalian cells which are responsible for generating the majority of the energy required by cells. Mitochondria contain their own genome, called mitochondrial DNA (mtDNA), which encodes 13 polypeptides in the oxidative phosphorylation (OXPHOS) system, two ribosomal RNA (rRNA) molecules, and 22 transfer RNA (tRNA) molecules. This constitutes only a small fraction of the mitochondrial proteins and structures since all the other proteins are encoded by nuclear DNA (nDNA) (Anderson *et al.*, 1981). MtDNA is more susceptible to variations than nDNA and there are thus, compared to nDNA, various non-pathogenic and pathogenic variants present in mtDNA (Richter *et al.*, 1988). This variation leads to single nucleotide polymorphisms (SNPs, single nucleotide variants, occurring in more than 1% of the population) which form unique fingerprints called haplogroups, which arose in people who migrated to different areas of the world (Herrnstadt & Howell, 2004).

Pathogenic variants in mtDNA can lead to various mitochondrial diseases. In addition, it is now commonly recognized that rare and common SNPs, as well as the cumulative effect of numerous rare non-synonymous variants, could also attribute to functional changes of the OXPHOS system and subsequent common disease phenotypes. Three known pathogenic mtDNA variants were detected at low levels in a number of patients with haplogroup U5 in a ME study cohort, during a previous study, conducted at the NWU. These were m.7497G>A, m.9185T>C and m.10197G>A (unpublished data), and they were the initial motivation for conducting the study presented here. Although there were strong indications that these three variants were pathogenic, they were detected at low allele frequencies (~5-20%) using next-generation sequencing (NGS). Due to the lack of any diagnostic examinations or conclusive treatments, an association between ME and known pathogenic variants could provide insightful information regarding the diagnosis and causes of the disease (Fukuda *et al.*, 1994). Patients suffering from ME are often accused of being lazy or avoiding work, thus indicating that a definitive cause or diagnosis could improve their own understanding of the disease as well as their psychological well-being (McInnis *et al.*, 2014).

The purpose of this study was thus to make sense of these mtDNA variants, as well as the possible role of other rare non-synonymous mtDNA variants, using functional investigations. To achieve this, cytoplasmic hybrid cells (cybrids) needed to be developed, using each of these patients' blood platelets to transfer their mtDNA to cells with the same nuclear background. MtDNA transfer to cybrid cells could be confirmed in a cost-effective manner using PCR-RFLP haplogroup analyses and relative mtDNA copy number (RMCN) determination, as described in Chapter 3. By sequencing selected cybrid cell lines, mtDNA (and mtDNA variant) transfer from the patients' blood platelets to the cybrid cells could also be confirmed.

These cybrids then needed to be analysed in comparison to various controls by investigating functional parameters of the OXPHOS system. The instrument used in this study, the Seahorse XF^{e}96 analyser, provides bioenergetics information about the cells and can thus give an indication as to whether any of the mtDNA variants have a significant impact on bioenergetics parameters or not. In preparation for the analysis of all the cybrid cells, using the extracellular flux (XF) analyser, numerous optimization and standardization methods needed to be developed. A further aim of this study was thus to develop standard protocols for the basic functioning of the instrument by obtaining various cell lines and optimizing their specific conditions so that they could be used for other studies later on. The knowledge and experience gained from optimizing these cell lines could then be used to optimize and perform the bioenergetics experiments utilizing the cybrid cells.

Subsequent studies at the NWU, on this cohort, were unable to consistently confirm the presence and accurately determine the variant allele frequency of the three pathogenic variants, m.7497G>A, m.9185T>C and m.10197G>A, in ME patients when using different NGS methods. Ion Torrent (Life Technologies) and MiSeq (Illumina) sequencing, as well as pyrosequencing (QIAGEN) methods were used without successful validation of any of these pathogenic variants. Thus, it should be noted that during this study, the initial motivation to primarily investigate these pathogenic variants was adapted to look at mtDNA variants in general, including rare and common SNPs.

Myalgic encephalomyelitis (ME) is also commonly known as *Chronic Fatigue Syndrome (CFS)*, however, in this study the term ME will be used since it has been shown to more appropriately and accurately describe the pathophysiology of the disease (Carruthers *et al.*, 2011). Based on the article by Vihinen (2015) where genetically muddled terms are discussed, the terms *variation* and *variant* will be used throughout this paper to describe a genetic alteration in DNA, RNA or protein compared to a reference condition. The terms *subject* and *subject group* will be used to refer to the combination of ME patients and healthy controls.

In Chapter 2, a comprehensive overview of the topics relevant to this study will be provided, along with the problem statement, aims and objectives, and an experimental strategy. All methods and materials used in this study will be discussed in Chapter 3. In Chapter 4, all results will be shown and discussed, while Chapter 5 will provide a summary for each of the objectives as well as the conclusions that were reached.

CHAPTER 2: Literature Study

2.1. Introduction

In this literature study, a basic overview of the mitochondrion, the OXPHOS system and mtDNA will be given to provide an understanding of other concepts that were used in this study. Commonly known mitochondrial disorders, originating mainly from mtDNA variations, will then be discussed along with homoplasmy, heteroplasmy, the threshold effect and the association between SNPs, mutational load, haplogroups and mitochondrial disease. The criteria used for determining whether or not an mtDNA point mutation or mt-tRNA variant is pathogenic will then be given. The focus will thereafter be shifted to the methods that were used in this study. A detailed description will be provided for the creation of cybrid cells. An overview of the various methods used for bioenergetics analyses will be given with a detailed description of the Clark-type oxygen electrode and the XF analyser. Real-time PCR was also used in this study but will not be discussed in this chapter since it is a well-known technique and the principle by which it works is commonly understood. Lastly, the problem statement, aims, objectives and experimental strategy will be discussed.

2.2. The mitochondrion

2.2.1. Mitochondrial structure and function

The mitochondrion is a cellular organelle that can be found in all mammalian cells containing a nucleus (Scheffler, 1999). It contains various partitions, namely the inner and outer membrane, inter-membrane space and the mitochondrial matrix (DiMauro & Schon, 2003). The main function of mitochondria is the production of ATP via a process called oxidative phosphorylation (OXPHOS). The mitochondria are also involved in pyruvate oxidation via the Krebs cycle (which is located within the mitochondrial matrix along with some urea cycle enzymes), metabolizing amino acids and fatty acids, the regulation of apoptosis, iron-sulphur complex and steroid synthesis, the control of cytosolic calcium concentration and as a source of reactive oxygen species (ROS) (Chinnery & Hudson, 2013; DiMauro & Schon, 2003).

2.2.2. Oxidative phosphorylation

The OXPHOS system is composed of five protein complexes (as shown in Figure 2.1), each containing numerous subunits: Complex I (NADH-ubiquinone oxidoreductase), complex II (succinate-ubiquinone oxidoreductase), complex III (ubiquinol-cytochrome c oxidoreductase), complex IV (cytochrome c oxidase) and complex V (ATP synthase). Ubiquinone (coenzyme Q_{10}) and cytochrome c, are electron carriers that also play a critical role during OXPHOS. Distinction between the OXPHOS system and the electron transport system (ETS) can be made since the

ETS does not include complex V and is thus comprised of only complexes I, II, III, and IV. Carbohydrates, fatty acids and amino acids are oxidized via glycolysis, pyruvate oxidation and the Krebs cycle to form NADH and $FADH_2$, which are in turn oxidized by complex I and complex II, respectively. Electrons derived by the oxidation of NADH by NADH dehydrogenase and $FADH_2$ by succinate dehydrogenase, are transferred to ubiquinone, along with electrons derived from ETF-ubiquinone oxidoreductase, dihydroorotate dehydrogenase and *s,n*-glycerophosphate dehydrogenase. Electrons are transferred from ubiquinone to complex III and thereafter to cytochrome c. From cytochrome c, electrons are transferred to complex IV where they are then finally transferred to molecular oxygen with the subsequent production of water (Gutman *et al.*, 1971; Hatefi *et al.*, 1962; Hatefi, 1985; Nicholls & Ferguson, 2013c). According to the chemiosmotic theory (Mitchell, 1961), complexes I, III and IV pump protons from the mitochondrial matrix to the inter-membrane space, as electron transfer occurs. This results in the formation of a pH gradient and a mitochondrial membrane potential, collectively called the proton motive force (pmf), across the inner mitochondrial membrane. The pmf acts as a driving force by allowing the protons to be pumped back into the mitochondrial matrix through ATP synthase, with the subsequent phosphorylation of ADP to form ATP. Proton leak back into the matrix, also occurs with and without ATP production. In this way, a proton circuit is formed whereby energy is produced from the oxidation of various substrates (Brand & Nicholls, 2011).

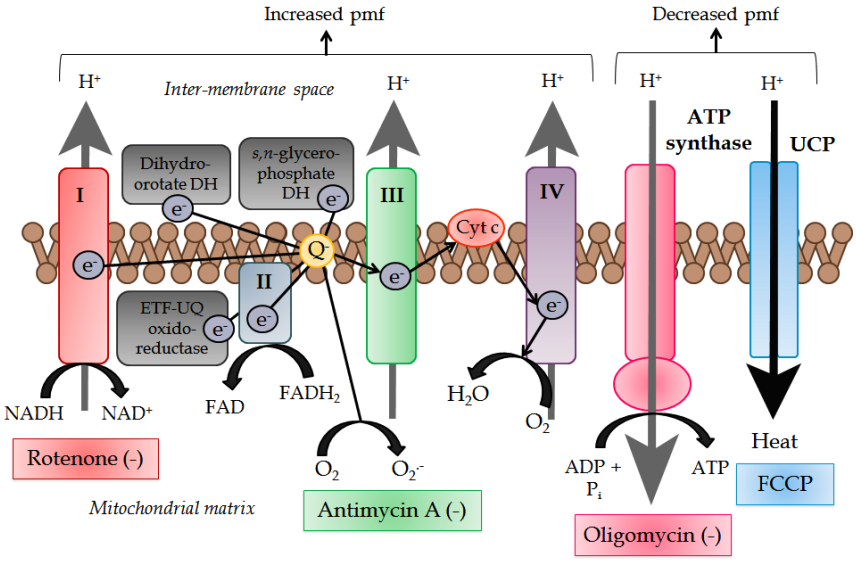

Figure 2.1: The *electron transport system*. Rotenone, antimycin A and oligomycin are inhibitors of complexes I, III and V respectively. FCCP is an uncoupler. DH = dehydrogenase; ETF = electron transfer flavoprotein; UQ = ubiquinone; UCP = uncoupler. Figure adapted from Brownlee (2001).

2.2.3. Mitochondrial DNA

mtDNA is a maternally inherited molecule that can be found within the mitochondrial matrix (Giles *et al.*, 1980). During fertilization, the entire sperm (including the mid-piece that contains between 50 and 75 mitochondria) inserts into the oocyte (which contains approximately 10^5

copies of mtDNA). The mtDNA of the sperm is thus thought to be diluted to such an extent that it is undetectable in the zygote (Ankel-Simons & Cummins, 1996). The ubiquitination of the mitochondrial membranes within sperm, as the sperm move down the reproductive tract, is also believed to remove paternal mtDNA (Sutovsky, 2003). A recent study confirmed the lack of any paternal mtDNA transfer to offspring, using extreme-depth re-sequencing, and concluded that the active elimination of paternal mtDNA was a more plausible hypothesis for the maternal inheritance of mtDNA than passive dilution due to the difference in the proportion of sperm and oocyte mtDNA (Pyle *et al.*, 2015).

MtDNA consists of ~16569 base pairs of double-stranded circular DNA and 37 genes. These genes encode 13 polypeptides in the OXPHOS system, two rRNA molecules, and 22 tRNA molecules. The two DNA strands (which lack introns) are called the heavy and light strands, and their transcription is promoted by a non-coding section of the mtDNA genome called the displacement-loop (D-loop) (Anderson *et al.*, 1981). Of the 92 known structural OXPHOS genes, 79 are encoded by nuclear DNA (nDNA) (Chinnery & Hudson, 2013). Unlike nDNA, there are numerous copies of mtDNA within each cell. In human cells there are between 1000 and 10 000 copies of mtDNA per cell (Shadel & Clayton, 1997). MtDNA forms nucleoids that are associated with the inner mitochondrial membrane and are made up of five to seven mtDNA copies that have been arranged into protein-DNA macrocomplexes (Wang & Bogenhagen, 2006). nDNA wrapped around histones is protected from mutagens, while nucleoids do not provide the same protection for mtDNA, allowing it to accumulate variations more easily (Richter *et al.*, 1988).

2.3. The association between mtDNA variants and mitochondrial disorders

2.3.1. Introduction

The mutation rate in mtDNA is approximately ten times greater than in nDNA (Brown *et al.*, 1979). MtDNA polymerase gamma (POLG) is an nDNA encoded enzyme responsible for mtDNA replication, and it is the only DNA polymerase found within the mitochondrion. As mentioned before, mtDNA is not wrapped around protective histones, making it more susceptible to variations. Another factor adding to the susceptibility of mtDNA to variations is that the ETS, which plays a role in ROS generation, and mtDNA (along with the associated POLG) are located in close proximity to one another within the mitochondrial matrix. This proximity exposes mtDNA and POLG to oxidative damage caused by ROS, which impairs DNA replication and repair. Mitochondria also lack certain repair mechanisms found in the nucleus, allowing for mtDNA replication errors and the occurrence of irreparable damage to mtDNA (Graziewicz *et al.*, 2002; Richter *et al.*, 1988). These variations can lead to the malfunctioning of

various aspects of the mitochondria which in turn lead to mitochondrial disease and the expression of a clinical phenotype.

Variations in mtDNA can occur in various forms such as population variants, well-known and rare pathogenic variants (which may be homoplasmic or heteroplasmic as described below), non-synonymous variants (variation causing an amino acid substitution) and synonymous variants (variation that does not cause an amino acid substitution) (Tuppen *et al.*, 2010; Vihinen, 2015). Common mtDNA population variants include single nucleotide polymorphisms (SNPs) which are defined as single nucleotide variants that occur in more than 1% of the population (Brookes, 1999; Collins *et al.*, 1998). MtDNA rearrangements can also occur and may involve partial mtDNA deletions (which are always heteroplasmic) (Holt *et al.*, 1988) and/or insertions (Poulton *et al.*, 1989).

All of the above mentioned variants can play a role in common complex diseases (such as cancer, diabetes, Alzheimer disease and Parkinson's disease) as well as in rare disorders, although many conflicting results exist. Despite the controversy surrounding this, in recent years there is a greater consensus and understanding regarding common complex diseases and mtDNA variants (Howell *et al.*, 2005; Hudson *et al.*, 2014; Taylor & Turnbull, 2005). Three hypotheses relating to the association between mtDNA variants and common complex, as well as rare diseases, will be discussed, namely: (1) the haplogroup association hypothesis; (2) known disease-causing variants at low allele frequencies; and (3) the mutational load hypothesis.

2.3.2. Haplogroups and the haplogroup association hypothesis

In 1987, a paper was published describing the link between mtDNA and the migration of various populations to different areas of the world. MtDNA, from a broad selection of geographic populations, was used to trace a common maternal ancestor that originated in Africa (Cann *et al.*, 1987). These groups of mtDNA lineages were later called haplogroups. Haplogroups can be determined by sequencing the HVR1 and HVR2 regions (highly variable regions which are subject to a very high mutation rate) within the D-loop, or by studying the SNPs found within a population, since each haplogroup has its own characteristic set of SNPs that developed as a result of each population's geographical migration (Herrnstadt & Howell, 2004). Haplogroups H, I, J, K, T, U, V, W and X are typically recognized as European haplogroups (Herrnstadt *et al.*, 2002). In Europe, haplogroup H is the most common haplogroup with a frequency of approximately 40% (Roostalu *et al.*, 2007), as opposed to haplogroup U which has a frequency of approximately 7% (Richards *et al.*, 1996) – both of these haplogroups being prominent in this study.

Different haplogroups have been associated with certain diseases (Lin et al., 2012). Based on the haplogroup association hypothesis, much research has been conducted on whether or not specific haplogroups provide certain populations with an evolutionary advantage, or whether they aggravate other deleterious variants when occurring together (Gómez-Durán *et al.*, 2012). Certain haplogroup markers (SNPs) have recently been found to increase the incidence of common late-onset human diseases (Hudson *et al.*, 2014). Although much focus has been placed on these haplogroup association studies, it has been found that very large cohorts are necessary for detecting trustworthy associations between haplogroup markers and complex diseases (Samuels et al., 2006). This, combined with inconsistent results for individual haplogroups and associations seen only in single studies (as multiple studies show conflicting results), have led to much debate regarding the haplogroup association hypothesis and have shown that articles based on haplogroup association studies must be more stringently evaluated prior to publication (Herrnstadt & Howell, 2004; Salas & Elson, 2015).

2.3.3. Homoplasmy, heteroplasmy, the threshold effect and low allele frequency mtDNA variants

Since mitochondria contain more than one copy of mtDNA, variations are able to occur at different frequencies within each cell. Homoplasmy occurs when all the copies of mtDNA within a cell are identical. Both normal (also known as wild-type) and variant mtDNA are able to exist together in one cell which leads to a state of heteroplasmy (Flier *et al.*, 1995). It is estimated that heteroplasmy can be found in 90% of all healthy individuals at very low allele frequencies (~1-10%), and it is highly probable that it may even be present in all individuals. The proportion of variant mtDNA within cells determines the clinical phenotype. A threshold of variant mtDNA must be reached for a mitochondrial defect to become evident. The threshold depends on the type of tissue since tissues more dependent on OXPHOS, will have a lower threshold than those that depend on anaerobic glycolysis. Heteroplasmy has previously been associated with numerous mitochondrial diseases, as discussed in Section 2.3.5, but it is also becoming increasingly evident in other complex diseases, such as diabetes mellitus, cancer, aging and neurodegenerative diseases, which present later in life (Rossignol *et al.*, 1999; Ye *et al.*, 2014).

In some cases, a slight excess of wild-type mtDNA is able to compensate for large percentages of variant mtDNA, and thus prevent the onset of a clinical phenotype. It is believed that wild-type mtDNA has an excess of mRNA, tRNA and OXPHOS subunits, as a fallback for increased energy requirements, or an OXPHOS defect, and is thus able to safeguard the mtDNA up to a threshold value when mtDNA variations occur (Rossignol et al., 2003). However, there is increasing evidence that the mtDNA content of cells is tightly regulated and that almost all mtDNA molecules are necessary for optimal mitochondrial function (Villani & Attardi, 1997). The

maintenance of wild-type mtDNA hypothesis proposes that molecular defects lead to a compensatory response of nonspecific mitochondrial proliferation of variant and wild-type mtDNA. However, once the variant mtDNA has reached a crucial level, further nonspecific proliferation leads to increased variant mtDNA replication at the cost of wild-type mtDNA, and is thus harmful to cell survival (Chinnery & Samuels, 1999). In general, the threshold for an mtDNA variant ranges between 60-90%, depending on the type of tissue or variation being studied, with mtDNA deletions averaging closer to ~60%. Mt-tRNA encoding genes, that are heteroplasmic for a specific variant, do not produce the same variant level in the resulting tRNA molecule, instead, the variant level appears to be lowered (variant tRNAs are tolerated over a broader variant load than protein-encoding genes), possibly indicating instability of variant tRNAs (Montoya *et al.*, 2009; Rossignol *et al.*, 2003; Schon *et al.*, 2012; Tuppen *et al.*, 2010).

In a recent study it was found that every 1 in 200 healthy individuals possessed low frequencies of common pathogenic mtDNA variants, which have the potential to become highly pathogenic with aging when a higher frequency could be reached, thus leading to mitochondrial dysfunction (Elliott *et al.*, 2008; Ye *et al.*, 2014). A novel variant in dividing cells is capable of reaching heteroplasmy within ~70 cell division generations thus making it possible for low frequency heteroplasmy to reach a high frequency within an average individual's life time (Coller *et al.*, 2001). MtDNA variants can also accumulate in non-dividing cells due to random genetic drift alone, over a much longer time period (Elson *et al.*, 2001).

2.3.4. Mutational load hypothesis

A third hypothesis, *the mutational load hypothesis*, suggests that numerous rare mtDNA variants may have a cumulative effect to increase the risk for certain diseases (Elson *et al.*, 2006). It is assumed that rare variants which alter an amino acid or rRNA/tRNA, have a greater probability of being slightly deleterious since purifying selection has been found to remove deviations in mtDNA population variation that are expected to be deleterious in later generations (Elson et al., 2004; Kivisild et al., 2006). The hypothesis that more than one variant, be it in nDNA or mtDNA, can contribute in various ways to a disease phenotype is not novel (Loeb & Loeb, 2000), but evidence for this is gaining (Liu et al., 2015).

Computational methods, such as the MutPred program, have been developed and are able to compare possible non-synonymous protein variants with known wild-type protein sequences, in order to predict protein functional site and structural feature changes. These changes are then stated as probabilities of gain or loss of structure and function, which can be used to aid in understanding specific molecular mechanisms that may cause a particular disease (Li *et al.*, 2009). This program has been satisfactorily verified in the context of mtDNA variation, where

higher pathogenicity (or MutPred) scores (>0.7) indicate a greater probability that the amino acid substitution is pathogenic (Pereira *et al.*, 2011; Soares *et al.*, 2013). The revised Cambridge reference sequence (rCRS) is used as the reference for each amino acid sequence (Andrews *et al.*, 1999), and the adjusted MutPred score takes the position on the phylogenetic tree for human mtDNA into account (Van Oven & Kayser, 2009).

2.3.5. Common mitochondrial disorders resulting from mtDNA variations

There are currently numerous well-known pathogenic variants found in mtDNA which are related to a clinical phenotype. The symptoms associated with these mtDNA variants vary greatly, as does the age of onset of the disease. Environmental factors may also play a role in the development of mitochondrial defects (Tuppen *et al.*, 2010). Altered nDNA can also result in mitochondrial diseases since nDNA encodes such a large portion of the mitochondrial proteins. In fact, most mitochondrial disorders result from nDNA variations (DiMauro & Schon, 2003). Many mtDNA variations are related to encephalomyopathies, since the brain and muscle mitochondria are required during high bursts of energy, and they will thus be most severely affected by any impaired mitochondrial activity (Nicholls & Ferguson, 2013a). A brief overview will be given of the common mitochondrial diseases that are caused by mtDNA variations, with numerous variations and their associated diseases shown in Figure 2.2.

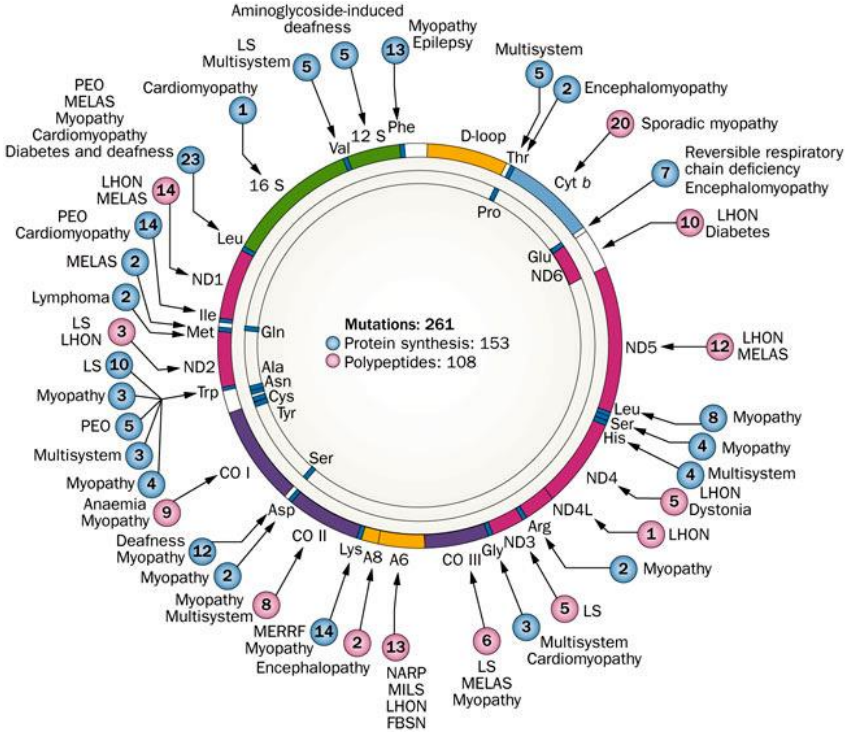

Figure 2.2: Schematic representation of well-known pathogenic mtDNA variations and their associated clinical phenotype, as well as the various genes encoded by the mtDNA genome. The numbers within the circles indicate the number of variations at each site. From DiMauro *et al.* (2013). (Copyright permission no. 3467200396243)

There are numerous maternally inherited mitochondrial disorders associated with heteroplasmic mtDNA point mutations. Mitochondrial encephalomyopathy, lactic acidosis and stroke-like episodes (MELAS), tends to affect complex I, and is typically associated with variations in the mt-tRNA$^{Leu(UUR)}$ and the MT-ND genes. Myoclonic epilepsy with ragged red fibers (MERRF), is a progressive neurodegenerative disorder most frequently caused by a variation in the mt-tRNA^{Lys} gene and which mainly affects complex IV. Neurogenic weakness, ataxia and retinitis pigmentosa (NARP) occur due to a variation in the MT-ATP6 gene and can result in Leigh syndrome when the variant level is greater than 95%. Hearing loss-ataxia-myoclonus syndrome typically affects the mt-tRNA$^{Ser(UCN)}$ gene.

Homoplasmic variations, which typically affect a specific tissue, include mitochondrial disorders such as Leber's hereditary optic neuropathy (LHON) and non-syndromic and aminoglycoside-induced sensorineural hearing loss (SNHL). LHON involves a progressive decline in visual sharpness with the eventual pain-free loss of central vision in both eyes and it is caused by variations in the mtDNA-encoded subunits of complex I (Tuppen *et al.*, 2010; Zeviani & Di Donato, 2004). LHON was the first maternally inherited disease to be linked to an mtDNA point mutation (Wallace *et al.*, 1988). SNHL is caused by a variation in the 12S rRNA gene.

Mitochondrial diseases associated with rearrangements (such as single deletions and duplicates) in mtDNA include Kearns-Sayre syndrome (KSS), progressive external ophthalmoplegia (PEO) and Pearson's syndrome. KSS presents as progressive external ophthalmoplegia and retinitis pigmentosa at an early age, while PEO presents as a less severe phenotype with no retinitis pigmentosa but rather exercise intolerance and proximal myopathy. KSS patients may also develop ataxia, neuropathy and cardiomyopathy, along with various other symptoms. Pearson's syndrome is associated with sideroblastic anemia with pancytopenia and sometimes exocrine pancreas deficiency (Tuppen *et al.*, 2010; Zeviani & Di Donato, 2004).

2.4. Association between myalgic encephalomyelitis and mtDNA variants

2.4.1. Introduction

Myalgic encephalomyelitis (ME), also known as chronic fatigue syndrome (CFS), is a neuro-immune disorder of the central nervous system which involves cardiovascular irregularities, along with deficient ion transport and energy metabolism. In criteria originally given by the CDC, a patient could be diagnosed with ME when persistently fatigued for more than six months without over-exertion and if at least four of the following symptoms were present for six months or longer: Reduced memory, malaise after exertion, restless sleep, myalgia, joint pain without redness or inflammation, headaches, repeated sore throat and sensitive cervical or axillary

lymph nodes. More recently, the International Consensus Criteria (ICC) has been developed to improve the distinction between ME and depression, as shown in Table 2.1. In these criteria, the six month time period is no longer necessary and focus is placed on the low threshold of physical or mental activity required to severely fatigue these patients for prolonged periods.

Table 2.1: International Consensus Criteria for diagnosing CFS/ME

Main Criteria	Symptom Categories	Details
1. Post-exertional neuro-immune exhaustion *(Compulsory)*	a. Noticeable physical and mental exhaustion due to exertion	Diagnosis of ME: *Mild:* 50% decrease in pre-illness activity level *Moderate:* Mostly housebound *Severe:* Mostly bedridden *Very severe:* Totally bedridden, unable to perform basic functions without help
	b. Continued exhaustion even after exertion is over	
	c. Worsening of pre-existing symptoms after exertion	
	d. Prolonged recovery time (usually >24 hours)	
	e. Considerable decrease in pre-illness activity level (≥50% less active than before) due to lack of stamina	
2. Neurological deficiency *(1 symptom in at least 3 categories)*	a. Mental impairments – Short-term memory loss or impaired/slowed processing of information	
	b. Pain – Headaches (severe/chronic/migraine) or significant pain	Pain may be experienced in muscles, tendons, joints, chest or abdomen.
	c. Sleep interruption – Disrupted sleeping patterns or unrefreshing sleep	May involve insomnia, prolonged sleep or reversed sleeping patterns.
	d. Neurosensory, perceptual and motor deficiencies	Such as impaired depth perception, inability to focus sight, muscle weakness, ataxia, etc.
3. Gastro-intestinal, genitourinary and immune deficiencies *(1 symptom in at least 3 categories)*	a. Flu-like symptoms that begin or worsen with exertion	Sore throat, sinusitis, inflamed cervical or axillary lymph nodes.
	b. Sensitivity to viral infections with a longer recovery period	
	c. Gastro-intestinal tract problems	Nausea, abdominal pain, irritable bowel syndrome, bloating
	d. Genitourinary problems	More frequent or urgent urination, nocturia
	e. Sensitivity to medication, food, smells or chemicals	
4. Energy production and transport deficiency *(At least 1 symptom)*	a. Cardiovascular	Dizziness, heart palpitations, hypotension, etc.
	b. Respiratory	Shortness of breath, difficulty breathing, weak chest wall muscles
	c. Irregular body temperature	
	d. Unable to endure extreme temperatures	

Table adapted from Carruthers *et al.* (2011).

A detailed medical history must be compiled and thorough mental and physical examinations must be performed along with various laboratory screening tests, in order to rule out any other underlying mental or physical condition which could be causing the ME symptoms. If a patient meets the first criterion of post-exertional neuro-immune exhaustion, but meets one or two less of the other criteria, they are diagnosed with atypical ME (Carruthers *et al.*, 2011; Fukuda *et al.*, 1994).

Most recently, the *Institute of Medicine of the National Academies* proposed revised diagnostic criteria for CFS/ME. Three fundamental symptoms must all be present: (1) a noticeable reduction in the ability to perform ordinary daily tasks compared to pre-illness onset (lasting for more than 6 months), together with recent onset fatigue which is not due to physical exertion and is not relieved with rest; (2) malaise after exertion which includes headaches, nausea, myalgia, tiredness and weakness; and (3) unrefreshing sleep. One of the following two symptoms must also be present: (1) Mental impairment and (2) orthostatic intolerance (symptoms experienced when standing straight that are minimized by lying down). These symptoms should exist for at least half the time (over a 6 month period) with intermediate to severe intensity. The name Systemic Exertion Intolerance Disease (SIED) was also proposed by this committee to replace the name CFS/ME since it describes a core characteristic of the disease (Clayton, 2015; Lengert & Drossel, 2015).

No diagnostic examinations or conclusive treatments currently exist for ME (Fukuda *et al.*, 1994), but there are various hypotheses attempting to explain the causes of ME. One of the biggest debates regarding ME is whether it is a physiological or psychological condition, with most research seeming to indicate that it is caused by close interaction between both of the above. ME mainly affects women, and due to the lack of a definitive diagnosis for ME, many women become depressed and anxious (compared to women with similar symptoms who have been diagnosed with well-known, medically accepted diseases) due to lack of social support (since ME has the stigma that the patient is simply avoiding work) and the uncertainty of living with a disease with no established diagnosis, causes or treatments (McInnis *et al.*, 2014).

Physiological factors believed to play a role include: Mitochondrial dysfunction (including oxidative stress), infection, nutritional deficiencies, excessive exercise, neuro-endocrine dysfunction (including altered autonomic nerve function) and immuno-inflammatory factors. Psychological factors include: Personality disorders, anxiety or depression disorders, stress (physical or emotional), injury or trauma (Morris & Maes, 2013; Shephard, 2001). Patients with major depression have up-regulation of the hypothalamic-pituitary-adrenal (HPA) axis and thus increased levels of cortisol. ME patients were found to have decreased cortisol levels thus indicating a physiological rather than a psychological condition (Evengård & Klimas, 2002). A variation in the corticosteroid-binding globulin gene, has been associated with numerous ME patients and the decreased levels of cortisol are believed to play an integral role in the altered immuno-inflammatory factors in ME patients (Torpy *et al.*, 2004). Thus far, most evidence seems to indicate that ME is an acquired rather than an inherited disease, but this is yet to be proven.

2.4.2. Association between myalgic encephalomyelitis and mitochondrial dysfunction

In some studies patients with ME have been found to have structurally altered muscle mitochondria (Behan *et al.*, 1991), decreased mitochondrial content as measured by citrate synthase activity (Smits *et al.*, 2011), bioenergetic irregularities in skeletal and cardiac muscle with decreased ATP production and ATP synthesis (Hollingsworth *et al.*, 2010), exercise intolerance with significantly increased lactate levels (which leads to the muscle pain experienced by ME patients) and decreased ATP synthesis, compared to control subjects both during and 24 hours after exercise (Paul *et al.*, 1999). In addition, ME patients were found to switch from OXPHOS to anaerobic respiration much earlier than healthy controls (Vermeulen *et al.*, 2010).

Much contradicting data exists for the role of mitochondrial dysfunction in ME patients, but in many studies, ME patients have been found to have numerous characteristics of mitochondrial disease - including the above mentioned symptoms - such as increased ROS/RNS, ETS defects, coenzyme Q10 deficiency and fatty acid oxidation. Activated immune-inflammatory pathways, in conjunction with oxidative (and nitrosative) stress, could form an integral role in producing mitochondrial dysfunction and thus the bioenergetic irregularities that have been found in ME patients (Morris & Maes, 2013). There have also been reports of uncommon mtDNA deletions in ME patients which may be a contributing factor to the decreased aerobic ATP production observed (Zhang *et al.*, 1995). In a recent study on post-exertional malaise in ME patients, they also found exceptionally low ATP levels during high intensity exercise, with correlating levels of increased cell death. Patients compensated for this with either upregulated glycolysis (along with increased acidosis and lactate) or by replenishing energy supply through purine nucleotide degradation (extending recovery time) (Lengert & Drossel, 2015).

Morris and Maes (2013) proposed that an enterovirus (such as Epstein Barr) or bacterial infection could lead to activated immuno-inflammatory pathways with the subsequent increase of pro-inflammatory cytokines, tumour necrosis factor α, interleukin 1β, nuclear factor κB and elastase, which in turn result in decreased ATP production, defective OXPHOS, increased ROS and RNS production and increased apoptosis. The increased ROS and RNS, together with decreased coenzyme Q10, decreased zinc and ω3 polyunsaturated fatty acids and increased lipid peroxidation, act together to further damage various complexes in the ETS and to impair OXPHOS. Evidence of increased antioxidant enzymes (in an attempt to compensate for the increased oxidative stress) has been found in ME patients along with decreased antioxidant molecules (Myhill *et al.*, 2009; Vernon *et al.*, 2006). Through various mechanisms, these pathways impair mitochondrial function and may account for the bioenergetic irregularities found

in ME patients, such as fatigue and post-exertional malaise, as well as some of the neurological abnormalities that have been observed.

In a recent study, researchers at the CHM (NWU) detected three known pathogenic mtDNA variants, in 14 cases, in a Caucasian cohort of 97 patients from South Africa and the UK, diagnosed with ME: m.7497G>A, m.9185T>C and m.10197G>A (unpublished data). Although there are strong indications that these variants are pathogenic (Jaksch *et al.*, 1998; Kirby *et al.*, 2004; Moslemi *et al.*, 2005), they occur at low allele frequencies (~5 – 20%) and were in the process of verification (including accurate allele frequencies) at the onset of this study. Strikingly, all of these variations were only detected in patients harbouring the U5 mtDNA sub-haplogroup. In other studies, haplogroup U patient cybrids have been found to show a decrease in mtDNA copy number, which in turn cause decreased mitochondrial protein synthesis and complex IV function, ultimately resulting in insufficient energy production and thus possibly playing a role in disease. Haplogroup U5 has also been associated with an increased risk of multiple sclerosis, psoriasis, ankylosing spondylitis, ischemic stroke, ulcerative colitis and Parkinson's disease (Hudson *et al.*, 2014).

2.4.3. m.7497G>A variant

The m.7497G>A variant is found within the MT-TS1 gene which encodes $tRNA^{Ser(UCN)}$. Numerous variations in this gene that were associated with sensorineural hearing loss, overlapping MELAS and MERRF, as well as ataxia and myoclonus have previously been described. Symptoms specifically related to the m.7497G>A variation included muscle weakness and exercise intolerance, with the possible development of deafness at a later stage. Variations in the $tRNA^{Ser(UCN)}$ gene appear to have a very high threshold of variant mtDNA (>95%) before a clinical phenotype is evident, with most patients being homoplasmic for the variation. The pathogenicity of the m.7497G>A variant is believed to be related to the secondary and tertiary structure of the $tRNA^{Ser(UCN)}$ molecule, which results in impaired translation and thus decreased levels of mt-$tRNA^{Ser(UCN)}$ and has also been found to cause a deficiency in complexes I and IV (Jaksch *et al.*, 1998; Mollers *et al.*, 2005).

2.4.4. m.9185T>C variant

The m.9185T>C variant is found within the MT-ATP6 gene which encodes a subunit of ATP synthase. ATP synthase contains a catalytic domain (F1) which converts ADP to ATP, and a proton channel domain (F0) which directs protons from the inter-membrane space to the mitochondrial matrix. The F1 domain is encoded solely by nDNA, while the F0 domain contains 10 subunits, two of which are mtDNA encoded subunits, namely ATPase 6 and 8 (encoded by the MT-ATP6 and MT-ATP8 genes). Numerous variations in the MT-ATP6 gene have previously

been associated with NARP, bilateral striatal necrosis (BSN), Leigh syndrome (a subacute necrotizing encephalomyopathy with psychomotor deterioration) and LHON. The m.9185T>C variation has been specifically associated with Leigh syndrome (predominantly), febrile illness, ataxia, NARP, peripheral neuropathy and Charcot-Marie-Tooth disease. The clinical phenotype has been found to have a very high threshold and to vary with very small differences in tissue heteroplasmy, where variant loads have been found to range from >85% heteroplasmic to homoplasmic for the variation with different symptoms and severity of disease. The variant is believed to affect complex V assembly and decrease ATP synthase activity (Castagna *et al.*, 2007; Childs *et al.*, 2007; Moslemi *et al.*, 2005; Pitceathly *et al.*, 2012; Saneto & Singh, 2010).

2.4.5. m.10197G>A variant

The m.10197G>A variant is found within the MT-ND3 gene which encodes NADH dehydrogenase (a subunit of complex I). The variation was first reported as a neutral polymorphism (Kirby *et al.*, 2004), but it was later considered to be pathogenic. Other MT-ND3 variations have previously been described to play a role in Leigh syndrome, early-onset encephalopathy and progressive neurologic decline (Chae *et al.*, 2007). Patients with the m.10197G>A variant were found to have severe Leigh syndrome and isolated complex I deficiency (Sarzi *et al.*, 2007). A case was also found within a Chinese family, where the variation was associated with LHON (Wang *et al.*, 2009). The variant has been found to range from heteroplasmic (80-90%) (Chae *et al.*, 2007) to homoplasmic with a correlation between the severity of the clinical phenotype and the variant load, with the high percentage indicating that an elevated threshold of variant mtDNA is required for symptoms to be expressed (Sarzi *et al.*, 2007).

2.5. Determining the pathogenicity of mitochondrial DNA variations

2.5.1. mtDNA point mutations

In order to determine whether or not an mtDNA variation is pathogenic, there are certain criteria that must be met. The criteria for point mutations include:

1. The variation must be found at high levels of heteroplasmy in patients and not in controls, but there are a few variants with tissue-specific presentations that may also be present in unaffected individuals;
2. The variation must be found in varied genetic backgrounds in order to ensure that it is not simply a SNP of a specific haplogroup or a neutral polymorphism;
3. The whole mtDNA genome must be sequenced to ensure that the best possible mtDNA variation has been selected, as well as to establish whether or not more than one pathogenic variation exists;

4. The variant load must correspond to the clinical phenotype, since most deleterious variations are heteroplasmic;
5. The variation must alter highly evolutionary conserved nucleotides. If a variation is found in a very old branch of the phylogenetic tree, then it is more likely to be pathogenic since most pathologic variations would be removed by negative selection and are thus not present for a long period of time. Pathogenic variations are able to survive for a longer period if another compensatory variation is also present.
6. The variation must have an effect on areas of the mitochondrial genome which encode amino acids that have an important function. Amino acids and nucleotides having largely varying chemical properties are more likely to undergo pathogenic substitution;
7. Lastly and most importantly; when transferring mtDNA, containing the variation, into another cell line to create cytoplasmic hybrid cells, the cellular or molecular defect must also be transferred.

There are, however, many exceptions to these criteria and all relevant factors, including where the variation occurs (tRNA, rRNA or structural gene), must be considered before drawing any conclusions (Montoya *et al.*, 2009).

2.5.2. mt-tRNA variants

The pathogenicity of mt-tRNA variants is much harder to elucidate since the genes encoding for mt-tRNA form only a small part of the mitochondrial genome and yet they appear to be responsible for a greater part of mitochondrial diseases. Some variations result in extremely harmful phenotypes, while others have no clinical significance (McFarland *et al.*, 2004). The criteria for determining mt-tRNA variant pathogenicity include the following:

1. The variation must not be a recognized, non-pathogenic SNP.
2. The variation must alter an area that is known to be highly conserved throughout evolution. This, however, has the disadvantage of allowing mt-tRNA variations, that are actually pathogenic, to be excluded, simply because they originate from regions that are poorly conserved. mt-tRNA variations should thus not be ruled out if they are not highly conserved.
3. The variation must occur at varying levels within the cells (i.e. heteroplasmic). This criterion is problematic since homoplasmic variations may also occur but they do not show the segregation of the biochemical defect as do heteroplasmic variations. This criterion may also allow non-pathogenic variations to be seen as pathogenic since they are heteroplasmic.
4. A larger proportion of variant mt-tRNA must correspond to a more severe phenotype.
5. Single fiber PCR must be performed by comparing normal and abnormal fibers from muscle (DiMauro & Schon, 2001; McFarland *et al.*, 2004). Single fiber PCR and the development of transmitochondrial cell lines are the gold standard for determining mt-tRNA pathogenicity.

mt-tRNA variants must not be ruled out if they do not show any results using single fiber or transmitochondrial cytoplasmic hybrid studies (Yarham *et al.*, 2011).

6. The secondary structure of the tRNA molecule must also be taken into account when determining mt-tRNA variation pathogenicity. It was found that almost three quarters of pathogenic variations occur in the stems, where the acceptor and anticodon stems are prime areas for pathogenic variations. Watson-Crick base pairing also plays a role where the interruption of C-G base pairing is found more in pathogenic variations than in neutral ones, and pathogenic variations occur in loop structures that are abnormal in size and that affect the tertiary folding of the mt-tRNA (McFarland *et al.*, 2004).

2.5.3. The use of mtDNA-depleted cells and cytoplasmic hybrid cells

To comply with the seventh point in the criteria for determining mtDNA point mutation pathogenicity and the fifth point in the criteria for determining mt-tRNA variant pathogenicity, it is necessary to develop cybrid cells by fusing mtDNA-depleted cells (ρ^0 cells) with enucleated cytoplasts or blood platelets containing the desired mtDNA variant. This creates a structured environment whereby the effects of specific mtDNA variations and their variant load in different individuals can be studied against identical nuclear backgrounds. This allows the mechanisms by which these variations harm cellular function to be studied (Chomyn *et al.*, 1991).

King and Attardi created the first transmitochondrial cybrid cell line in 1989 by transferring mtDNA from cytoplasts to ρ^0 143B osteosarcoma cells (King & Attardi, 1989). In 1994, Chomyn described a method using blood platelets rather than cytoplasts to donate mtDNA. This simplifies the overall procedure since blood platelets do not contain nuclei and no enucleation procedure is thus necessary (Swerdlow, 2007). It is also a less invasive procedure since fibroblasts no longer need to be obtained from patients and fibroblast cultures do not need to be established (Chomyn, 1994).

The ρ^0 cells can be developed by culturing cells in the presence of ethidium bromide (EtBr) over a prolonged period of time (King & Attardi, 1996). EtBr is a positively charged DNA intercalating agent which is attracted to the negatively charged mitochondrial matrices. The mtDNA polymerase attempts to integrate EtBr into the growing mtDNA strands causing mtDNA replication to be inhibited. EtBr does not remove any existing mtDNA, it simply prevents further mtDNA replication, forcing the cells to split their mtDNA as they divide. The mtDNA is thus effectively diluted out of the cells with each successive cell division (Swerdlow, 2007). Very low doses of EtBr are administered so that the replication of nDNA is not affected (King & Attardi, 1996). Other methods used to develop ρ^0 cells include the use of ditercalinium (an mtDNA POLG inhibitor), expression of a dominant negative mtDNA POLG construct, exposure to

dideoxynucleoside analogues (which interfere with mtDNA replication), rhodamine 6-G (which interferes with mitochondrial ETS function) and expression of mitochondrial targeted EcoRI (Inoue *et al.*, 1997; Jazayeri *et al.*, 2003; Kukat *et al.*, 2008; Nelson *et al.*, 1997; Williams *et al.*, 1999). These treatments leave the cells with mitochondrial shells that lack a functional ETS or ATP synthase. Together with the adenine nucleotide translocator (ANT), which accepts ATP^{4-} and releases ADP^{3-}, the F_1 subunits of ATP synthase are still capable of hydrolyzing glycolytic ATP which allows ρ^0 cells to maintain a non-ideal but sufficient pmf (Nicholls & Ferguson, 2013a).

King and Attardi found that cells were unable to continue growing when exposed to EtBr, even with high levels of glucose. This led to the discovery that these ρ^0 cells were pyruvate and uridine auxotrophs. Pyrimidines, such as uridine, are required since the enzyme dihydroorotate dehydrogenase (located in the mitochondrial inner membrane) cannot function without OXPHOS. When treated with EtBr, OXPHOS becomes non-functional, resulting in lack of pyrimidine synthesis. The ρ^0 cells function mainly by the glycolysis pathway resulting in the production of pyruvate. Thus it was surprising to find that these cells were pyruvate auxotrophs. A proposed theory was that the lack of an ETS within these cells decreased the NAD^+ levels and allowed the build-up of NADH, due to elevated glycolysis and complex I dysfunction. The additional pyruvate was then reduced to lactate by lactate dehydrogenase with the subsequent oxidation of NADH to NAD^+ and H^+. This lowered the amount of pyruvate entering the Krebs cycle and restored redox balance (King & Attardi, 1996).

The aim of this study was to use mtDNA (from patients with ME and control subjects) obtained from blood platelets and to fuse these blood platelets with ρ^0 cells, using polyethylene glycol (PEG) (Figure 2.3). The cybrids obtained from both patients and the controls were to be cultured, and various biochemical and molecular experiments performed on them. Since both control and patient cybrids contained the same nuclear background and were cultured under the same conditions, it was presumed that any differences observed between controls and patient cybrids, were due to variations in mtDNA (Swerdlow, 2007).

Before the discovery of PEG, UV-inactivated Sendai virus was used to induce cell fusion (Radomska & Eckhardt, 1995). The exact mechanism behind PEG-mediated cell fusion is not yet fully understood, but theories have been proposed. In order for cellular membranes to fuse, their molecular arrangement must be altered. PEG is a greatly hydrated polymer which is believed to thermodynamically remove water from between cells and thus allow the membranes to come into molecular contact by forcing cells to aggregate. Dehydration causes an imbalance in the lipid packing pressure, due to the effect of PEG on the outer monolayer of the lipid

bilayer. This leads to the formation of a single bilayer septum which decays until it eventually forms a fusion pore (Lentz, 1994; Lentz & Lee, 1999). Other methods that have been used for cell fusion includes electrofusion, which fuses the membranes of adjacent cells using a pulsed electric field. Dielectrophoresis is used by subjecting the cells to an alternating AC electric field which causes the cell to form dipoles and the dipoles begin to attract to one another, forming a chain as they move towards a common point within the electric field. A DC pulse is then applied creating a strong electric field which fuses the cells by creating a transient pore in the cell membrane. Thereafter, an AC pulse is again applied to keep the cells together as they fuse (Berg, 1988). While electrofusion has been shown to be more reliable and reproducible, it requires specialized apparatus.

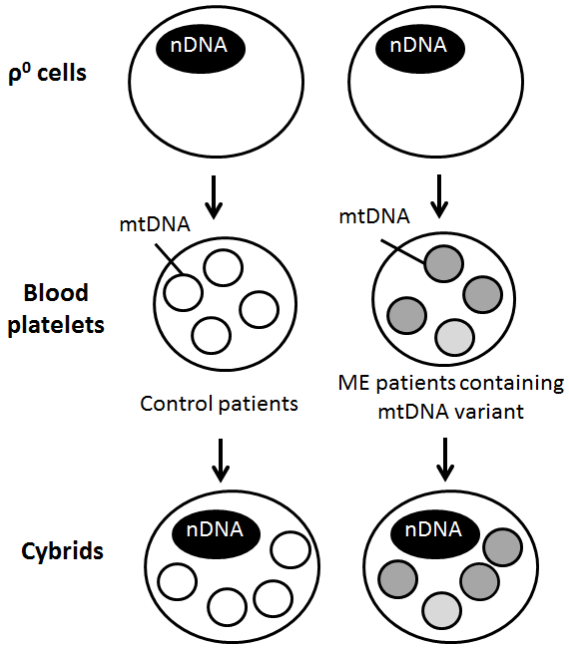

Figure 2.3: The fusion of ρ^0 cells with blood platelets, obtained from control and ME patients, to form cybrid cells which have the same nDNA but varying mtDNA. Image adapted from Swerdlow (2007).

When working with cybrids there are certain considerations that should be made. It is presumed that only the mtDNA is being studied when working with cybrids, but the nuclear background of the ρ^0 cells will inevitably have an effect on the cybrids. Most cell lines used for cybrids are tumour cell lines that are aneuploid and thus have an unusual number of chromosomes, which can have very varied effects on different ρ^0 cell lines (Swerdlow, 2007). Tumour cell lines are also anaerobic cell lines depending mainly on glycolysis for ATP production, while the cells in which most mitochondrial defects occur are aerobic cells that depend on OXPHOS for ATP production. It has also been found that the production of ρ^0 cells and cybrids leads to up-regulation of nuclear transcripts involved in OXPHOS. This can alter the phenotype seen in cells compared to patients (Tuppen *et al.*, 2010). In addition to fusing 143B ρ^0 cells with ME patient

and control blood platelets, rhabdomyosarcoma (RD) ρ^0 cells were also used to observe the effect of a more aerobic cell line (since RD cells are derived from human muscle cells).

The following tests can be performed to ensure that ρ^0 cells truly are mtDNA free: Southern blotting, determining the absence of oxygen usage or the absence of functional ETS activity, proving pyruvate/uridine auxotrophy, and the lack of mtDNA amplification by PCR (Swerdlow, 2007). In this study the focus lay on determining pyruvate/uridine auxotrophy, mtDNA copy number and the absence of oxygen utilization or functional ETS activity.

2.6. Applying bioenergetics parameters to evaluate mtDNA pathogenicity in cellular models

2.6.1. Introduction

Bioenergetics is the study of how energy is transferred within living organisms. Within the field of biochemistry in humans, bioenergetics refers more specifically to the energy changes occurring across the inner mitochondrial membrane and how oxidation reactions, involving the transfer of electrons between coenzymes and proteins, are linked to this energy-conserving membrane (Nicholls & Ferguson, 2013d).

The proton current across the inner mitochondrial membrane can be determined since it is proportional to the rate of oxygen usage (rate of respiration), for a specific substrate, due to the tight coupling between electron transport and proton translocation in isolated mitochondria and cells. As discussed in Section 2.2.2., electrons may be transferred to the ETS through complex I or complex II, depending on the substrate. It is most commonly accepted that for every $2e^-$ transferred from NADH or any other ubiquinone-linked dehydrogenase to $½O_2$, 10 H^+ ions or 6 H^+ ions are translocated from the mitochondrial matrix to the inter-membrane space, respectively (Brand & Nicholls, 2011). Methods for determining the oxygen utilization of cells can thus provide us with a large amount of information concerning the mitochondrion. According to Brand and Nicholls (2011), the best assay for measuring mitochondrial dysfunction in cells is the cell respiratory control (which will be discussed in Section 2.6.3), and in isolated mitochondria, the mitochondrial respiratory control (which will be discussed in Section 2.6.2). Ideally, both respiration and membrane potential should be measured to obtain a more detailed understanding of the mechanisms involved in mitochondrial dysfunction, but respiration alone is much more informative than pmf.

In this section, the two most commonly used methods for measuring respiration, the Clark-type oxygen electrode and XF analyser will be discussed in detail, while less common or problematic methods used for measuring respiration and membrane potential will be discussed briefly.

2.6.2. Clark-type oxygen electrode

The Clark-type oxygen electrode, developed by Leland Clark in 1954 (Clark Jr, 1956), can be used to measure the oxygen usage of isolated mitochondria and cells. As shown in Figure 2.4a, a cell suspension or isolated mitochondria are incubated in an oxygen electrode chamber (of between 0.2 and 2 mL) in media containing sucrose, KCl (or another suitable reagent for providing osmotic assistance), calcium, a pH similar to that of the cytoplasm, and inorganic phosphates (P_i). There is an O_2-permeable membrane separating the incubation medium from the electrodes and a stirrer to prevent the exhaustion of O_2 at the membrane. The Clark-type O_2 electrode can be dropped down into the media until all the air is released through the addition port (through which compounds can be added to the medium) where it gradually uses up O_2 which is measured by the current between a silver reference electrode and a platinum electrode (Nicholls & Ferguson, 2013b).

The first experimental design using the oxygen electrode for isolated mitochondria (Chance & Williams, 1955) proposed the following: Mitochondria with P_i, addition of ADP, addition of substrate which together with the ADP allows rapid respiration, exhaustion of ADP, and lastly, lack of O_2. This experiment has since been slightly adapted (as seen in Figure 2.4b):

1. Mitochondria are incubated in the presence of P_i (no respiration occurs).
2. A substrate is added so that a stable respiration rate is attained. The protons are unable to move through ATP synthase, but a slow rate of respiration is still achieved due to proton leak.
3. 3_{ADP}: ADP is added which allows the protons to move through ATP synthase with the subsequent conversion of ADP and P_i to ATP. This allows respiration to occur rapidly due to the drop in pmf, controlled by ATP turnover (as well as substrate supply and oxidation).
4. 4_{ADP}: The limited amount of ADP becomes depleted and the ATP/ADP ratio reaches equilibrium (as in state 2) with the concurrent slowing of respiration due to the rise in pmf.

   4_{oligo}: Instead of adding a limited amount of ADP, an ATP synthase inhibitor such as oligomycin can be added to slow down respiration and stop all protons from re-entering ATP synthase. This is especially necessary if contaminating ATPases exist (due to broken mitochondria), allowing ATP recycling to occur and thus preventing respiration from slowing. Similarly to state 2, it is controlled mainly by proton leak and ~10% by substrate oxidation.

   3_u: FCCP (an uncoupler) is added causing uncontrolled respiration where the protons are able to flow freely back into the mitochondrial matrix, thus showing maximal respiration as controlled by substrate availability, metabolism and electron transport. This state is useful for determining whether or not there is dysfunction in one of the ETS components, substrate translocases or dehydrogenases.
5. Eventually all the O_2 becomes depleted so that a state of hypoxia occurs.

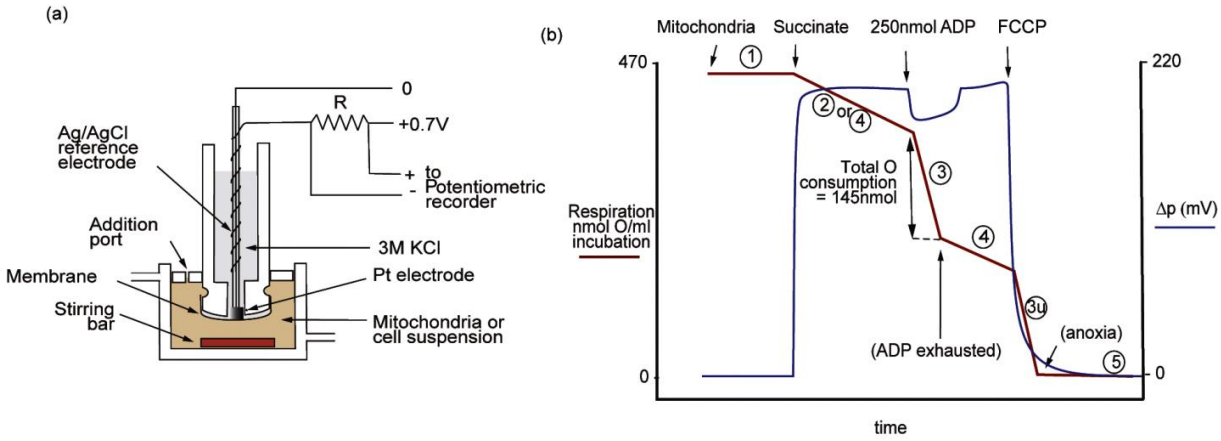

Figure 2.4: (a) The classic Clark-type O_2 electrode. (b) The classic experiment conducted on isolated mitochondria by adding substrate, ADP, and FCCP in order to determine the increase in respiration in response to ADP. (From Nicholls & Ferguson, 2013. Copyright permission no. 3401830802336.)

There are two factors that can be used to assess the performance of mitochondria in this experiment. Firstly, and most importantly, the mitochondrial respiratory control ratio (RCR) is the respiration in state 3_{ADP} divided by the respiration in state 4. A high RCR suggests that the mitochondria have a low proton leak but a high rate of ATP production and substrate oxidation, whereas a low RCR suggests mitochondrial dysfunction. Secondly, the P/O ratio which is the mol of ATP produced, divided by the mol of $½O_2$ used. This ratio indicates the maximum amount of ATP that can be produced when $2e^-$ move from their substrate to $½O_2$. This ratio will only show mitochondrial dysfunction if the coupling efficiency of the mitochondria is affected, and is thus a poor measure of mitochondrial dysfunction. By measuring both respiration and membrane potential (discussed in Section 2.6.5), slight changes in proton leak and coupling efficiency can be observed, but by itself, the mitochondrial respiratory control provides the most important information.

One of the main disadvantages of the Clark-type oxygen electrode is that it can only be used on a large amount of cells that are in suspension. The effect of removing adherent cells from their normal environment and exposing them to rapid stirring in suspension must be considered when studying the metabolic status of these cells (Brand & Nicholls, 2011; Nicholls & Ferguson, 2013b). The following section discusses an apparatus which overcomes these disadvantages.

2.6.3. Extracellular flux analyser

The XF analyser (also known as the Seahorse XF analyser) allows the analysis of cells and organelles in a 24- or 96-well format so that much fewer cells are required than for the Clark-type oxygen electrode. Cultured cells adhere to the plate naturally, but isolated mitochondria (or other organelles) or cells that grow in suspension must be centrifuged (Brand & Nicholls, 2011).

The XF analyser is able to measure both OXPHOS and glycolysis of cells simultaneously in real time. When O_2 is available, cells consume the O_2 along with glucose, amino acids, fatty acids and glutamine. The XF analyser measures the rate at which O_2 is used up from the medium, the so-called oxygen consumption rate (OCR). During glycolysis, glucose is converted to pyruvate, and if no O_2 is available or if OXPHOS is not functional, pyruvate is converted to lactate with the concurrent release of NAD^+ and protons. The XF analyser measures the rate at which these protons are released, the so-called extracellular acidification rate (ECAR) (Ferrick *et al.*, 2008).

The XF analyser makes use of a culture plate (in which the cells are seeded) and a sensor cartridge, which contains one probe and four injection ports for each well (as shown in Figure 2.5). Each probe contains two fluorophores embedded in the base of the polymer; one of the fluorophores is quenched by O_2 while the other is sensitive to protons. The fibre optic bundles of the XF analyser insert into these probes during analyses and emit light to excite the fluorophores while measuring the change in fluorophore emission due to O_2 and H^+. In the 96-well format, the probes are lowered so that the cells are encapsulated in 3 µL of medium. The injection ports surrounding the probes allow up to four different compounds to be loaded in the sensor cartridge (where they are held by capillary action) and they can then be injected one-by-one during the assay (using compressed air), mixed into the media by the raising and lowering of the fibre optic probe, and the effect of each compound on the cells can be measured.

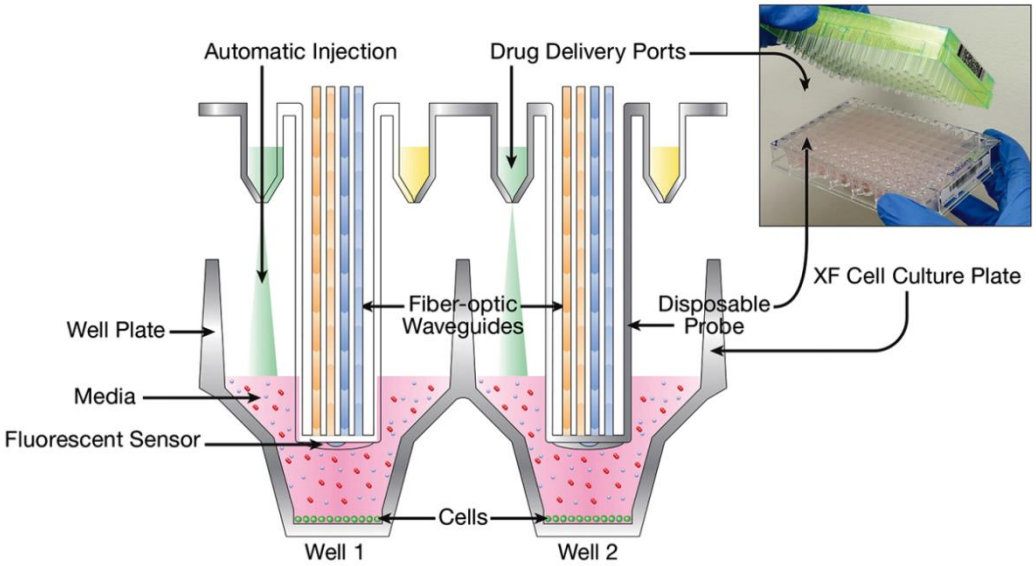

Figure 2.5: Schematic representation of two wells in a Seahorse culture plate showing the probes containing the embedded fluorophores as well as the drug injection ports. Insert: Photo of a 96-well cell culture plate and cartridge. (With permission from www.seahorsebio.com)

Specific compounds are loaded into the injection ports in order to perform a “Mito Stress test” in which OXPHOS is stressed to observe its maximal respiration or mitochondrial dysfunction.

A typical Mito Stress test design is as follows (as shown in Figures 2.1 and 2.6):

1. Basal respiration is measured as it is controlled by proton leak and re-entry pathways through ATP synthase.
2. Oligomycin, an ATP coupler, which blocks the proton channel of the F_0 part of ATP synthase, is injected. This blocks all protons from re-entering the mitochondrial matrix through ATP synthase and thus any remaining respiration is due to natural proton leak only.
3. FCCP, an ATP accelerator which acts as an uncoupler by transporting H^+ ions across the mitochondrial membrane instead of through the proton channel of ATP synthase. It causes a rapid decrease in the mitochondrial membrane potential with the subsequent greatly increased consumption of O_2 (and thus also OCR) and energy, without any production of ATP. The ECAR is also increased since the cells attempt to restore energy balance by increasing their ATP production through glycolysis.
4. Rotenone, a complex I inhibitor that prevents electrons from being transferred to ubiquinone, and antimycin A, a complex III inhibitor which disturbs the formation of a proton gradient and thus inhibits ATP production, are then injected simultaneously. These two compounds together terminate all mitochondrial respiration, so that any remaining respiration is non-mitochondrial. ECAR is increased as the cells attempt to produce energy via glycolysis.

(Seahorse Bioscience. http://www.seahorsebio.com)

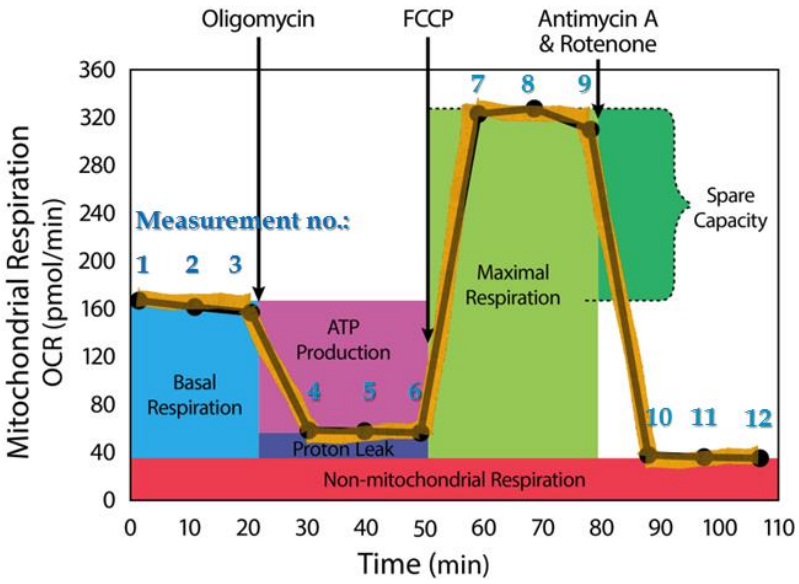

Figure 2.6: Mito Stress test profile showing the changes in OCR after injections of oligomycin, FCCP, rotenone and antimycin A. The parameters that are being measured are also shown: Basal respiration, proton leak, ATP production, maximal respiration, spare respiratory capacity and non-mitochondrial respiration. (With permission from www.seahorsebio.com)

Since the XF analyser was the chosen method for this study, each of the parameters shown on Figure 2.6 will be discussed in detail along with the coupling efficiency and cell respiratory control ratio.

BASAL RESPIRATION

The basal respiration rate is normally taken as the OCR measurement before injection of mitochondrial inhibitors. The basal respiration is primarily controlled by ATP production and secondarily, by proton leak and substrate oxidation (Ainscow & Brand, 1999; Brown *et al.*, 1990). It thus responds mainly to changes in ATP demand, but it is also sensitive to various substrates or hormones within the incubation medium. The basal respiration can be seen as the minimum level of respiration that is required by cells in order to meet the energy demands placed on OXPHOS.

ATP PRODUCTION AND PROTON LEAK

Inhibition of proton flux through ATP synthase by oligomycin, prevents electron transfer between the other four complexes due to the high proton gradient across the inner mitochondrial membrane. This results in decreased OCR which corresponds to the basal rate of mitochondrial ATP synthesis. Protons pumped across the mitochondrial membrane during respiration, that are not linked to ATP production but do use oxygen, represent proton leak and the rate of this proton leak can be determined by any remaining respiration (above non-mitochondrial respiration) after oligomycin has been injected. The cells are forced to shift to glycolysis for ATP production during this period, as they are no longer able to meet the basal respiratory level required to maintain OXPHOS during the given energy demands of the cell.

Increased ATP production is indicative of a higher energy demand while decreased ATP production is indicative of a lowered energy demand, insufficient substrate and/or greatly impaired OXPHOS. An increased proton leak into the mitochondrial matrix may be indicative of increased uncoupling protein activity, deficient respiratory chain complexes or damage to the inner mitochondrial membrane. The increased proton leak causes electron slippage, where oxygen is used up without the proton transfer that usually accompanies complexes I, III and IV. Oxidative stress is also known to increase proton leak and ATP production.

COUPLING EFFICIENCY

The coupling efficiency is calculated by the following equation:

Coupling efficiency = 1 – (Oligomycin response/Basal respiration) x 100

The coupling efficiency is expected to change in almost any dysfunction as it is sensitive to changes in all bioenergetic aspects, and since it is a ratio, it is internally normalized.

MAXIMAL RESPIRATION AND SPARE RESPIRATORY CAPACITY

The maximal respiration rate is attained after the addition of FCCP and is equivalent to state 3_u in the Clark-type oxygen electrode. A distinction must be made between OXPHOS capacity and ETS capacity since the maximal respiration discussed in this section refers to the ETS capacity. OXPHOS capacity can only be measured using saturating ADP concentrations, a condition that cannot be measured in intact cells due to the lack of ADP and inorganic phosphate equilibration across plasma membranes. The ETS capacity is limited by the maximum rate of substrate absorption and metabolism, and the activity of the ETS. This will be typically greater than OXPHOS capacity if limited by the phosphorylation system during coupled respiration. When the phosphorylation system does not exert control over coupled respiration, the ETS and OXPHOS capacity will typically be identical.

The spare respiratory capacity shows the capacity of electron transport and substrate reserve to react to an increase in energy requirement and it can be determined using either of the following two equations:

Spare respiratory capacity = Maximal respiration (due to FCCP) - Basal respiration

Spare respiratory capacity (%) = Maximal respiration (due to FCCP)/Basal respiration x 100

The maximal rate can often be increased by adding pyruvate so that glycolytic capacity is not a limiting factor. FCCP must be added at a concentration where there is maximal uncontrolled respiration without excessively decreasing the membrane potential due to decreased substrate supply. This is as a result of uncouplers acidifying the cytosol and disrupting endosomes. Mitochondria in highly excitable cells, such as nerve and heart cells, are also subject to large transfers of calcium and other ions, which make use of the proton gradient and thus increase the OCR without any ATP production.

During oxidative stress the spare respiratory capacity of the cells is used up and may result in cell death if respiration drops below the basal respiration threshold. Decreased spare respiratory capacity may indicate mitochondrial dysfunctions not evident in basal respiration, due to the cells being subjected to a higher ATP demand, where substrate oxidation may be limiting instead of ATP turnover (in basal respiration). Decreases in maximal respiration/spare respiratory capacity may be indicative of either reduced substrate supply, or possible impairment of mitochondrial mass or integrity.

NON-MITOCHONDRIAL RESPIRATION

Most cells have a small percentage (~10%) of non-mitochondrial oxygen consumption due to certain detoxification, pro-inflammatory and desaturase enzymes. These enzymes seem to

have a negative effect on the bioenergetic status of cells. By blocking all mitochondrial OXPHOS activity using rotenone and antimycin A, the percentage of non-mitochondrial respiration can be determined. This non-mitochondrial respiratory rate is deducted from all other rates. This rate has been found to differ, and tends to increase when subjected to stressors such as ROS and RNS.

CELL RESPIRATORY CONTROL RATIO AND BIOENERGETIC HEALTH INDEX

Similar to the mitochondrial RCR, the cell RCR is the respiration rate after uncoupling (FCCP), divided by the respiration after oligomycin addition. This ratio is sensitive to substrate oxidation and proton leak, while ATP turnover does not play a role. The cell RCR has the same advantages as the coupling efficiency where it is internally normalized and is capable of revealing various types of mitochondrial dysfunction.

Since the bioenergetics parameters measured using the Mito Stress test are interactive and only show small differences between experimental groups, the overall bioenergetic profile is often difficult to ascertain. A new concept has recently been proposed to overcome this, called the Bioenergetic Health Index (BHI). The BHI is an equation which incorporates all positive and negative characteristics of bioenergetic function into a single value. The idea is that by measuring the BHI in blood platelets or leukocytes (which can act as biomarkers since they are subject to circulating factors which are associated with metabolic stress) of different patients, a clinical test can be established for measuring bioenergetic dysfunction. The proposed equation looks as follows (a, b, c and d are exponents, which can be used to alter the relative effect of each respiratory parameter):

$$BHI = log \frac{(spare\ respiratory\ capacity)^a \times (ATP\ production)^b}{(non\text{-}mitochondrial)^c \times (proton\ leak)^d}$$

A recent paper from Kramer *et al.* (2015) made use of the BHI where they equated all exponents to one and excluded individual samples with undetectable proton leak or non-mitochondrial respiration, due to the instrument's limitations. Absolute values for the BHI cannot be given since it varies widely depending on the experimental conditions, but it does allow statistical comparisons (intra-plate) to be made between experimental and control groups using a single index, rather than studying multiple parameters. (Brand & Nicholls, 2011; Chacko *et al.*, 2014; Gnaiger, 2014; Kramer *et al.*, 2015)

2.6.4. Other methods for measuring respiration

The OROBOROS Oxygraph-2k (O2k) is another instrument that can be used for determining respiration using an electrode similar to the Clark-type electrode. The O2k is a method of high

resolution respirometry, compared to the XF analyser, which is more suitable for high-throughput analyses. The O2k has only two chambers (compared to the multiple wells available with the XF analyser) and cells or isolated mitochondria must be kept in suspension. The O2k is only capable of measuring oxygen usage, but additional modules can be purchased such as sensors which allow simultaneous real-time measurement of ROS and mitochondrial membrane potential using fluorescent dyes. The O2k is not restricted to a set number of injections and is thus able to provide much more information in a single analysis compared to the XF analyser (Gnaiger & Fasching, 2014).

2.6.5. Methods for measuring mitochondrial membrane potential

The mitochondrial membrane potential is much less sensitive to changes in mitochondrial function, compared to respiration (which undergoes large changes), but measuring the mitochondrial membrane potential can provide numerous mechanistic insights (such as proton leak and coupling efficiency) into mitochondrial dysfunction when performed in conjunction with respiration analyses that provide the RCR.

In isolated mitochondria, this can be done by incubating mitochondria with media containing small doses of cations that are able to permeate through the lipophilic membranes. An electrode is placed in the medium to measure the decrease in cations within the medium as they are accumulated within the mitochondrial matrix (which is negatively charged, thus attracting the positively-charged cations). Absorbance or fluorescence can also be used instead of an electrode if a suitable membrane-permeant cation is used (Brand & Nicholls, 2011).

The mitochondrial membrane potential of cells can be measured using flow cytometry and fluorescent dyes that are positively-charged and are able to permeate the cell membrane. These dyes are actively absorbed by the cell's mitochondria where they accumulate in the mitochondrial matrix and inter-membrane space, due to the proton gradient across the inner mitochondrial membrane which creates a charge, and because of their solubility. Fluorescence microscopes can then be used to monitor the fluorescent signals. Alternatively, radioactive tracers can also be used. Although this is a fast and simple method, the disadvantage of these dyes is that they may inhibit complexes of the respiratory chain, so their concentrations must be carefully optimized (Brand & Nicholls, 2011; Scaduto Jr & Grotyohann, 1999).

2.6.6. Additional bioenergetic methods

In both isolated mitochondria and cells, various enzymes and complexes within the respiratory chain, Krebs cycle or metabolism can be studied to determine whether or not their function is altered during mitochondrial dysfunction. Although analyses of their activity, concentrations and

expression are relatively easy to conduct, no one enzyme is rate-limiting and control shifts between enzymes and processes under different conditions so the specific functioning of that complex or enzyme under physiological conditions is very difficult to determine. Mitochondrial proliferation, size, shape and dispersal may be indications of changed mitochondrial function. Oxidative stress due to reactive oxygen species may also occur during mitochondrial dysfunction and may thus also be a useful assay (Brand & Nicholls, 2011).

ATP assays can be performed using the luciferin-luciferase bioluminescent assay to determine the concentration of ATP (Crouch *et al.*, 1993). These assays are, however, not a good indication of mitochondrial dysfunction since they indicate changes in the adenine nucleotide pool size, rather than the bioenergetic state of the mitochondria, and the ATP/ADP concentrations change so quickly that the sensitivity of these assays are limited (Brand & Nicholls, 2011; Zhang *et al.*, 2012).

Various other indicators can be used for detecting possible mitochondrial dysfunction. Cell viability assays are fast and cost-effective. They can be conducted using a tetrazolium salt (e.g. MTT which measures mitochondrial dehydrogenase activity) or water-soluble tetrazolium derivatives which are reduced to form purple formazan products and allow cell viability to be measured by colorimetric analyses. Cells can be cultured in a medium containing galactose so that the cells are forced to rely on OXPHOS more than glycolysis and any OXPHOS dysfunction may then become more obvious. Assays to determine the lactate production may be useful since increased lactate production may suggest that mitochondrial dysfunction lead to an increase in glycolysis as a compensatory mechanism (Brand & Nicholls, 2011; Ishiyama *et al.*, 1996).

A final tool that can be used for determining mitochondrial bioenergetics is the metabolomics approach where stable isotope-labeled carbon substrates are included in the cell medium and the intermediate metabolic isomers formed by the cells are then traced using mass spectrometry. It is also possible to do this, using radioactive isotopes, but non-radioactive isotopes have become the method of choice (Paul Lee *et al.*, 2010; Zhang *et al.*, 2012).

2.7. Problem statement, aims and strategy

2.7.1. Problem statement

The possible involvement of mtDNA in ME forms the problem statement of this study and will be addressed via a number of aims and objectives, as described in the next section. Essentially, this study will investigate two questions relating to the involvement of mtDNA sequence variation in ME:

- The first question is whether known pathogenic mtDNA variants detected at sub-clinical levels in ME patients have a functional effect on energy metabolism? As described previously, before the onset of this study, three known pathogenic mtDNA variants were discovered in a number of patients in the current ME study cohort, namely m.7497G>A, m.9185T>C and m.10197G>A. Although there were strong indications that these variants were pathogenic, they were detected at low allele frequencies (~5-20%) using NGS and their presence and frequencies were validated in the duration of this study. An important aspect of making sense of mtDNA variation is to determine whether an mtDNA variant is pathogenic or not. Criteria can be used to evaluate pathogenicity, and one of these criterions involves the development of cybrid cells whereby the variations in question are transferred to cells with the same nuclear genetic background. By comparing the energy production capacity (using the XF analyser) of control cells and cybrid cells containing the ME variants, the pathogenicity of these variations may be determined.
- The second question asks whether the combination of rare non-synonymous variants in the mtDNA of patients have a functional effect on energy metabolism? This question is based on the so-called “mutational load” hypothesis described in Section 2.3.4.

2.7.2. Aims and objectives

The following two *aims* have been formulated for this study, to address the two mentioned research questions, both of which involved a functional investigation:

1. The first is to set up the techniques and optimize the protocols for an *in vitro* functional (bioenergetics) investigation suitable for this study. This will be done using an XF analyser called the Seahorse XF^{e}96 analyser and several cell lines, including the host cell lines used in the second aim of this study.
2. The second is to develop cybrid cells using blood platelets from ME patients in the study cohort, including those initially identified to harbour the mtDNA variants, m.7497G>A, m.9185T>C and m.10197G>A, and healthy controls. These cybrid cell lines will then be used to investigate the two research questions.

The *objectives* are to:

1. Set up and develop the techniques and protocols for using the Seahorse XF^{e}96 analyser for bioenergetics studies.
2. Confirm the presence of mtDNA variants in selected patients using NGS and calculate the MutPred scores (see Section 2.3.4 and 3.6) of each subject.
3. Create cybrid cells using blood platelets from healthy controls and from patients with one or more of the ME mtDNA variants and confirm mtDNA transfer to the cybrid cells using PCR-RFLP haplogroup analysis.
4. Determine the (relative mtDNA copy number) RMCN of the cybrid cells on the day of the Seahorse XF^{e}96 analysis using real-time PCR.
5. Analyse the energy production capacity of the various cybrid cells using the Seahorse XF^{e}96 analyser, determine the bioenergetic parameters for each patient and perform statistical analyses.
6. Use different ρ^0 cells (RD rhabdomyosarcoma cells instead of 143B osteosarcoma cells) in order to observe the effect of a different nuclear background and different cell line.
7. Determine whether or not the three ME mtDNA variants are pathogenic according to specific criteria and if any variation of bioenergetics profiles between patient and control cybrids can be attributed to mutational load or possibly, to haplogroup variation.

2.7.3. Experimental strategy

Figure 2.7 illustrates the experimental strategy which was used in this study. In fulfilment of Aim 1, six different cell lines were obtained from American Type Culture Collection (ATCC, Manassas, USA) and cultured so that reserve cells could be frozen for future use. Each of these cell lines were then optimized on the XF analyser so that future studies and analyses can be performed using these cell lines. The optimization was also essential for obtaining practical experience on the XF analyser in order to be able to perform more accurate analyses.

For Aim 2, blood samples were collected from all healthy controls and ME patients and the blood platelets were isolated and frozen. These patients formed part of a previous study performed by the CHM (NWU), thus providing the information required for patient selection. Patients believed to harbour one or more of the three pathogenic mtDNA variants were sequenced again using the Ion Torrent to confirm heteroplasmy level and mutational load. These sequencing results along with previous sequencing data were used to calculate the MutPred score for each patient and control. These blood platelets were then fused with 143B ρ^0 cells using PEG to form cybrid cells. Cells were cultured for six weeks and mtDNA transfer was confirmed via haplogroup analyses using the PCR-RFLP approach. Both control and patient (containing the ME variants) cybrid cells were then analysed using the Seahorse XF^{e}96

analyser, after three and six weeks of cell culture. Cells obtained the day of seeding for the XF analysis were used to determine the RMCN using real-time PCR. The RMCN served as an additional measure to confirm that mtDNA transfer to ρ^0 cells was successful and to determine the effect (if any) of the RMCN on the bioenergetic profile for each patient. Bioenergetic results were normalized using the CyQUANT DNA proliferation assay kit (Invitrogen). Statistical analyses were then performed on the data obtained from the XF analyser, which included all of the bioenergetic parameters (as calculated by the Seahorse Bioscience report generators). The bioenergetic profiles were then studied to determine whether or not a link could be found to the mutational load hypothesis or haplogroup variation, as well as to determine the possible pathogenicity of the three mtDNA variants.

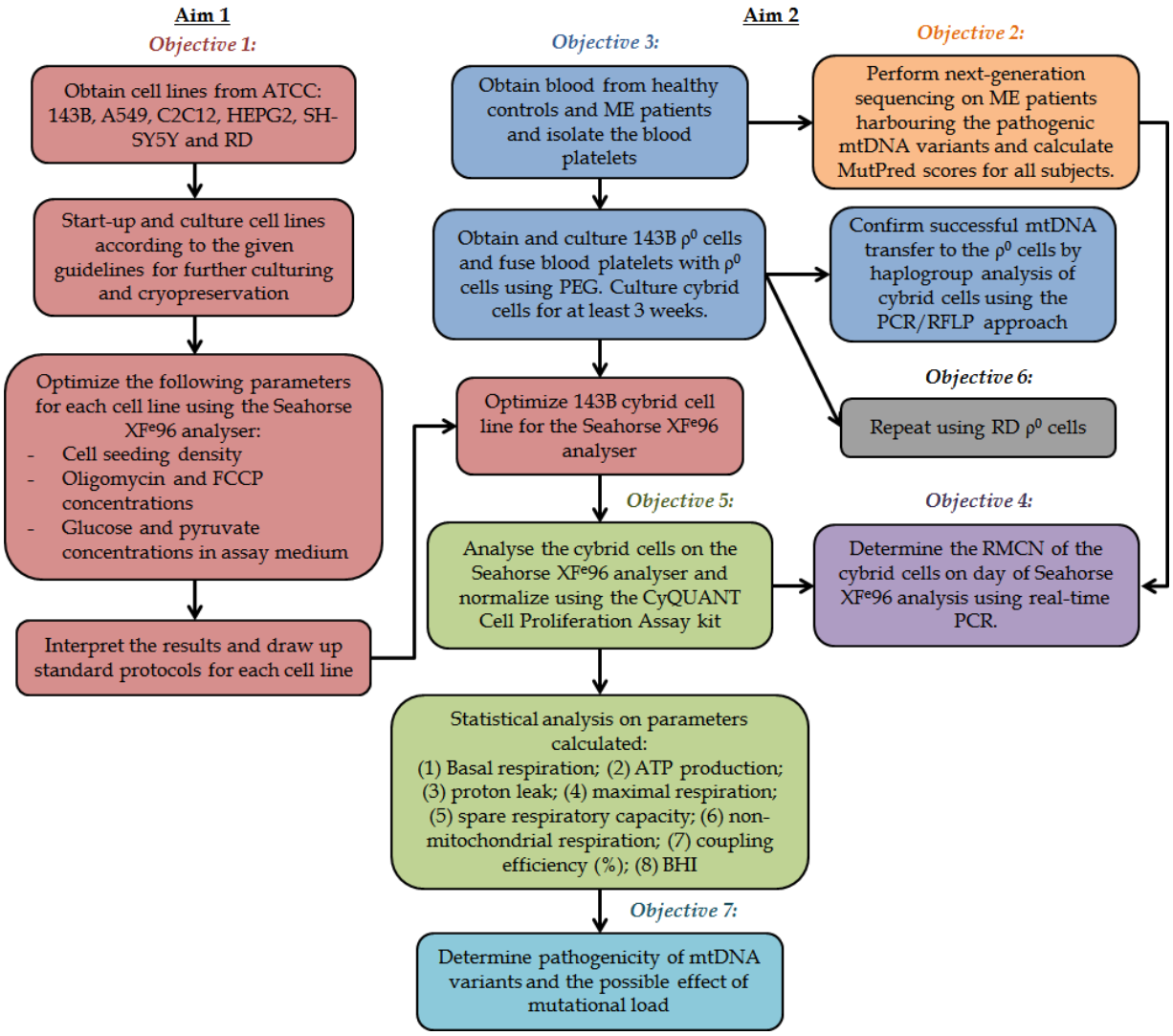

Figure 2.7: Experimental strategy illustrating the aims and objectives of this study. Aim 1 is depicted on the left and involves the optimization of selected cell lines on the Seahorse XF^e96 analyser. Aim 2 on the right depicts the development of cybrid cells from the blood platelets of patients diagnosed with ME (and healthy controls) and the analysis thereof on the Seahorse XF^e96 analyser.

CHAPTER 3: Methods and Materials

3.1. Introduction

As discussed in Section 2.7, selected cell lines from ATCC were obtained and cultured according to the specifications given by the supplier. 143B and RD ρ^0 cells were also obtained and cultured under specific conditions. Various parameters were then optimized for each of these cell lines and standard protocols were drawn up so that specific experiments could later be performed, using the Seahorse XF^{e}96 analyser. These methods were all novel for the laboratory at which they were performed and will thus be described in detail in this chapter. Fresh blood was obtained from selected ME patients and healthy controls, in order to isolate and store blood platelets. Blood from patients suspected to harbour one or more of the three mtDNA patients was used for NGS (this will not be discussed in detail in this chapter) to confirm the heteroplasmy level of these mtDNA variants. MutPred scores were also obtained from NGS that had been previously (as well as during this study) performed on all patients. The ρ^0 cells were fused with these patient blood platelets to form cybrids. A test run was first performed, and after confirming that the protocol was successful, cybrids were created for all of the patients. After confirming successful mtDNA transfer to the cybrids, using PCR-RFLP haplogroup analyses, these cybrids were then analysed in batches on the Seahorse XF^{e}96 analyser, using the protocols that had been previously optimized. The RMCN was also determined for each cybrid cell line using real-time PCR and will be reported in this chapter, but since the optimization of the real-time PCR method was performed in a prior study, it will not be discussed here in detail. Various bioenergetic parameters were then calculated using the data obtained from the Seahorse XF^{e}96 analyser and statistical analyses were performed.

3.2. Patients and ethics

Ethical approval had previously been obtained from the NWU (approval number NWU 00 102-12-S1). Prior to this study, researchers at the CHM (NWU) detected three known pathogenic mtDNA variants, using NGS in 14 cases in a Caucasian cohort of 97 patients from South Africa and the UK diagnosed with ME: m.7497G>A, m.9185T>C and m.10197G>A (unpublished data). The current study focused only on the South African patients, where 18 of a possible 41 patients clinically presenting with ME symptoms were selected based on their haplogroups and accessibility. All patients were female, between the broad age category of 18 to 66 and were clinically assessed for ME by answering a medical symptom questionnaire (MSQ), and the Piper Fatigue Scale (PFS) questionnaire. Non-European haplogroups (N, M and L) were excluded from the study, while the European haplogroups U, H, J, T and R were included. Of the 18 patients that were selected, six cases (all with the U5 haplogroup) had been found to have one

or more of the three pathogenic mtDNA variants present. An additional seven subjects were also included in the study as healthy controls. These seven subjects were selected using the MSQ and PFS questionnaire to ensure that they presented with no ME symptoms, as well as according to their haplogroups (same as ME patients) and gender (female). The haplogroups along with the corresponding number of patients and controls is shown in Table 3.1.

Table 3.1: Allocation of patients with different haplogroups

Haplogroup	Number of Cases	Sample Numbers
Patients clinically diagnosed with ME:		
U5 (with mtDNA variants)	6	SA5, SA6, SA11, SA25, SA26, SA36
U	2	SA1, SA19
R	1	SA16
J	1	SA35
H	7	SA7, SA9, SA12, SA20, SA23, SA24, SA39
T	1	SA31
Healthy controls:		
U	3	HC1, HC2, HC3
H	2	HC6, HC7
J	2	HC4, HC5
Total	*25*	

Factors such as gender and age were not applicable in this study, since mtDNA alone was used from patients and controls, and these factors were thus not mentioned here in detail or entirety.

3.3. Materials

Cell lines obtained and purchased from ATCC (Manassas, Virginia, USA) included the following (with the cell type and catalogue number included in brackets): 143B (human osteosarcoma, CRL-8303), RD (human rhabdomyosarcoma, CCL-136), SH-SY5Y (human neuroblastoma, CRL-2266), C2C12 (mouse myoblast, CRL-1772), HEPG2 (human hepatocellular carcinoma, HB-8065) and A549 (human lung carcinoma, CCL-185). 143B ρ^0 and RD ρ^0 cells were obtained as generous gifts from Prof. JAM Smeitink (Radboud Nijmegen University Medical Centre, Nijmegen, The Netherlands) and Prof. Lodovica Vergani (University of Padova, Department of Neurosciences, Padova, Italy), respectively.

Reagents used for cell culture and for the creation of cybrids were as follows: Dulbecco's Modified Eagle Medium (DMEM, 41966052), DMEM containing high glucose, no glutamine and no calcium (21068028), advanced MEM (12492021), F12 medium (21765029), F12 Kaighn's medium (F12K, 21127022), penicillin:streptomycin (15140122), L-glutamine (25030081), GlutaMAX (35050038), sodium pyruvate (11360039) and trypsin (15400054) were obtained from Gibco®, purchased from Thermo Fisher Scientific™, Fairland, South Africa. Fetal Bovine

Serum (FBS, BC/S0615-GI) was obtained from Biochrom, purchased from The Scientific Group, Randburg, South Africa. Glucose solution (G8644), uridine (U3003), 5-bromo-2'-deoxyuridine (BrdU, B5002), phosphate buffered saline (PBS, P4417), DMEM (D5030), phenol red (P0290), polyethylene glycol (PEG, 81210), DMSO (D2650) and LookOut Mycoplasma PCR Detection Kit (MP0035) were purchased from Sigma Aldrich, St. Louis, USA.

Reagents obtained and purchased from Seahorse Bioscience (North Billerica, Massachusetts, USA) include: XF calibrant (100840-000), XF Cell Mito Stress Test Kit (103015-100) and XF^e96 flux pack (102416-100).

In Section 3.9, the O'RangeRuler 50 bp (SM0613) and the enzymes used were NlaIII (FD1834), AluI (FD0014), DdeI (FD1884), BstNI (FD0554) and HinfI (FD0804) and they were all obtained from Fermentas (Vilnius, Lithuania), purchased from Inqaba Biotec, Pretoria, South Africa. The KAPA blood PCR mix was obtained from KAPA Biosystems, purchased from Lasec SA (Cape Town, South Africa). The GelRed Nucleic Acid Gel Stain was obtained from Biotium, purchased from Anatech (Johannesburg, South Africa). The oligonucleotide forward and reverse primers for fragments SC-B, SC-C, SC-D, SC-F, SC-G and SC-H, as originally described by Taylor *et al.* (2001) were obtained from Inqaba Biotec (sequences are shown in Tables 3.2 and 3.3, in Sections 3.6 and 3.9.1 respectively).

3.4. Cell culture conditions

Each cell line was cultured according to the specifications given by ATCC. All cell lines were cultured in medium, supplemented with 10 % (v/v) FBS, 100 units/mL penicillin and 100 µg/mL streptomycin, and incubated at 37°C in 5% CO_2. 143B, RD and C2C12 cells were cultured in DMEM, with the addition of 100 µg/mL BrdU to the 143B medium. SH-SY5Y cells were cultured in 1:1 (v/v) advanced MEM:F12, HEPG2 cells in advanced MEM, and both were supplemented with 2 mM L-glutamine. The A549 cells were cultured in F12K medium. When culturing ρ^0 cells, 50 µg/mL uridine was added to the medium and it was also essential to ensure that the medium contained 1 mM sodium pyruvate as explained in Section 2.5.3. The RD ρ^0 cells were cultured in 30% (v/v) FBS and were supplemented with 6 mM L-glutamine. During the sub-culturing process, all cells were trypsinized using PBS (0.01 M phosphate buffer, 0.0027 M potassium chloride and 0.137 M sodium chloride, pH 7.4) and 1x trypsin-EDTA (0.5 % w/v trypsin-EDTA in H_2O). All cell lines were cryopreserved in their cell growth media, supplemented with 5% (v/v) DMSO, with the exception of the 143B and 143B ρ^0 cells which were cryopreserved in 90% (v/v) FBS and 10% (v/v) DMSO. All cells were tested for mycoplasma contamination, using the Lookout Mycoplasma Detection Kit from Sigma Aldrich.

3.5. Bioenergetics analyses using the Seahorse XF^{e}96 analyser – *Objective 1*

Specific conditions had to be optimized before performing any bioenergetics analyses on new cell lines. These conditions varied depending on the aim and type of analysis that would be performed, but certain standard conditions could be optimized for each cell line. In this section, the basic protocol for any Seahorse XF^{e}96 analyser experiment was first described, followed by the protocol to be used when optimizing the standard conditions for a new cell line. As only OXPHOS function was investigated in this study, the conditions described here are targeted to the parameters for OXPHOS function (i.e. Mito Stress test from Seahorse Bioscience).

3.5.1. Standard bioenergetics analysis procedure for the Seahorse XF^{e}96 analyser

The standard XF analysis required at least two days. The first day involved the design of a new protocol, using version 2.2 of the Seahorse Wave software (Seahorse Bioscience), hydration of the sensor cartridge and the seeding of the cells into a 96-well microtiter Seahorse cell culture plate. On the second day, unbuffered assay medium was prepared, cell culture medium was replaced with the unbuffered assay medium, the injectable compounds were prepared and loaded into the ports of the sensor cartridge, and finally the analysis was conducted using the XF analyser. The methods and reagents used were in accordance with the instructions given by the supplier (www.seahorsebio.com). The standard assay design template used for planning all XF analyser experiments is shown in Appendix A. The Seahorse Wave software analyses the data using an algorithm (Gerencser *et al.*, 2009) that corrects for oxygen diffusion and background noise, to obtain more accurate OCRs.

The unbuffered assay medium stock was prepared by autoclaving 1L of ddH_2O (distilled H_2O) and then dissolving one bottle of DMEM powder (Sigma Aldrich) and 1.85 g/L sterile-filtered NaCl into the autoclaved H_2O. The following were also added: 2 mM GlutaMAX, 3 mg/L phenol red and 0.85 mM NaOH. This was stored at 4°C for up to 3 months. The Mito Stress kit reagents (oligomycin, FCCP, rotenone and antimycin A), in powdered form, were reconstituted with DMSO to obtain a final concentration of 2.5 mM for each compound, followed by aliquoting and storage at -20°C.

DAY 1

To hydrate the sensor cartridge, 200 µL XF calibrant was added to each well of the utility plate (a plate which has the same design as the cell culture plate but which is used solely for hydrating the sensor cartridge), and the sensor cartridge was then lowered onto the utility plate so that all sensors were immersed in calibrant. The sensor cartridge and utility plate were then placed in a non-CO_2 incubator for 24 hours. The XF analyser was switched on 3-24 hours prior to the actual analysis in order to allow the temperature to equilibrate to 37°C.

Cells were harvested by trypsinization and re-suspended in the cell growth medium. To 900 µL PBS, 100 µL of the cell suspension was added and counted using the Sceptor 2.0 Handheld Cell Counter (60 µM tips, Merck Millipore). Growth medium was then added to the cell suspension to obtain the appropriate cell concentration so that when seeding 80 µL of cell suspension per well, the correct cell seeding density was obtained. The four corner wells were filled with medium only (no cells), for background correction. The cell culture plate was left in the laminar flow cabinet for one hour to enhance even cell dispersal and to minimize edge effects due to a temperature gradient. The cells were then incubated at 37°C in a CO_2 incubator for 24 hours before being analysed.

DAY 2

Approximately 150 mL unbuffered assay medium was prepared per 96-well microtiter plate, by supplementing the stock unbuffered assay medium with sodium pyruvate and glucose, at concentrations optimized for each cell line. This assay medium was then warmed at 37°C after which the pH was adjusted to 7.4 using NaOH.

After the seeded cells had been incubated for 23 hours, the cell culture medium was removed and replaced with the unbuffered assay medium. This was done using the XF prep station, an automated instrument capable of washing the cells in a 96-well microtiter Seahorse cell culture plate and delivering precise final volumes of media to each well. The media, H_2O and 'clean' bottles were filled with assay media, ddH_2O and 70% ethanol, respectively. The manifold was firstly primed with "Clean" and then with "H_2O". Thereafter, the media change was performed, which involved priming the manifold with assay medium followed by two aspiration and dispense cycles (200 µL assay media was dispensed each time). Finally there was a third aspiration and dispense cycle which left each well with 175 µL assay medium, as set by the user. The cell culture plate was then incubated in a non-CO_2 incubator for one hour, before being inserted into the XF analyser. Unbuffered assay medium and a non-CO_2 incubator were used to allow the pH of the assay medium to reach equilibrium and to de-gas the plate (to allow CO_2 diffusion from the plate, assay media and cells) for accurate ECAR measurements.

The injectable compounds were then prepared – oligomycin, FCCP, rotenone and antimycin A. These compounds were added to the assay medium, to obtain the appropriate concentration, and then loaded into the injection ports of each well at 25 µL per port (including background correction wells and any wells not containing cells, because the compounds are pneumatically injected using compressed air). The loaded sensor cartridge and utility plate were then placed into the XF analyser and the protocol was initiated so that calibration could begin. Once calibration was complete (approximately 25 minutes), the utility plate was ejected and the cell

culture plate was then loaded into the XF analyser for the assay to run. The assay consisted of four steps, as described in Section 2.6.3: A basal reading, oligomycin injection, FCCP injection and finally rotenone and antimycin-A injection. Each of these four steps consisted of three cycles of 3 minutes mix, and 3 minutes measure. There were thus 12 measurements in total (as depicted on Figure 2.6), three replicate measurements per basal and injection readings.

3.5.2. Optimization of Seahorse XF^{e}96 analyser conditions

Certain XF analyser conditions had been optimized for the RD and A549 cell lines in previous studies performed under supervision of the author (Kenosi, 2014; Mereis, 2014). Selected data from these studies was used in the present study for further optimization. For each new cell line, the cell seeding density per well and the oligomycin concentration were optimized first. A range of four cell seeding densities were selected, based on literature and recommendations by Seahorse Bioscience. Four oligomycin concentrations were selected: 0, 0.5, 1 and 2 µM. The plate design is shown in Figure 3.1a.

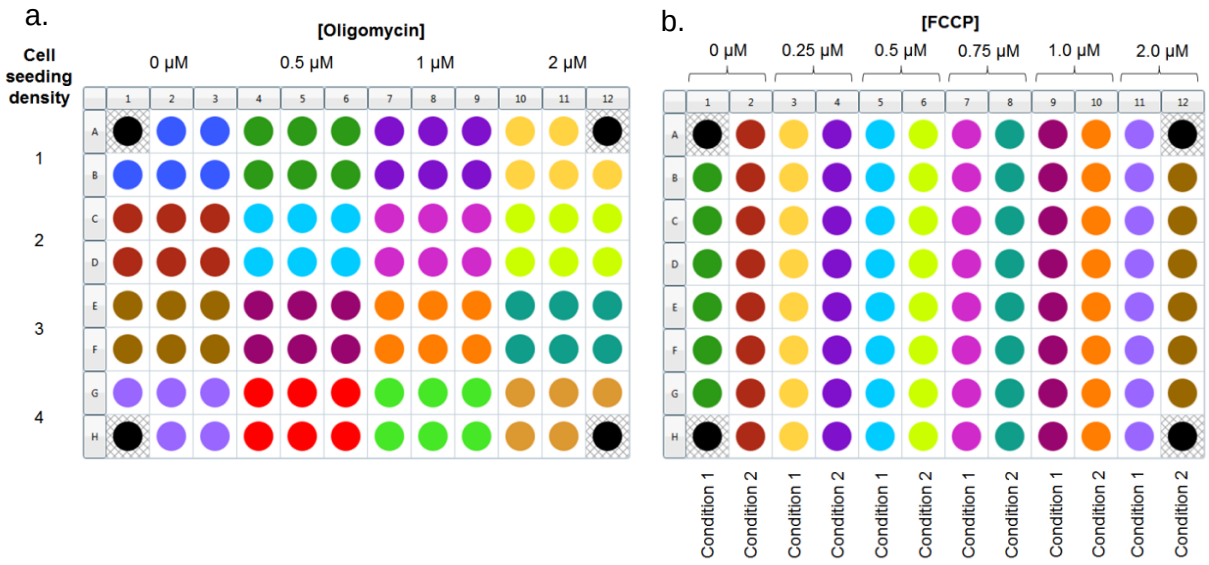

Figure 3.1: Micro-titer (96-well) plate design for optimization of (a) cell seeding density and oligomycin concentration and (b) FCCP concentration on two separate plates. (a) On day 1, four different cell seeding densities were selected for cell seeding (in rows A and B cells were seeded at density 1, rows C and D at density 2, etc.) and on day 2 four different oligomycin concentrations were selected and loaded into port A of the sensor cartridge (rows 1-3 were loaded with assay media only, rows 4-6 with 0.5 µM oligomycin, etc.). (b) On a separate plate on day 2 (all wells contain the same cell seeding density and oligomycin concentration), six FCCP concentrations were selected and loaded into port B of the sensor cartridge (rows 1 and 2 were loaded with assay media only, rows 3 and 4 with 0.25 µM FCCP, etc.), and if required, an extra condition could also be tested. Each colour represented a specific treatment combination.

The following condition to be optimized was the FCCP concentration. Six FCCP concentrations were selected, for example: 0, 0.25, 0.5, 0.75, 1 and 2 µM. Since there were 16 replicates per FCCP concentration, there was space on this plate (shown in Figure 3.1b) to compare any two other conditions as well (e.g. two different cell seeding densities, two different oligomycin concentrations, two different cell lines, etc.).

The final conditions to be optimized were the concentrations of glucose and sodium pyruvate in the assay medium. Typically, the pyruvate concentration was kept at 1 mM, while the glucose concentration ranged between 0 and 25 mM (as shown in Figure 3.2). As with the FCCP optimization, there was sufficient space on the plate to optimize two other conditions as well. Plates that were analysed prior to assay media optimization (shown in Figure 3.1), were supplemented with 5 mM glucose (physiological level) and 1 mM pyruvate (supraphysiological level since the physiological level in blood is usually 200 µM) (Dranka *et al.*, 2011).

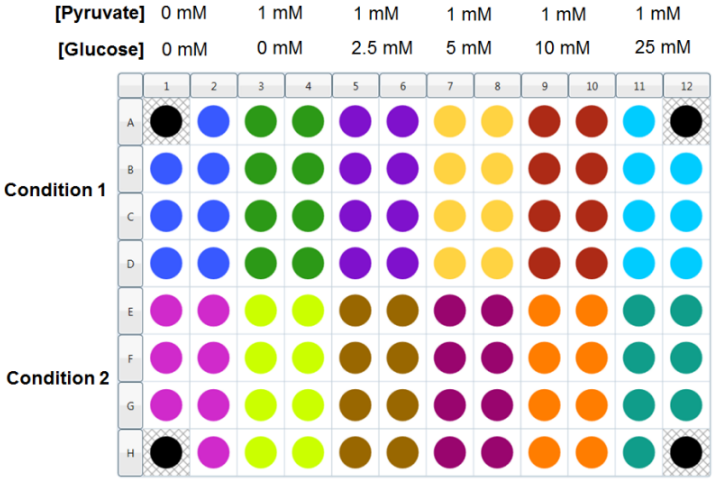

Figure 3.2: Micro-titer (96-well) plate design for optimization of glucose and pyruvate concentrations in assay media. An additional condition could also be optimized on this plate if desired. Assay media was supplemented with 1 mM pyruvate in rows 3-12 (no pyruvate was added to rows 1 and 2), and glucose concentrations ranging from 0-25 mM (rows 1-4 contained no glucose, while rows 5 and 6 contained 2.5 mM glucose, etc.). Each colour represented a different combination of treatments. All other conditions were kept on the plate.

3.6. Next-generation sequencing of the whole mtDNA genome and mutational load analysis using MutPred scores – *Objective 2*

Before the onset, as well as during this study, the full mtDNA sequence of the U5 patient group (who putatively contained the three pathogenic mtDNA variants) and the healthy control group (introduced during this study) were sequenced using the Ion Torrent PGM (Life Technologies). DNA isolated from the patients' blood (obtained in Section 3.7.1) and DNA isolated from cybrid cells obtained in Section 3.11, was used to confirm mtDNA transfer (along with mtDNA variant

transfer) from the patient blood to the cybrid cells, as well as to confirm the heteroplasmy level of the three mtDNA variants in the U5 patient group and the mutational load. This data also existed for all other ME patients in this study cohort as they had been sequenced in a previous study. Minimal detail will be given here as the methods and bioinformatics used to identify the variants and allele frequencies, were done with the assistance of Marianne Pretorius (PhD student, CHM, NWU) and according to protocols described by Van der Walt (2012).

After DNA isolation (Section 3.8), the entire mtDNA genome was amplified in two separate reactions to form two overlapping mtDNA fragments, using the primers as shown in Table 3.2. Each 50 µL reaction consisted of 0.2 µL AccuPrime Taq DNA Polymerase high fidelity (12346086, obtained from Invitrogen®, purchased from Thermo Fisher Scientific™, Fairland, South Africa), 1x AccuPrime Buffer I, H_2O (molecular grade), 40 ng DNA and 0.2 µM forward and reverse primers (see Table 3.2). The thermal cycler conditions were set according to the recommendations given by the AccuPrime supplier.

Table 3.2: Sizes of the two overlapping mtDNA fragments produced, using two specific forward and reverse primer pairs for NGS

Fragment	Nucleotide position of forward primer	Nucleotide position of reverse primer	Product size (bp)
1	***SC-H:*** *13539 – 13559* 5'-ATCATACACAAACGCCTGAGC-3'	***SC-C:*** *6200 – 6220* 5'-GGTAAGAGTCAGAAGCTTATG-3'	9250
2	***SC-D:*** *6113 – 6133* 5'-AATACCCATCATAATCGGAGG-3'	***SC-G:*** *8017 – 7996* 5'-TTGACCTGTTAGGGTGAGAAGA-3'	7546

Table adapted from Taylor *et al.* (2001).

Post-PCR amplicon clean-up was thereafter performed using the PureLink Pro 96 PCR Purification Kit obtained from Invitrogen®, purchased from Thermo Fisher Scientific™, Fairland, South Africa. The two fragments for each patient were then combined in equimolar amounts at a ratio of 5.6:4.9 (Fragment 1:Fragment 2). This was then followed by an automated library preparation procedure and sequencing, at an average base coverage of ~2000x on an Ion Torrent personal genome sequencing (PGM) platform at the NWU, Potchefstroom.

The bioinformatics used, involved the formatting and aligning of high quality mtDNA sequence data to the reference mtDNA genome (GenBank NC_012920.1), using Torrent Suite software and the generation of a variant caller file that was used for annotation. Haplogroups were assigned using Mitomaster (Lott *et al.*, 2013).

As discussed in Section 2.3.4, a modified mutational load analysis (adjusted MutPred score) was also performed, to assess whether or not any association was found between the cumulative effects of non-synonymous variants and ME. This was done using the variant caller

file obtained after sequencing and reference sequence (rCRS) alignment. This variant file listed all variants and their consensus sequences, and was then used to remove all variants with an allele frequency (heteroplasmy level) of <50%. A list of all known non-synonymous variants in the mitochondrial genome, and their corresponding MutPred scores, were obtained using the MutPred program (mutpred.mutdb.org/about.html). This list was compared to the variants obtained for each subject, and any variants not found on the MutPred list were removed. All remaining variants for each subject were then assigned MutPred scores. Thereafter, the sum of all MutPred scores for each subject was calculated and divided by the number of variants per subject, to obtain an "adjusted MutPred score" for the whole mtDNA genome of each subject. To obtain the adjusted MutPred score for specific mitochondrial complexes or genes, the same procedure was followed using variants present only in the relevant gene or complex. Each MutPred score (ranging between 0 and 1) represented the probability that the amino acid substitution was pathogenic or disease-causing, where 0 indicated no pathogenicity and 1 indicated maximum pathogenicity. Scores >0.5 were referred to as "actionable hypotheses", while scores >0.75 were referred to as "confident hypotheses" (Li *et al.*, 2009).

3.7. Development of cybrid cells – *Objective 3*

The isolation of blood platelets and development of the cybrid cells was performed using the method originally described by King and Attardi (1989) and later modified by Chomyn (1994), as discussed in Section 2.5.3.

3.7.1. Isolation of blood platelets

Four EDTA vials of blood were collected from all healthy controls and patients, all with known mtDNA haplogroups, and processed within a few hours. The volume of blood was determined and 1/9th volume 10 x citrate in physiological saline (NaCl 0.15 M and trisodium citrate 0.1 M, pH 7.0) was added. The two were gently mixed by inversion to avoid platelet activation caused by vigorous mixing. The mixture was centrifuged at 200 x g for 20 min. Of the supernatant (platelet-rich plasma), ~75% was collected whilst leaving at least 3 mm of plasma above the red blood cells in order to prevent the inclusion of any red or white blood cells. The collected plasma was centrifuged at 1500 x g for 20 min at 15°C. The supernatant was discarded and the pellet containing the blood platelets was re-suspended in 2 mL physiological saline (0.15 M NaCl and 0.015 M Tris-HCl buffer, pH 7.4). After all the clumps had been broken up by gentle pipetting, physiological saline was added to a final volume of 11 mL and the blood platelet suspension was then divided equally into two 15 mL centrifuge tubes. To each centrifuge tube, 0.785 mL DMSO and 1.57 mL FBS was added and the tubes were then frozen at -80°C (Chomyn, 1994).

3.7.2. Fusion of blood platelets and ρ^0 cells

A 42% (w/v) PEG solution was prepared by autoclaving 2.1 g PEG 1500 for 15 min and then adding 0.5 mL DMSO and 2.4 mL DMEM minus Ca^{2+} before the PEG began to solidify. This solution was then stored at 37°C until it was ready to be used.

One 15 mL centrifuge tube containing 4.5 – 5.5 mL platelet suspension for each patient, was thawed at 37°C and then centrifuged at 1500 x g for 15 min at 15°C. While the blood platelets were being centrifuged, the ρ^0 cells were washed with PBS and then detached from the 25 cm^2 flask using 1x trypsin. DMEM (2-3 mL) supplemented with 5% (v/v) FBS was then added to the ρ^0 cells to inactivate the trypsin, and the ρ^0 cells were counted using the Sceptor 2.0 Handheld cell counter (Merck Millipore). The ρ^0 cells were pelleted by centrifugation at 180 x g for 5 min and then re-suspended in DMEM minus Ca^{2+} at a density of 5 x 10^5 cells/mL.

Once the blood platelets had completed the 1500 x g centrifugation step, almost all supernatant was carefully removed, leaving behind 50-100 µL over the pellet. Of the ρ^0 cell suspension containing 5 x 10^5 cells/mL, 2 mL was gently added to the pellet of blood platelets without disturbing them. The ρ^0 cells were then centrifuged onto the platelet pellet at 180 x g for 10 min. All supernatant was then removed and 100 µL of the 42% (w/v) PEG solution was added to gently re-suspend the mixture of platelets and ρ^0 cells. Thereafter, 10 mL ρ^0 cell medium (DMEM supplemented with 10%, v/v, FBS, 100 units/mL penicillin, 100 µg/mL streptomycin and 50 µg/mL uridine) was added and the cells were mixed into the medium. The 143B ρ^0 cell medium also contained 100 µg/mL BrdU. Half of the cybrid cell suspension (5 mL) was transferred to a 25 cm^2 flask and incubated at 37°C with 5% CO_2. The remaining cybrid cell suspension was centrifuged at 200 x g for 5 min, the supernatant removed and the cells suspended in 1 mL cryopreservation medium for both the 143B (DMEM containing 10%, v/v, DMSO and 20%, v/v, FBS) and RD cybrid cells (DMEM containing 10%, v/v, DMSO and 30% FBS). The cryovial was then stored at -80°C.

After 2-3 days of incubation, the medium in the plates was replaced with selective medium (DMEM supplemented with 10%, v/v, FBS, 100 units/mL penicillin, 100 µg/mL streptomycin, and 100 µg/mL BrdU for the 143B cells) so that only those cells that were true cybrids were able to continue growing and any ρ^0 cells still remaining would die, since they were pyruvate and uridine auxotrophs. The selective medium was replaced every 3-5 days. After approximately two weeks of the cells being cultured in selective medium, they were further cultured until the required quantities of cells were obtained to be analysed as described in Section 3.11 (Chomyn, 1994). Cells were also frozen away for DNA analysis by centrifuging at 500 x g for 5 min, removing the supernatant and storing them at approximately -20°C.

3.8. DNA isolation and quantification

DNA was isolated from blood and cells that had been frozen in Sections 3.7 and 3.11, according to the standard protocol for human or animal tissue and cultured cells, and the support protocol for genomic DNA and viral DNA from blood samples, from Macherey-Nagel's NucleoSpin® Tissue kit (Macherey-Nagel**,** Düren, Germany).

Cell lysis was achieved by re-suspending the cells in 200 µL Buffer T1 (which contains an alkaline-SDS detergent), while blood samples did not require pre-lysis and 200 µL blood could be used as is for each patient. Hereafter, both blood and cell samples were treated in the same way. Of the Proteinase K, 25 µL was added along with 200 µL Buffer B3 (which contains a high concentration of chaotropic salts to cause precipitation). Samples were incubated at 70°C for 10-15 min. To the sample, 210 µL ethanol (96-100%) was then added in order to adjust the DNA binding conditions and to allow DNA binding to the silica column. After robustly vortexing the sample, it was transferred into a NucleoSpin® Column. The column was centrifuged for 1 min at 11000 x g after which the flow-through was discarded. Contaminants were then removed by washing the silica column in two separate steps. Buffer BW (500 µL) was first added and centrifuged at 11000 x g for 1 min. After discarding the flow-through, 600 µL Buffer B5 was added to the column and once again centrifuged at 11000 x g for 1 min. The column was then placed into a clean collection tube and the silica membrane was then dried by centrifuging the column at 11000 x g for 1 min. The NucleoSpin® Column was placed into a 1.5 mL microcentrifuge tube and 100 µL pre-warmed (70°C) Buffer BE (slightly alkaline with a low concentration of chaotropic salts) was added to the column which was centrifuged at 11000 x g for 1 min to elute the pure DNA.

The DNA was quantified using the NanoDrop® ND100 spectrophotometer (NanoDrop Technologies, Thermo Fisher Scientific, USA) which determines the concentration of the DNA at a wavelength of 260 nm. All DNA was then diluted to 2.5 ng/µL in PCR-grade H_2O.

3.9. Haplogroup determination using the Polymerase Chain Reaction (PCR) and Restriction Fragment Length Polymorphism (RFLP) approach – *Objective 3*

3.9.1. Principle of haplogroup determination using PCR-RFLP approach

All healthy controls and patient haplogroups were determined in a previous study when the entire mtDNA genome was sequenced to determine whether or not any one or more of the three mtDNA variants were present and at which allele frequencies (heteroplasmy levels), as discussed in Section 3.6. The haplogroups (as explained in Section 2.3.2) of all the healthy control and ME patient cybrids were determined using PCR-RFLP in order to confirm mtDNA transfer from the blood platelets to the ρ^0 cells.

DNA was isolated from all the healthy controls and patient cybrid cells according to the protocol described in Section 3.8. The PCR-RFLP approach used in this section had been previously described (Smit, 2009) and it involved the PCR amplification of specific fragments of the mtDNA genome, followed by their digestion, using certain restriction enzymes. If certain haplogroup-defining SNPs were present in those mtDNA fragments, they were cut by specific restriction enzymes. The haplogroup could then be determined based on whether or not a specific mtDNA fragment was cut by a specific restriction enzyme (Ghezzi *et al.*, 2005). Table 3.3 indicates the sizes of the mtDNA fragments that were produced in the PCR reaction as well as the nucleotide sequences of the forward and reverse primers used for each fragment. Table 3.4 shows the restriction enzymes that were used to cut each mtDNA fragment, at what position of the mtDNA genome they cut and the haplogroup obtained according to whether or not the restriction enzyme cut a specific mtDNA fragment. Figure 3.3 summarizes Tables 3.3 and 3.4.

Table 3.3: Sizes of the PCR fragments produced using specific forward and reverse primer pairs targeting areas on the mtDNA genome for haplogroup identification

Fragment	Nucleotide position of forward primer	Nucleotide position of reverse primer	Product size (bp)
B	*2364 – 2386* CTGACAATTAACAGCCCAATATC	*4249 – 4228* GAATGCTGGAGATTGTAATGG	1886
D	*6113 – 6133* AATACCCATCATAATCGGAGG	*8017 – 7996* GAGTACTACTCGATTGTCAACG	1905
F	*9767 – 9784* CATTTCCGACGGCATCTA	*11748 – 11727* GCTAGGCAGAATAGTAATGAGG	1982
G	*11614 – 11635* CATTGCATACTCTTCAATCAGC	*12350 – 12309** GTGTGCATGGTTATTACTTTTATTTGG AGTTGCACCAAGATT	736
H	*13539 – 13559* ATCATACACAAACGCCTGAGC	*15431 – 15409* TGCTAAAGGTTAATCACTGCTG	1893

* Mismatched oligonucleotide used to create a restriction site for HinfI.
Table adapted from Taylor *et al.* (2001).

Table 3.4: Diagnostic RFLP markers for European haplogroup identification

	PCR Fragment	*B*	*D*	*F*	*G*	*H*
Haplogroup	**Restriction enzyme**	*Nla III* *4216*	*Alu I* *7025*	*Dde I* *10394*	*Hinf I* *12308*	*BstN I* *13704*
J		Yes		Yes		No
H			No	No		
U			Yes	No	Yes	
T		Yes	Yes	No	No	
Others DdeI -		No	Yes	No	No	

Only haplogroups and enzymes relevant to this study are shown. Table adapted from Ghezzi *et al.* (2005).

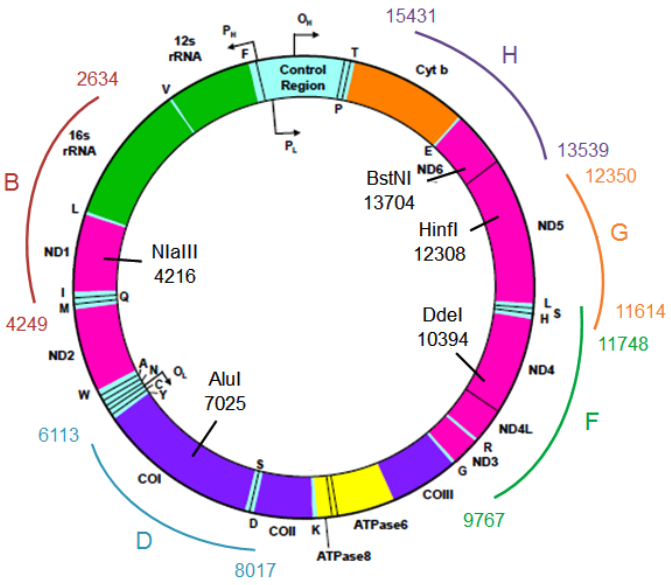

Figure 3.3: Schematic representation of the mitochondrial genome with the five mtDNA fragments (B, D, F, G and H) produced by the PCR reaction shown around the outside of the mtDNA genome, and each of the restriction enzymes (along with the position for where they cut each mtDNA fragment) shown along the inside of the mtDNA genome. Figure not drawn to scale and adapted from MITOMAP (Lott *et al.*, 2013).

3.9.2. PCR reaction and gel electrophoresis

For a 25 µL PCR reaction, the following reagents were used: 1 x KAPA blood PCR mix, H_2O (molecular grade), 0.8 µM forward and reverse primers and 5 ng DNA. The primers used were for fragments B, D, F, G and H, as shown in Table 3.3. The PCR cycle included the following steps: Incubation at 95°C for 10 min; 30 cycles of 95°C for 1 min, 55°C for 1 min and 72°C for 2 min; and finally, incubation at 72°C for 5 min. To test whether or not PCR fragments were successfully produced, PCR mixes were loaded along with 1x Loading Dye Solution (6x: 10mM Tris-HCl pH 7.6, 0.03% bromophenol blue, 0.03% xylene cyanol FF, 60% glycerol and 60 mM EDTA) onto a 1 % (w/v) agarose gel in 1 x TAE buffer (40 mM Tris-acetate and 1 mM EDTA, pH 8.0), containing 1x GelRed Nucleic Acid Gel Stain. As a DNA size marker, bacteriophage λ DNA sample treated with HindIII was also loaded onto the gel. The samples were then run at ~7 V/cm. The gel was photographed under UV exposure with a G:Box gel-documentation system from Syngene™, using GeneSys™ version 1.1.2.

3.9.3. RFLP reaction and gel electrophoresis

For the RFLP analyses, the following reagents were used in a final volume of 25 µl: PCR DNA (10-15 µL), H_2O (molecular grade), 1x FastDigest restriction enzyme buffer (Buffer FD) and 0.5 µL FastDigest restriction enzyme. Each RFLP reaction contained one specific mtDNA fragment and one specific restriction enzyme (as indicated in Table 3.4). The reaction mixtures were

mixed thoroughly and incubated at 37°C for 30 minutes. To identify the fragmentation pattern of each PCR fragment, the samples were run on a 2.5 % (w/v) agarose gel in 1 x TBE buffer (45 mM Tris-borate and 1 mM EDTA, pH 8.0) containing 1x GelRed Nucleic Acid Gel Stain. As DNA size marker, O'RangeRuler (50 bp increments), which contains 6x O'Range Loading Dye (10 mM Tris-HCl pH 7.6, 0.15% orange G, 0.03% xylene cyanol FF, 60% glycerol, and 60 mM EDTA), was used. Samples were loaded with 1x O'Range Loading Dye, run at ~7 V/cm and visualized and documented as described in Section 3.9.2.

3.10. Determination of Relative mtDNA Copy Number (RMCN) using real-time PCR – *Objective 4*

DNA was isolated (Section 3.8) from cybrid cells that were obtained on the day of cell seeding for the XF analyser (Section 3.11) so that the RMCN, at the time of the XF analysis, could be determined using real-time PCR. This was done by relatively quantifying a nuclear gene (β-globin) and an mtDNA gene (MT-ND2) using real-time PCR. The $2^{-\Delta\Delta CT}$ method (Applied Biosystems User Bulletin No. 2, P/N 4303859) was used to calculate the RMCN in this study. In order to obtain the $\Delta\Delta C_T$ value, C_T values were obtained from the real-time PCR instrument. The average C_T value was calculated for both MT-ND2 and β-globin, and the average C_T for β-globin was subtracted from the average C_T for MT-ND2. This represented the $\Delta\Delta C_T$ value and could then be substituted into the $2^{-\Delta\Delta CT}$ formula. The final answer after substitution represented the number of mtDNA molecules that existed for each nDNA molecule (Livak & Schmittgen, 2001), and since there are two copies of nDNA within each human cell, this answer was then multiplied by two (Ye *et al.*, 2014). For ρ^0 cells, a value of less than one was expected.

The real-time PCR method used was previously described (Meissner-Roloff, 2009) and optimized (van Dyk, 2013) and the experimental procedure used, was described in the TaqMan Gene Expressions Assay Protocol (P/N 4333458). TaqMan® Gene Expression Assays (20x), containing the two primers (18 µM per primer) and a 6-FAM™ dye-labelled TaqMan® MGB probe (5 µM) in an optimized reaction mix, were obtained from Applied Biosystems and purchased from Thermo Fisher Scientific™ (Fairland, South Africa) for the nuclear β-globin gene (Hs00758889_s1) and the mitochondrial ND2 gene (Hs02596874_g1). Each 20 µL reaction mixture for the two genes was prepared separately as follows: 1x TaqMan® Gene Expression Assay, 1x TaqMan® Gene Expression Master Mix, 5 µL PCR-grade H_2O and 4 µL DNA (2.5 ng/µL).

Each sample was loaded in triplicate for each gene, into a 96-well real-time PCR microplate. The samples were then analyzed in an ABI 7300 real-time PCR system and the C_T values were obtained using version 1.4 of the 7300 System Sequence Detection Software (Applied

Biosystems). The PCR cycling conditions were set to 95°C for 10 min followed by 40 cycles of 95°C for 15s and 60°C for 1 min, where detection occurred after the 60°C for 1 min step.

The PCR efficiency for each of these genes was previously determined (van Dyk, 2013), using the REST software tool (Pfaffl *et al.*, 2002). A PCR efficiency percentage can be obtained using this software where 0% indicates no amplification and 100% represents the exact doubling of the target molecule in one PCR cycle (Bustin *et al.*, 2009). The PCR efficiencies obtained for β-globin and MT-ND2 were 91% and 82%, respectively. Both PCR efficiencies obtained were relatively high, with an almost exact doubling of target molecules (especially in the case of β-globin) in each PCR cycle. Since an alternative quantification option, such as using mtDNA standards, wasn't available in this study, it was decided that this real-time PCR approach would be used.

3.11. Respiration rate determination of cybrids using the Seahorse XF^{e}96 analyser – *Objective 5*

Cybrids created for all 25 patients and healthy controls were analysed on the XF analyser using the protocol described in Section 3.5.1. The following optimized conditions (as determined in Table 4.1, Section 4.2.5) were used for the 143B cybrids: cell seeding density of 13 000 cells/well, oligomycin concentration of 1 µM, FCCP concentration of 0.5 µM and in the assay medium, a glucose concentration of 5 mM and pyruvate concentration of 1 mM. On average, there were five to eight replicate wells per sample. Problems were encountered when culturing the RD ρ^0 cells *(objective 6)* which led to their exclusion from the study, but this will be discussed further in Section 4.7. Plate layout for the XF analyser was designed so that all ME patients were analysed on Plate 1 (Figure 3.4), ME patients with haplogroup U and healthy controls were analysed on Plate 2 (Figure 3.5) and ME patients with non-U haplogroups and healthy controls were analysed on Plate 3 (Figure 3.6). In Figures 3.4, 3.5 and 3.6, the colours refer to cases (case numbers also indicated) on the plate, while the black markers refer to blanks (no cells).

The cybrids cultured in Section 3.7.2 were analysed (as shown in Figures 3.4 - 3.6) at two separate time intervals, three and six weeks after they were developed. Passage numbers for all cybrid cell lines were kept the same at these time intervals: at week 3 they were passage #4 and; at week 6 they were passage #11. At both time intervals, each of these three plates were analysed in duplicate. There were thus 12 plates run in total: Six plates were run at week 3 and six plates at week 6. All six plates were seeded on the same day at each time interval, and duplicate plates were seeded simultaneously.

Cells remaining after seeding for the XF analyser, were centrifuged at 500 x g for 5 min. After the centrifugation step, the supernatant was discarded and the remaining cell pellet was stored at approximately -20°C to be used as described in Sections 3.8, 3.9 and 3.10. Directly after removing each Seahorse cell culture plate from the XF analyser, all assay media was carefully removed from each well (by blotting the plate on paper towels) and the cell culture plate was frozen at -80°C overnight (cell culture plates can be kept frozen for up to four weeks before analysing them) to aid in cell lysis during normalization, as discussed in the following section.

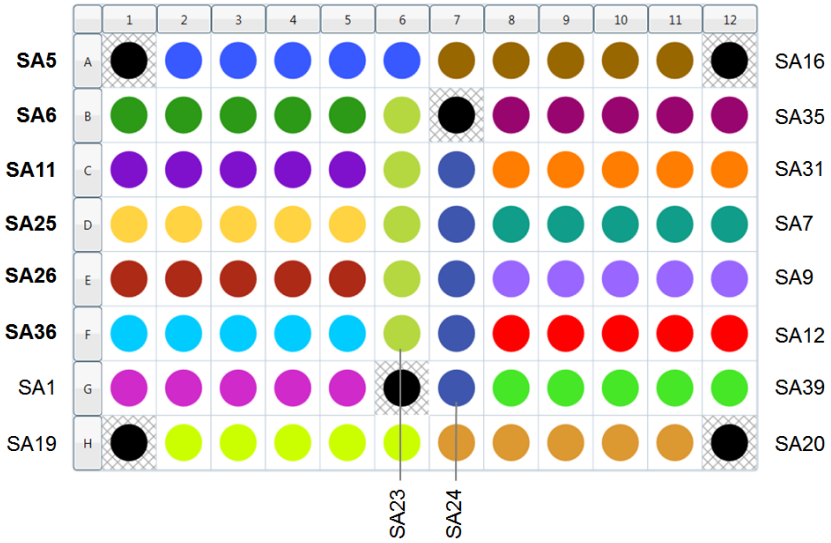

Figure 3.4: Micro-titer (96-well) Plate 1 layout for all ME patients. This allowed for a comparison between patients suspected to harbour the mtDNA variants (in bold) and all other ME patients that did not have the mtDNA variants.

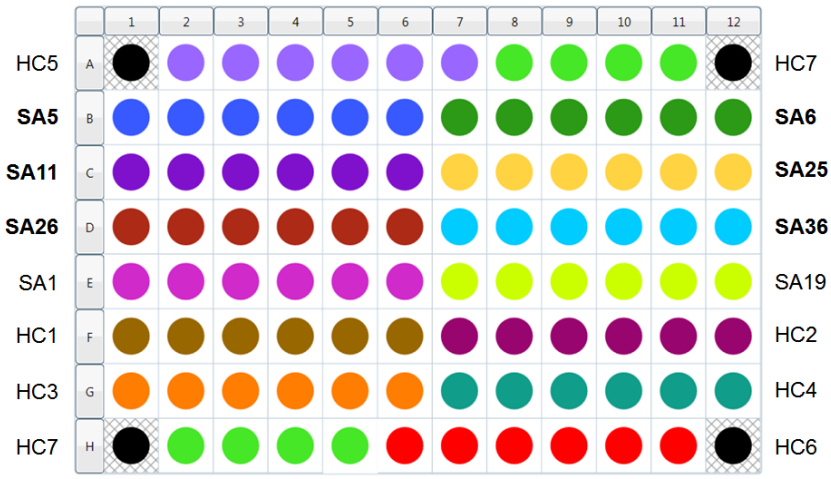

Figure 3.5: Micro-titer (96-well) Plate 2 layout for ME patients with haplogroup U and healthy controls. This allowed for a comparison between ME patients suspected to harbour the mtDNA variants (in bold) and healthy controls who did not have ME.

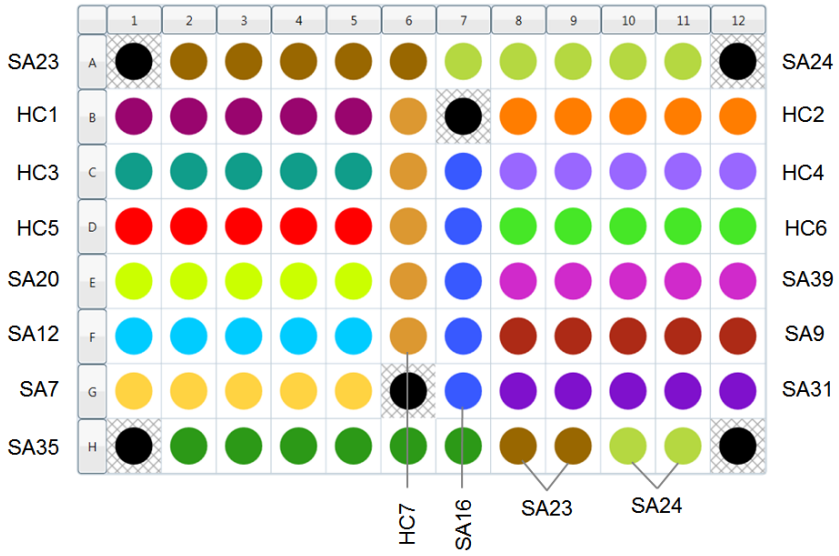

Figure 3.6: Micro-titer (96-well) Plate 3 layout for ME patients with non-U haplogroups and healthy controls. This allowed for a comparison between all other ME patients (without the mtDNA variants) and the healthy controls.

3.12. Normalizing cell DNA content using the CyQUANT Cell Proliferation Assay kit

All Seahorse cell culture plates that had been analysed in Section 3.11, were normalized according to the DNA content per well in order to account for any differences in cell seeding density between wells. This was done using the CyQUANT Cell Proliferation Assay kit (C7026) obtained from Molecular Probes®, purchased from Thermo Fisher Scientific™, Fairland, South Africa. The experimental procedure followed, was in accordance with the instructions given by the supplier (MP07026).

The cell culture plate was allowed to thaw at room temperature while preparing the reagents. In 15 mL nuclease-free distilled H_2O (enough for one 96-well plate), concentrated cell-lysis buffer stock solution was diluted 20-fold and CyQUANT GR stock solution was diluted 400-fold and the solution was kept protected from light. To each well, 150 µL of the CyQUANT GR dye/cell-lysis buffer was added. The sample was incubated at room temperature for 4 minutes, protected from light, and after mixing the sample by gently pipetting up and down, the entire volume was transferred to a black 96-well microplate. The sample fluorescence was then measured at ~480 nm excitation and ~520 nm emission maxima, using a Synergy HT microplate reader (BioTek instruments) and absorbance values were obtained using version 1.11.5 of the Gen5 Data Analysis software (BioTek Instruments). The absorbance values obtained were then entered into the Seahorse Wave software using the normalization function.

3.13. Statistical analyses performed on bioenergetics data – *Objectives 5 and 7*

Statistical analyses were performed on the data obtained in Sections 3.10, 3.11 and 3.12 in order to answer specific questions. For all statistical analyses, version 22 of SPSS Statistics (IBM) was used. The approach used to statistically analyse the data obtained from these sections is summarized in Figure 3.7.

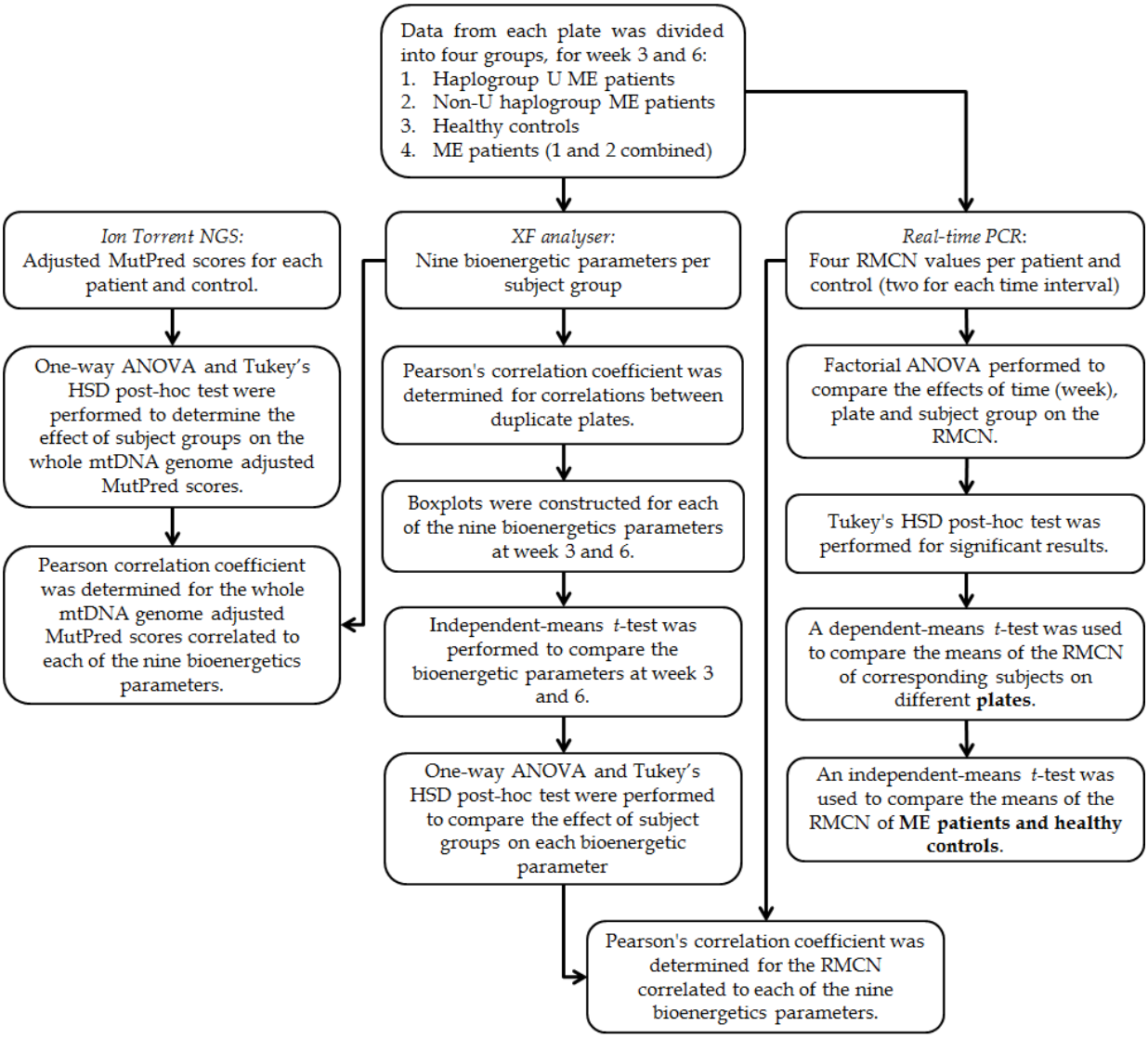

Figure 3.7: Strategy depicting the approach used for statistical analysis of the RMCN results, bioenergetics parameters and whole mtDNA genome adjusted MutPred scores.

Due to the small size of the cohort used in this study, it was not possible to determine whether the sampling distribution was normal or not. Despite this, parametric tests were used for all statistical analyses since numerous statisticians have argued that even if data is non-normally distributed, the *t* and F tests are relatively insensitive to violations of the parametric test assumptions (Blair & Higgins, 1980). For all statistical analyses performed, a p-value of less than 0.05 indicated that a significant difference existed between the groups.

A one-way ANOVA is used to determine whether or not a significant difference exists between the means of three or more independent groups. In Section 4.3.2, a one-way ANOVA was used to compare the MutPred scores of different subject groups (haplogroup U ME patients, non-U haplogroup ME patients, healthy controls and ME patients), and in Section 4.6.3, it was used to compare the OCR values of subject groups for each bioenergetic parameter. Tukey's HSD post-hoc test, a type of student *t*-test, was performed for both of these one-way ANOVAs in order to correct for multiple testing and to determine which groups within the sample differed.

A factorial ANOVA, which allows the influence of two or more factors (as well as their combined effect) on a dependent variable to be tested, was performed on the RMCN results shown in Section 4.5. The main effects of time (week 3 or week 6), plate (1, 2 or 3) and subject group (haplogroup U ME patients, non-U haplogroup ME patients and healthy controls) on the RMCN were studied. Where significant differences were obtained, Tukey's HSD post-hoc test was performed. Where necessary, parametric dependent-means *t*-tests, where the means of two experimental conditions were compared and the same subjects were used for both, and independent-means *t*-tests, where the means of two experimental conditions were compared and different subjects were used for both, were performed (Field, 2009).

All outliers in the bioenergetics data obtained from Section 3.11 were identified using the Tukey method which defines outliers as data points that lay 1.5 interquartile ranges below the first quartile or above the third quartile of the dataset (Tukey, 1977). In Section 4.6.3, boxplots were constructed for each bioenergetic parameter at week 3 and week 6, for each of the four subject groups. The whiskers of the boxplots indicated the minimum and maximum values (the range), while box indicated the interquartile range. The bottom edge of the box was the first quartile while the upper edge of the box was the third quartile, and the line in the middle of the box indicated the median of the data. Outliers (1.5 inter-quartile ranges) were depicted as circles and extreme outliers (3 inter-quartile ranges) were depicted with an asterisk on the boxplots. In Section 4.6.3, an independent-means *t*-test was also performed to compare each of the bioenergetic parameters at week 3 and week 6.

In Sections 4.6.2, 4.6.4 and 4.8, Pearson's correlation coefficient was used to correlate duplicate plates as well as bioenergetics parameters to the RMCN and to the whole mtDNA adjusted MutPred score. It was used to indicate whether or not a significant correlation existed between two variables. The value of the correlation coefficient lay between -1 and 1, where -1 indicated a perfect negative correlation, 0 indicated no correlation and +1 indicated a perfect positive correlation. A p-value of <0.05 provided an indication that the correlation coefficient obtained was statistically meaningful (Field, 2009).

CHAPTER 4: Results and Discussion

4.1. Introduction

In this chapter, the results pertaining to each objective (see Section 2.7) were shown and discussed. Firstly, the optimization results from the XF analyser, for various selected cell lines, were shown, and the optimized conditions discussed. The NGS results were thereafter shown along with the MutPred scores. The results confirming patient haplogroups were provided as proof of mtDNA transfer from patient blood platelets to ρ^0 cells, along with the RMCN for all cybrid cell lines. The bioenergetics parameters obtained using the XF analyser were then analysed and discussed. Lastly, the development of the RD ρ^0 cells and cybrids was discussed and the mutational load of the patients was investigated.

4.2. Bioenergetic respiratory rates obtained from the Seahorse XF^{e}96 analyser during optimization of selected cell lines – *Objective 1*

Although only two of the cell lines optimized were used for the rest of the objectives in this study, it was considered important to evaluate and report the *optimization of extracellular flux conditions* as an objective, by including other cell lines frequently used in bioenergetics investigations. Bioenergetic profiles obtained from each of the selected cell lines (as described in Section 3.5.2) were used to determine the optimized conditions (cell seeding density, oligomycin and FCCP concentrations, and the glucose and pyruvate concentrations in the assay media) for the Seahorse XF^{e}96 analyser. The standard concentration of rotenone and antimycin A used for all XF analyses was 1 µM. Specific measurement numbers (shown in Figure 2.6, Section 2.6.3) were used to determine each of these optimized conditions. Each plate that was analysed had replicate wells for each treatment group. The mean and standard deviations for specific treatments (and specific measurements) were calculated and outliers were identified using the Tukey method, described in Section 3.13. Optimization plates were not normalized using the CyQUANT Cell Proliferation Assay Kit, since the conditions being optimized could be relatively determined. Each cell line was shown on the graphs in a different colour and the data for each cell line was obtained from separate plates that were run on the XF analyser.

4.2.1. Cell seeding density

As shown in Figure 3.1a (Section 3.5.2), four different cell seeding densities were present on the first plate that was analysed for the optimization of each cell line. Optimized cell density was first assessed by looking at the cell confluency, ensuring that cells were evenly distributed within each well, and that wells were consistent within a plate. Prior to oligomycin injection, the two

rows seeded for each selected cell seeding density were identical. Since the measurement #3 basal reading was used to calculate the mean OCR value for each of the four cell seeding densities, all wells from the two rows of each cell seeding density were used, rather than the six replicates shown for each treatment in Figure 3.1a. A scatterplot was drawn (Figure 4.1) where the cell seeding densities were plotted against the mean OCR values to determine the cell seeding density that provides the maximal basal respiration and which remains within the range of 20–160 pmol/min. The ECAR should range from 10–190 mpH/min, but since all ECAR values did fall within this range, they will not be shown here (Seahorse Bioscience, www.seahorsebio.com). A second identical scatterplot (Figure 4.2) was drawn, but the OCR values were normalized (using the Seahorse Wave software) according to the cell seeding density per well. These normalized OCR values were expected to remain constant with increasing cell seeding density.

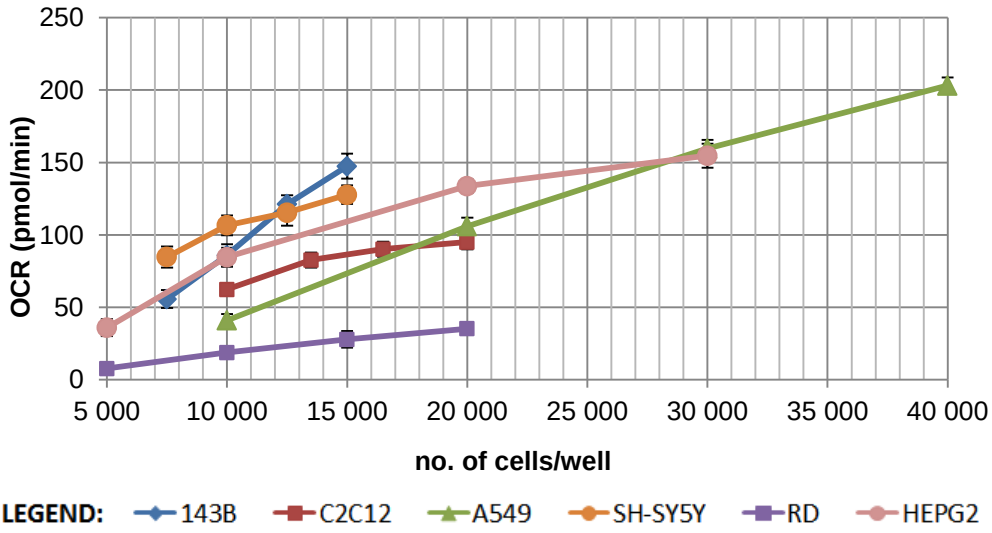

Figure 4.1: Graph of basal respiration (measurement #3) showing the relationship between cell seeding density and OCR for six cell lines. Each data point represented the mean OCR (N = 22-24) ± standard deviation.

It is well-known that cells undergo three phases during cell culture, namely: the lag phase, the exponential phase and the stationary phase. Immediately after reseeding, cells undergo a period of zero cell growth as they recover from trypsinisation and prepare to re-enter the cell cycle. Thereafter, they undergo exponential cell growth with cell population doubling. As the culture surface becomes over confluent and substrate is depleted within the media, cell proliferation decreases, cells retract from the cell cycle and, in some instances, may undergo apoptosis. Cell morphology may also be influenced in overgrown cultures. Cells that have reached this plateau of growth can remain viable after subculture, but they may take longer to recover during the lag phase (Vunjak-Novakovic & Freshney, 2006). As shown in Figure 4.1, all cell lines had an increase in OCR as the cell seeding density per well increased (as expected).

The 143B, RD, A549 and SH-SY5Y cell lines appeared to show a linear increase in OCR, while the C2C12 and HEPG2 cell lines appeared to reach this plateau for the selected cell seeding density ranges. Should broader cell seeding density ranges have been selected, it would be likely that all cell lines would eventually reach this plateau, once the cells had become over confluent and their growth had begun to decrease due to contact inhibition (GIBCO, 2015).

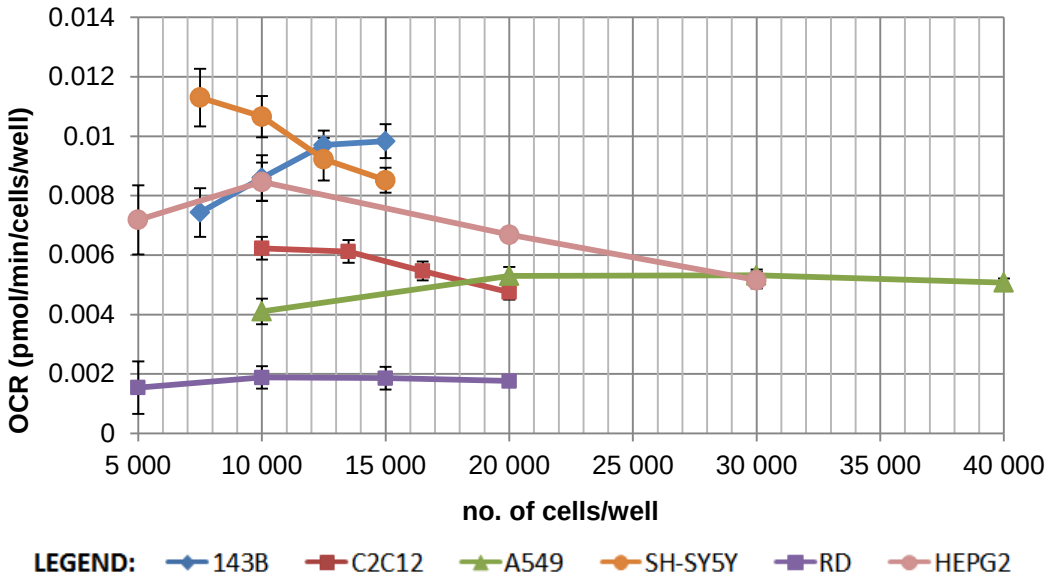

Figure 4.2: Graph of basal respiration (measurement #3) showing the relationship between cell seeding density and the OCR, normalized to the number of cells/well for six cell lines. Each data point represents the mean normalized OCR (N = 22-24) ± standard deviation.

Each cell line was normalized according to the number of cells per well (shown in Figure 4.2), in order to compare the normalized OCR and different cell seeding densities. The OCR was expected to remain constant with increasing cell seeding density, and a decrease in OCR with increased cell seeding density was an indication that the maximum number of cells that should be used per well for optimal functioning, had been reached. The A549 and RD cells appeared to remain constant across the entire cell seeding range, thus indicating that any cell seeding density within that range could be selected. The C2C12 and SH-SY5Y cell lines appeared to remain linear from 10 000 – 13 500 and 7 500 – 10 000 cells/well respectively. The OCR decreased thereafter, indicating that the optimized cell seeding density fell within these ranges for the two cell lines. The 143B cell line increased at first, and only became constant between 12 500 and 15 000 cells/well, indicating that the optimized cell seeding density fell within this range. Finally, the HEPG2 cell line OCR appeared to increase until it reached 10 000 cells/well, after which it began to decrease again, thus indicating that the optimal range lay between 10 000 and 15 000 cells/well. The optimized cell seeding densities selected in Table 4.1 (Section 4.2.5) were estimated using Figures 4.1 and 4.2, and by studying cell confluency and morphology at the time of the analysis.

4.2.2. Oligomycin concentration

Also shown in Figure 3.1a (Section 3.5.2) are the four different oligomycin concentrations (between 0 – 2 µM) that were used on the first optimization plate. After the optimized cell seeding density had been selected (as described above), the mean OCR values (at measurement #4) were calculated for each of the four oligomycin concentrations at the optimized cell seeding density. A titration curve was then drawn, where the oligomycin concentration was plotted against the OCR values, to determine the oligomycin concentration at which maximal ATP synthase inhibition was obtained.

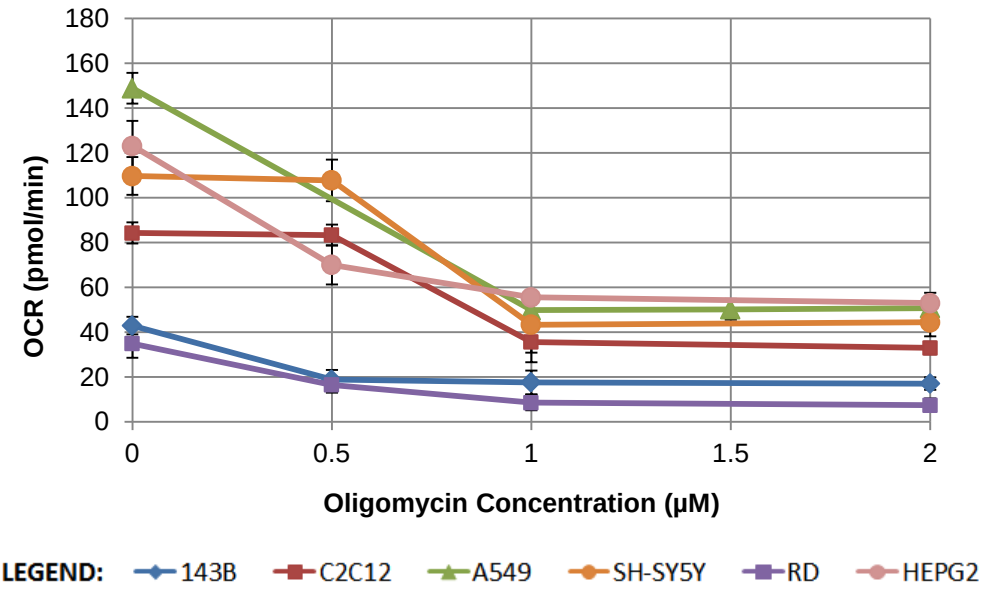

Figure 4.3: Oligomycin dosage curve of OCR values obtained from measurement #4 (first measurement after oligomycin injection) for six cell lines. Each data point represented the mean OCR (N = 5-6) ± standard deviation.

As can be seen in Figure 4.3, 0.5 µM oligomycin did not appear to have much of an inhibitory effect on the C2C12 or SH-SY5Y cell lines, whilst all the other cell lines showed a dramatic decrease in OCR. For all cell lines, 1 µM oligomycin appeared to be sufficient to cause maximum inhibition of ATP synthase and no further inhibition was seen at oligomycin concentrations above 1 µM.

4.2.3. FCCP concentration

The six different FCCP concentrations (between 0 – 2 µM) are shown in Figure 3.1b (Section 3.5.2) for the second optimization plate that was run using the optimized cell seeding density and oligomycin concentration for each cell line. The mean OCR values for each of the FCCP concentrations were calculated using the readings from measurement #7. A titration curve was drawn plotting the FCCP concentrations against the OCR values, to determine the FCCP concentration that gave the highest attainable maximal respiration.

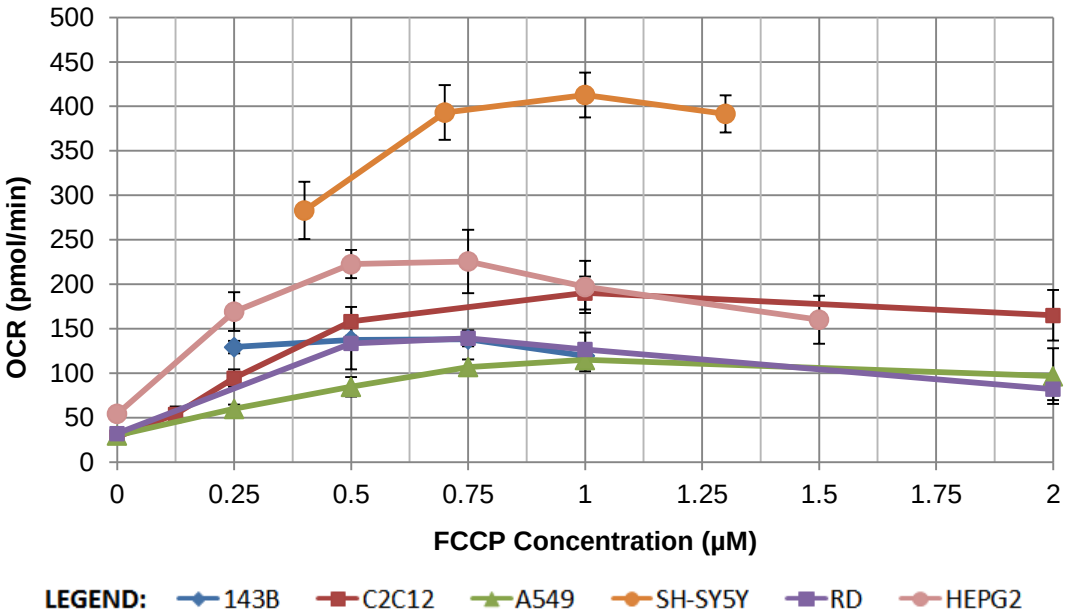

Figure 4.4: FCCP dosage curve of OCR values obtained from measurement #7 (first measurement after FCCP injection) for six cell lines. Each data point represented the mean OCR (N = 6-12) ± standard deviation.

All cell lines produced the same bell-like curve, as seen in Figure 4.4, with a concurrent increase in OCR with increasing FCCP concentration up to an optimal level, followed by a decrease in OCR due to excessively decreased membrane potential, caused by FCCP disrupting the endosomes and acidifying the cytosol. The optimized concentrations shown in Table 4.1 were determined by choosing those that produced the highest maximal respiration values before the OCR decreased again.

4.2.4. Glucose and pyruvate concentration in assay media

Figure 3.2 (Section 3.5.2) shows the glucose (0 – 25 mM) and pyruvate (0 and 1 mM) concentrations that were used in the assay media after the optimized cell seeding density, oligomycin and FCCP concentrations had been determined. Mean OCR values were calculated for each combination of glucose and pyruvate concentrations at measurements #3 and #7. Two bar graphs (for basal and maximal respiration, Figures 4.5 and 4.6 respectively) were drawn using these OCR values to determine the concentrations which provided a balance between the optimized basal and maximal respiration OCR values.

Glucose and pyruvate concentrations had to be selected based on the purpose of the given experiment and whether a higher basal respiration or higher spare respiratory capacity (difference between maximal respiration, Figure 4.6, and basal respiration, Figure 4.5) was required. For all cell lines a pyruvate concentration of 1 mM (supraphysiological) and a glucose

concentration of 5 mM (physiological) appeared to be adequate for obtaining sufficiently increased basal respiration and spare respiratory capacity.

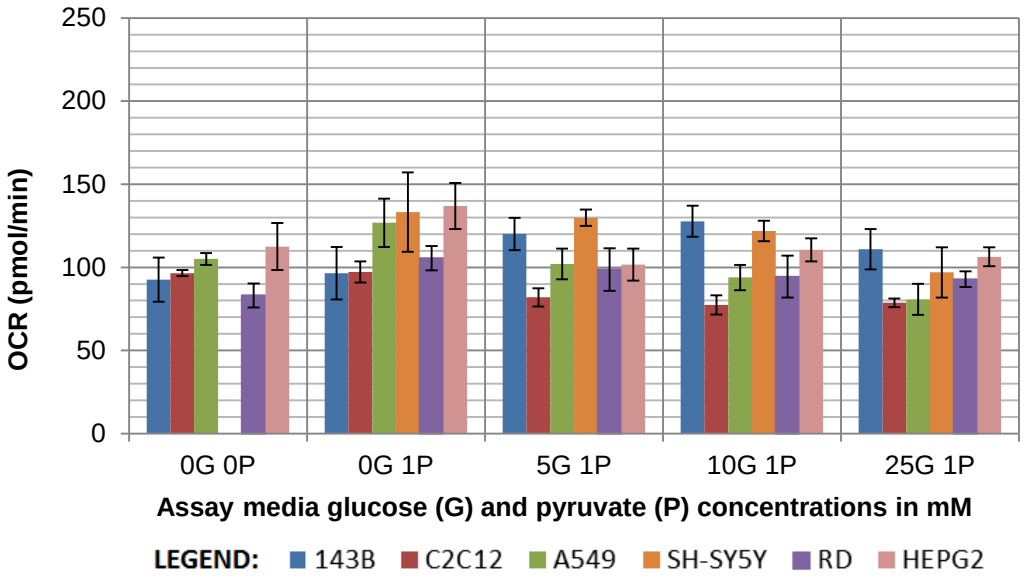

Figure 4.5: Bar graph depicting the basal respiration (measurement #3) of each cell line at five different glucose and pyruvate concentrations. Gaps indicate conditions that were not tested. Each bar represented the mean OCR (N = 6-12) ± standard deviation.

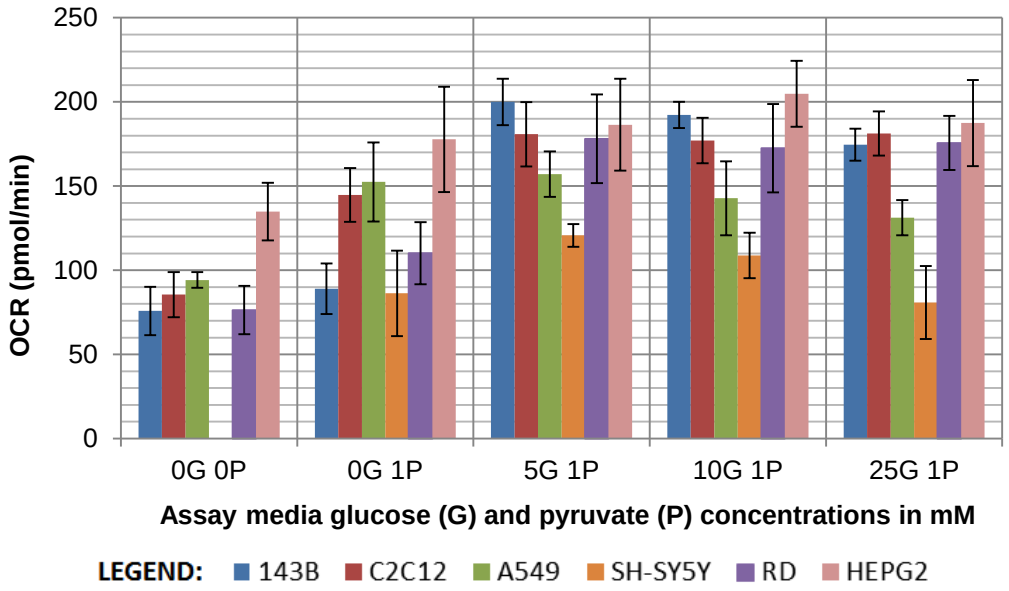

Figure 4.6: Bar graph depicting the maximal respiration (measurement #7) of each cell line at five different glucose and pyruvate concentrations. Gaps indicate conditions that were not tested. Each bar represented the mean OCR (N = 6-12) ± standard deviation.

4.2.5. Conclusion

Optimized conditions of extracellular flux analyses for six cells lines were determined, as was the objective of this section, and are summarized in Table 4.1. The recommended optimized conditions found in literature for each of the six cell lines were also shown in Table 4.1. Not

shown in the table were the selected optimized glucose and pyruvate concentrations for the assay media of 5 mM and 1 mM, respectively. Seahorse Bioscience recommends 10 mM glucose and 1 mM pyruvate, but these concentrations vary greatly in literature, depending on the nature of the study. In this study, no difference was seen between a glucose concentration of 5 mM and 10 mM, thus indicating that either of the two concentrations would be acceptable.

Table 4.1: Summary of selected optimized conditions from this study for six cell lines compared to recommended conditions found in literature.

Cell line	Cell seeding density (cells/well)	Recommended cell seeding density (cells/well)	[Oligomycin] (µM)	Recommended [oligomycin] (µM)	[FCCP] (µM)	Recommended [FCCP] (µM)
143B	13 000	20 000[a]	1	1.5[a]	0.5	0.5[a]
C2C12	15 000	10 000 – 20 000[b]	1	1[b]	1	0.5[b]
A549	25 000	15 000 – 20 000[b]	1	1[b]	0.75	0.5[b]
SH-SY5Y*	12 000	10 000 – 20 000[c,d]	1	1[c]	0.8	0.5[c]
RD	20 000	No XF96 data, only XF24	1	1[e]	0.75	1.25[e]
HEPG2	15 000	10 000 – 30 000[b]	1	1[b]	0.5	0.5[b]

* The SH-SY5Y cell line was incubated for 48 hours and not 24 hours, to improve cell adhesion to the cell culture plate. Various incubation times were obtained for this cell line in literature.
[a] (Gong *et al.*, 2014); [b] www.seahorsebio.com. Seahorse Bioscience recommends that the cells be incubated 24-28 hours prior to XF analysis; [c] (den Hollander *et al.*, 2015); [d] (Cocco *et al.*, 2015); [e] (Vaughan *et al.*, 2013).

As shown in Table 4.1, the oligomycin concentration of 1 µM appeared to be adequate for all cell lines and it may thus not be necessary to optimize this condition for all new cell lines, unless otherwise suggested in literature. At the onset of this study, Seahorse Bioscience recommended rotenone and antimycin A concentrations of 1 µM each, but more recently they suggested that 0.5 µM was sufficient. Future studies will thus make use of 0.5 µM rather than 1 µM rotenone and antimycin A for all cell lines. When comparing the optimized conditions obtained in this study to those found in literature, it can also be seen that numerous discrepancies exist. This emphasizes the point, as also advised by the supplier, that thorough optimization of reaction conditions for bioenergetics investigations is essential, even if the conditions are reported in literature, and will greatly improve the outcomes of subsequent investigations.

4.3. Whole mtDNA genome sequencing data and MutPred scores – *Objective 2*

4.3.1. Detection and verification of the known pathogenic mtDNA variants and their allele frequencies

As discussed in Section 3.2, the whole mitochondrial genome of selected ME patients was sequenced, using NGS, in a previous unpublished study performed at the CHM (NWU). Six South African patients were found to possess one or more of three known pathogenic mtDNA

variants (m.7497G>A, m.9185T>C and m.10197G>A) at low allele frequencies. These six patients were all found to harbour the U5 mtDNA sub-haplogroup. At the onset of this study, verification of these mtDNA variants was in progress as researchers were unable to consistently confirm the presence and accurately determine the variant allele frequency of the three pathogenic variants in ME patients when using different NGS methods. These patients were sequenced twice by other researchers, and once during this study, using the Ion Torrent PGM (Life Technologies). Selected patients were also sequenced by independent institutions using MiSeq (Illumina) sequencing and pyrosequencing (QIAGEN), at Inqaba Biotec (Pretoria, South Africa) and Newcastle University (Newcastle, UK), respectively.

The results of the mtDNA variant verification from other institutions are shown in Table 4.2, where the counts represent the number of times each of the two possible mtDNA nucleotides (wild-type to the left of the slash, and the variant on the right) was detected. The pyrosequencing, which can be considered the most sensitive method due to its reading depth and inclusive controls, *was unable to detect any of these mtDNA variants*. NGS performed during this study using the Ion Torrent PGM and fresh blood samples did not detect any of the three mtDNA variants either, in any of the six patients.

Table 4.2: Variant allele frequency results and counts of three known pathogenic mtDNA variants determined using NGS

Patient	mtDNA Variant	Ion Torrent (Batch 1)		MiSeq	
		Counts	*Frequency of variant allele*	*Counts*	*Frequency of variant allele*
SA5	m.7497G>A	101/21	17.2%	712/145	16.9%
	m.9185T>C	150/28	15.7%	1995/256	11.4%
	m.10197G>A	53/5	8.6%	597/120	22.2%
SA6	m.7497G>A	162/22	12%	1456/165	10.2%
	m.9185T>C	294/24	7.5%	3547/262	6.9%
		Ion Torrent (Batch 2)		**Ion Torrent (Batch 3)**	
		Counts	*Frequency of variant allele*	*Counts*	*Frequency of variant allele*
SA11	m.7497G>A	180/12	6.2%	434/35	7.5%
	m.9185T>C	326/23	6.6%	803/48	5.6%
	m.10197G>A	199/5	2.5%	305/19	5.9%
SA25	m.7497G>A			334/5	1.5%
	m.9185T>C	276/3	1.1%	654/16	2.4%
	m.10197G>A			206/4	1.9%
SA26	m.7497G>A	110/10	8.3%	307/23	7%
	m.9185T>C	209/8	3.7%	548/32	5.5%
	m.10197G>A	50/5	9.1%	146/8	5.2%
SA36	m.7497G>A	213/10	4.5%	367/12	3.2%
	m.9185T>C	479/20	4%	754/26	3.3%
	m.10197G>A			235/6	2.5%

The inconsistency between different batches sequenced using the Ion Torrent prior to this study made verification very difficult. Patient samples and controls (known to lack any of these three

pathogenic mtDNA variants) were sent to Inqaba Biotec to be sequenced using MiSeq (Illumina) in order to verify the results seen using the Ion Torrent. The results obtained from Inqaba Biotec (as shown in Table 4.2) seemed to confirm the original findings of the Ion Torrent, but the results for the control subjects also showed low allele frequencies for the pathogenic mtDNA variants (results not shown). This revealed that these low allele frequency variants could indeed be artefacts from sequencing, and thus a false indication of their presence.

A real-time PCR method was also developed in a previous study (van Heerden, 2013), in an attempt to screen for these three mtDNA variants in patients, by designing primers and probes that would only allow amplification of a specific mtDNA fragment in the presence or absence of the specific mtDNA variant. The real-time PCR approach was also found to be inconsistent, and a PCR-RFLP approach was then followed. Both of these methods proved unsuccessful in verifying the presence of the three mtDNA variants. Combined with the negative result obtained using pyrosequencing, the Ion Torrent results obtained in the current study (where none of the three pathogenic mtDNA variants were detected) was the final evidence that these variants were, in fact, not present in any of the ME patients.

Due to the high rate and context-specific nature of sequencing errors, one of the many challenges of NGS is distinguishing true variation from instrument artefacts (DePristo *et al.*, 2011). Despite the detection of these three mtDNA variants at low allele frequencies, using two different platforms (the Ion Torrent PGM and MiSeq), it was eventually concluded that these detections were merely artefacts. Much deeper coverage was obtained, and updated Ion Torrent software tools were used in the Ion Torrent sequencing performed during this study, compared to the previous studies, which may explain why the variants were not detected previously. Despite these unfortunate, but at least well-tested results, the aim of investigating mtDNA involvement could be further investigated from the other objectives that remained.

4.3.2. mtDNA sub-haplogroups and MutPred scores

As discussed in Sections 2.3.4 and 3.6, the mtDNA sub-haplogroups and MutPred scores were also determined using the NGS results from the Ion Torrent PGM. The whole mtDNA genome MutPred scores and mtDNA sub-haplogroups are shown below in Table 4.3, and will be used for further statistical analyses of the bioenergetics parameters in Section 4.8. The MutPred scores per mitochondrial gene and complex are shown in Table B1, Appendix B, but they will not be used for any further calculations due to the small cohort used in this study and thus provide insufficient data for each mitochondrial gene. In future studies with larger cohorts, the MutPred scores for each mitochondrial complex would be the next step in data analysis.

Table 4.3: Adjusted whole mtDNA genome MutPred scores and the mtDNA sub-haplogroups of each subject

Subject	mtDNA sub-haplogroup	Total adjusted MutPred score*	Subject	mtDNA sub-haplogroup	Total adjusted MutPred score*
ME Patients			**ME Patients**		
SA5	U5b1c2b	0.310	**SA12**	H1c1	0.411
SA6	U5b1c2b	0.341	**SA20**	H1ak1	0.411
SA11	U5b2a1b	0.365	**SA23**	H3b1b1	0.425
SA25	U5a2b1a	0.340	**SA24**	H1b1+16362	0.454
SA26	U5a1d2a	0.351	**SA39**	H3+73	0.361
SA36	U5a1d2a	0.344	**Healthy Controls**		
SA1	U2e1	0.310	**HC1**	U2e1'2'3	0.359
SA19	U4c2a	0.302	**HC2**	U5a1c1a	0.381
SA16	R 1	0.495	**HC3**	U5b2b3a	0.429
SA35	J1c2c1	0.361	**HC4**	J1c2c	0.361
SA31	T2b+!16296	0.367	**HC5**	J1c2c1	0.361
SA7	H1a1	0.411	**HC6**	H3b1b1	0.425
SA9	H1c3	0.428	**HC7**	H48	0.376

* mutpred.mutdb.org/about.html. MutPred score indicated the probability that the amino acid substitution was pathogenic or disease-causing, where 0 indicated no pathogenicity and 1 indicated maximum pathogenicity.

All subjects (ME patients and healthy controls) showed adjusted MutPred scores of <0.5, which were not "actionable hypotheses" and thus not considered to be harmful, as described in Section 3.6. A one-way ANOVA was performed to compare the MutPred scores of the haplogroup U ME patients, non-U haplogroup ME patients, healthy controls and ME patients as a whole (U and non-U haplogroups combined). A significance difference was seen between the four groups with $F(3) = 5.038$ ($p = 0.005$), thus meriting the use of Tukey's HSD post-hoc test, as shown in Table 4.4. These results showed that non-U haplogroup ME patients had significantly higher MutPred scores than the haplogroup U ME patients, while no significant difference was observed between ME patients and healthy controls.

Table 4.4: Tukey's HSD post-hoc test showing differences between the MutPred scores for each subject group.

Group 1	Group 2	Mean difference (Group 1 – Group 2)	SEM	p
Haplogroup U ME patients (N = 8)	Non-U haplogroup ME patients (N = 10)	-0.0795	0.0206	**0.002***
Haplogroup U ME patients (N = 8)	Healthy controls (N = 7)	-0.0517	0.0225	0.115
Non-U haplogroup ME patients (N = 10)	Healthy controls (N = 7)	0.0278	0.0214	0.567
ME patients (N = 18)	Healthy controls (N = 7)	-0.0075	0.0193	0.980

* Indicates significant p-values of <0.05. SEM = standard error of the mean.

In addition to the NGS performed using the blood of all the ME patients, four random cybrid cell lines (SA5, SA20, SA25 and SA35) were also sequenced to establish whether or not the same mtDNA sub-haplogroup and MutPred scores were found in the cybrid cells compared to patients' blood. In all four cases identical results were obtained indicating that mtDNA along with mtDNA variants were successfully transferred from patient blood platelets to ρ^0 cells, as required by point 7 in the criteria for determining mtDNA point mutation pathogenicity (Section 2.5.1). This was then further investigated for all of the other patients in the following section, using the less expensive (but also less sensitive) PCR-RFLP approach.

4.4. MtDNA haplogroup determination using gel electrophoresis images – *Objective 3*

As discussed in Section 3.9, two sets of gel photos were obtained, one depicting the PCR products that had been amplified for each mtDNA fragment of each patient, and the second depicting the RFLP products where each mtDNA fragment, of each patient, had been cut by a specific restriction enzyme. An example of the PCR gel photo and the sizes of the PCR products obtained will be shown here for two patients (since gel photos for all other patients were identical), while RFLP gel photos for all patients will be shown.

Each RFLP gel photo represented one of five fragments of mtDNA (B, D, F, G or H) which were digested by specific restriction enzymes. Each gel photo contained a ladder and the sizes of the fragments produced could be identified by comparing them to the ladder that had fragment sizes which were known. Differences in fragment sizes between the patient samples could be clearly identified and were highlighted to indicate the absence or presence of a specific SNP. Within each section of DNA that was amplified, there were numerous restriction sites for each specific enzyme, where only one of those restriction sites represented a SNP. The sizes of the fragments of DNA that were produced when each specific section of the mtDNA genome was cut with a certain restriction enzyme (shown in Table 4.5), were calculated using a program at http://pga.mgh.harvard.edu/web_apps/web_map/start, which determined the locations of the restriction sites for each enzyme.

In Table 4.5, fragments not underlined were those that were formed from restriction sites present in almost all humans, while the underlined fragments were those specific to the SNPs that were only present in certain haplogroups. If the SNP was not present, the underlined fragment in the row marked 'negative' was visible; whereas, if the SNP was present, that same fragment was cut into two parts, as shown by the underlined fragments in the row marked 'positive'. In the RFLP gel photos, all the underlined and non-underlined fragments were indicated, while only the underlined fragments were highlighted in red (SNP not present) or

green (SNP present). A process of deduction was used to determine the haplogroup of each patient using Table 3.4 (Section 3.9.1).

Table 4.5: Sizes of expected fragments after restriction enzyme digestion

mtDNA Fragment	Restriction Enzyme (position where it cuts)	Negative for SNP	Positive for SNP
B	NlaIII (4216)	527, 460, **407**, 295, 120, 77	527, 460, **374**, 295, 120, 77, **33**
D	AluI (7025)	419, 375, 305, 219, **188**, 167, 139, 92	419, 375, 305, 219, 167, **157**, 139, 92, **31**
F	DdeI (10394)	695, 459, 422, **275**, 130	695, 459, 422, **234**, 130, **41**
G	HinfI (12308)	336, 221, **180**	336, 221, **138**, **42**
H	BstNI (13704)	**1893**	**1726**, **167**

GEL ELECTROPHORESIS PHOTO FOR PCR PRODUCTS

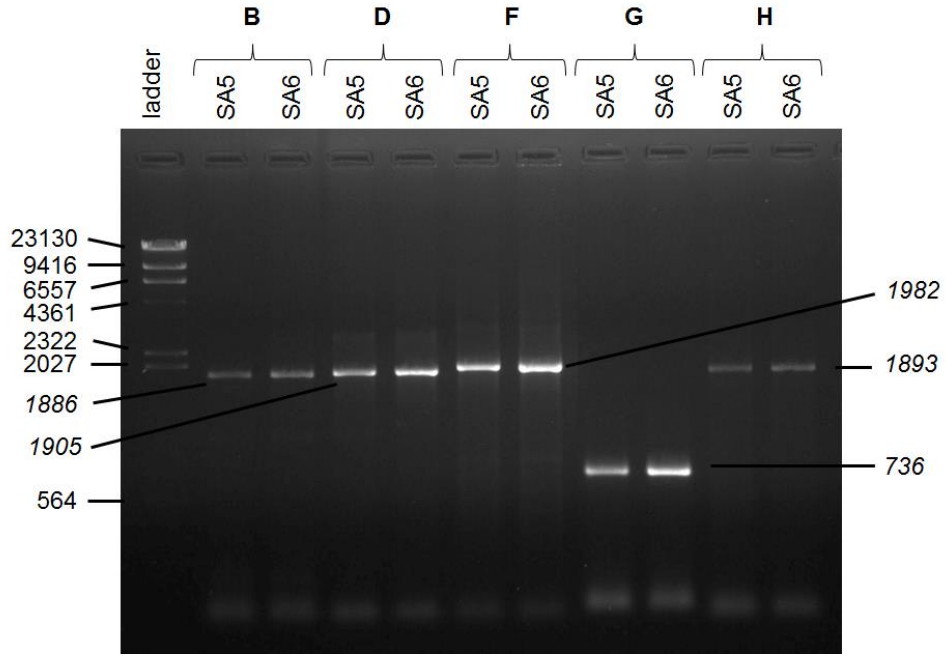

Figure 4.7: Agarose gel electrophoresis photo showing the size (in bp) of PCR products formed for each mtDNA fragment (B, D, F, G and H). The expected fragment sizes were shown in Table 3.3 (Section 3.9.1). Bacteriophage λ, digested with HindIII, was the ladder that was used, and patients SA5 and SA6 were shown here.

GEL ELECTROPHORESIS PHOTOS FOR RFLP PRODUCTS

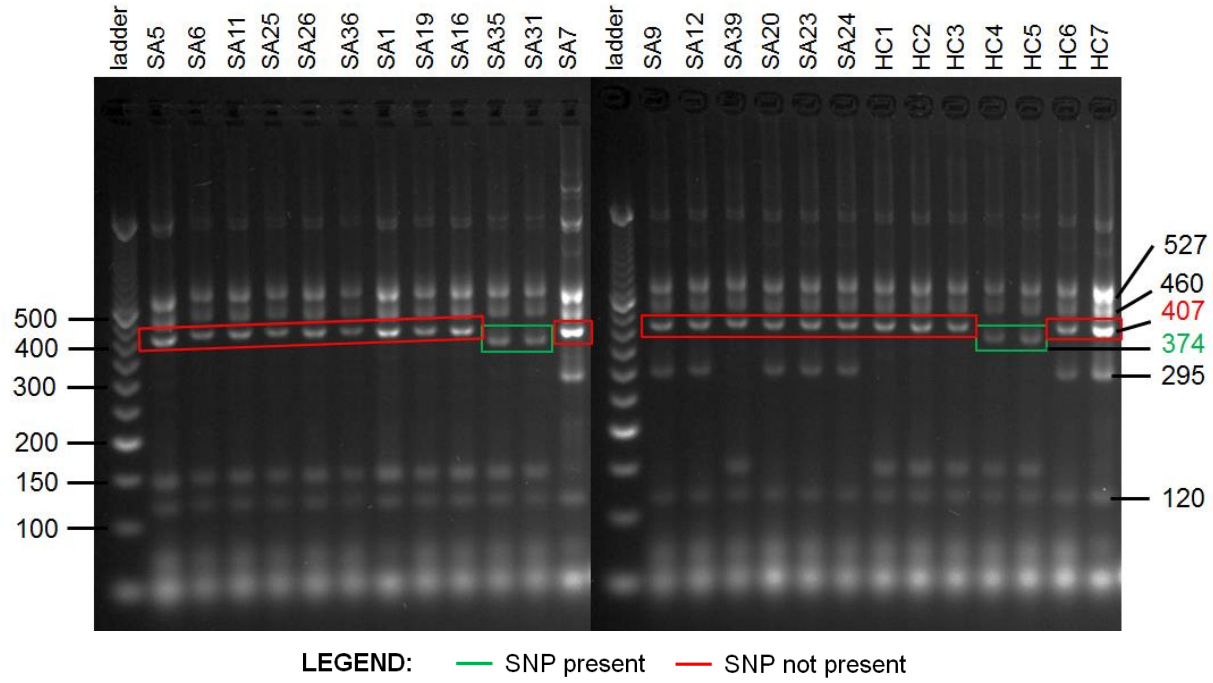

Figure 4.8a: Agarose gel electrophoresis photo for all ME patients and healthy controls, showing mtDNA fragment B that was digested by the restriction enzyme NlaIII.

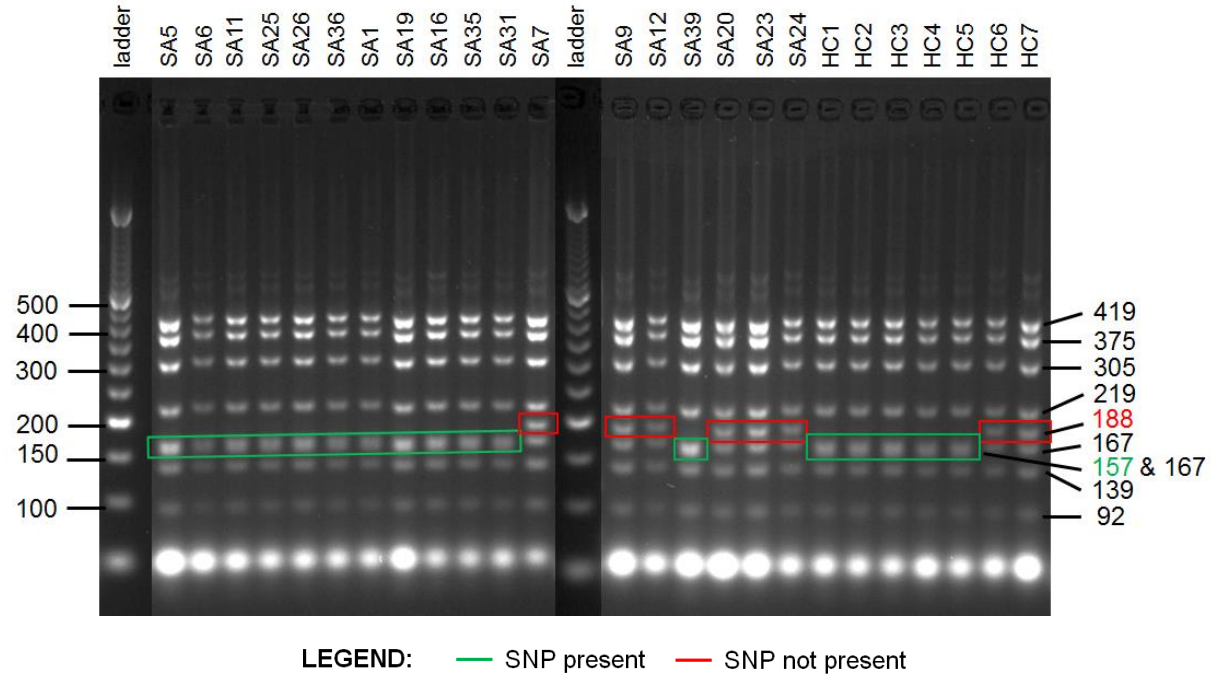

Figure 4.8b: Agarose gel electrophoresis photo for all ME patients and healthy controls, showing mtDNA fragment D that was digested by the restriction enzyme AluI.

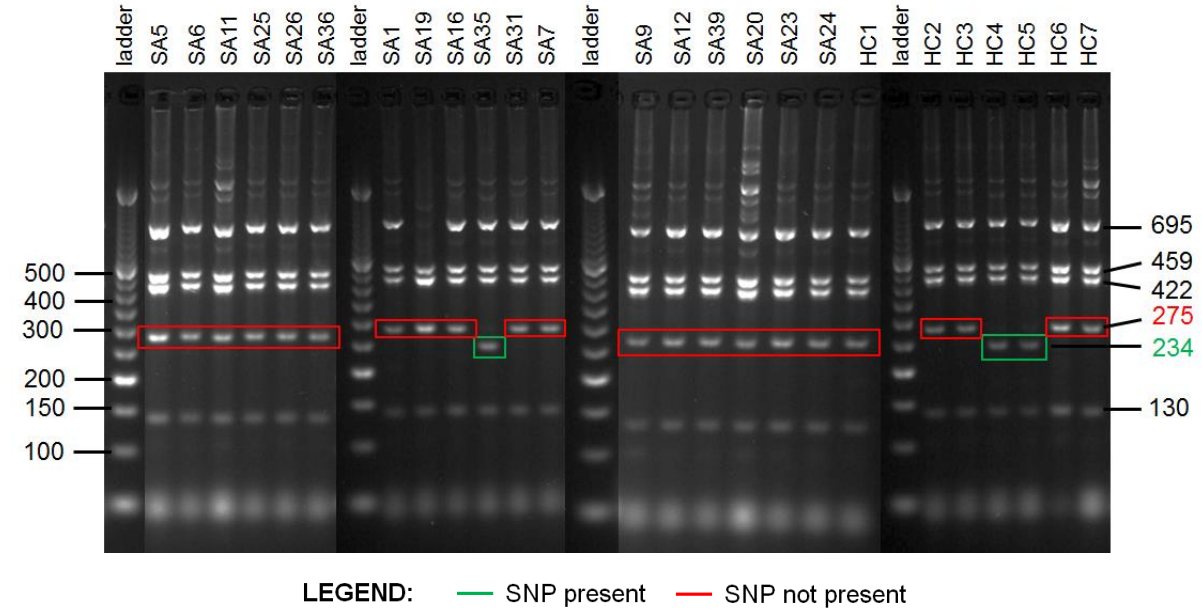

Figure 4.8c: Agarose gel electrophoresis photo for all ME patients and healthy controls, showing mtDNA fragment F that was digested by the restriction enzyme DdeI.

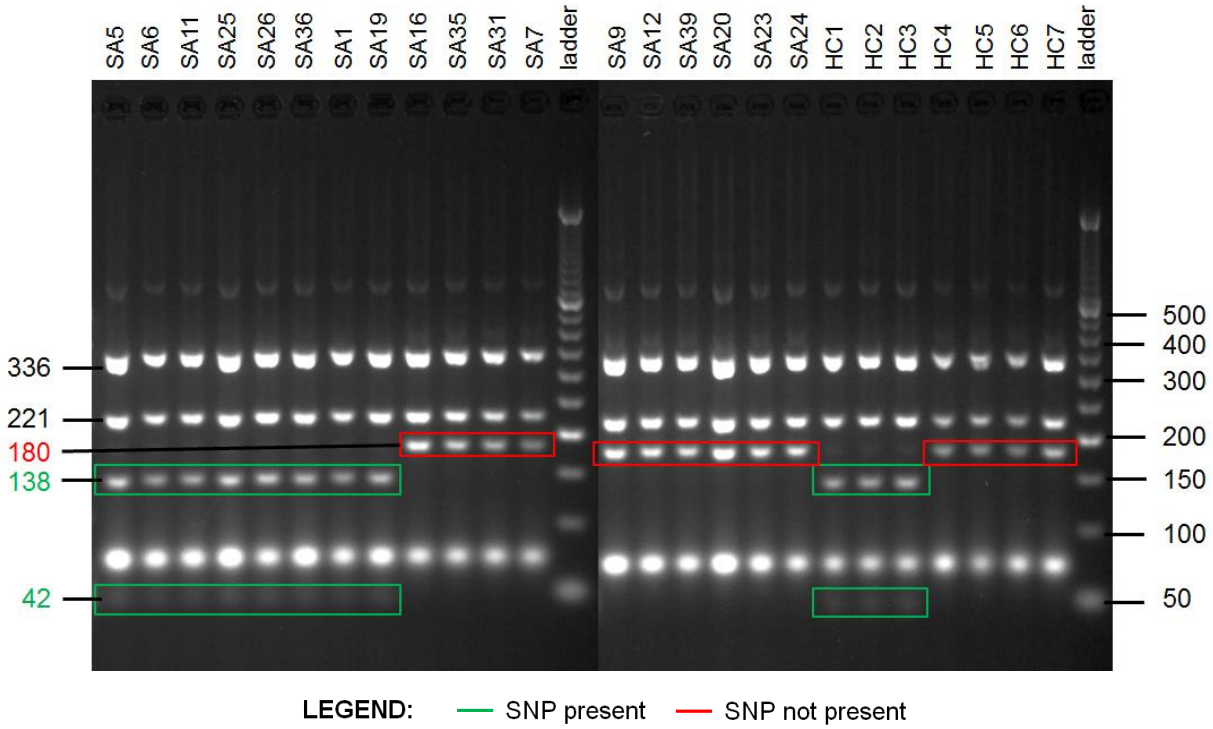

Figure 4.8d: Agarose gel electrophoresis photo for all ME patients and healthy controls, showing mtDNA fragment G that was digested by the restriction enzyme HinfI.

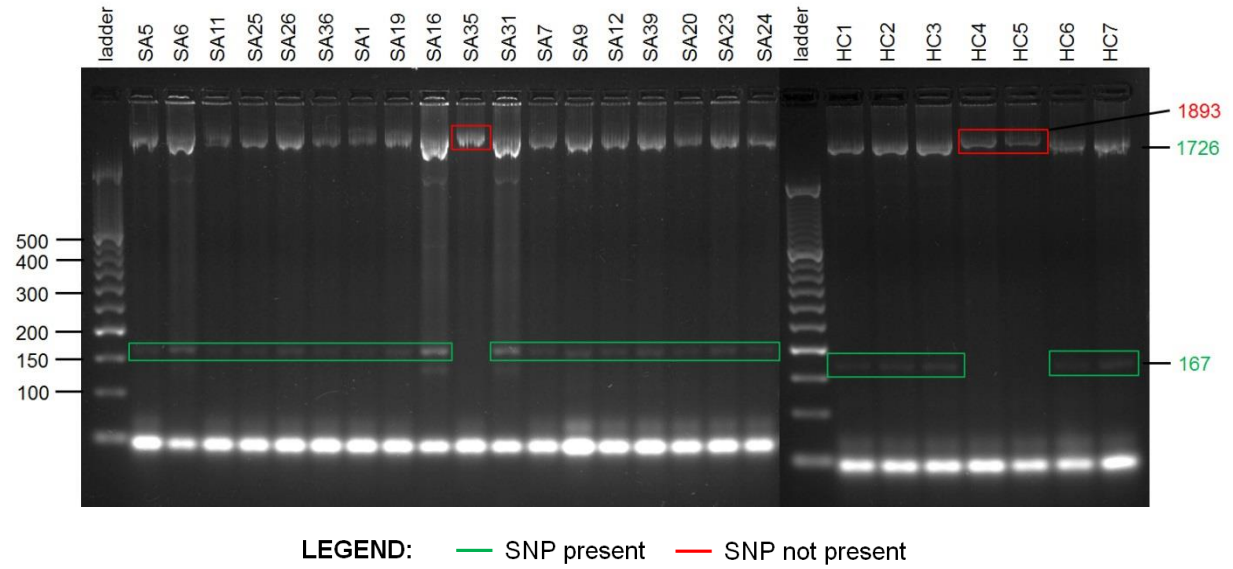

Figure 4.8e: Agarose gel electrophoresis photo for all ME patients and healthy controls, showing mtDNA fragment H that was digested by the restriction enzyme BstNI.

Many of the smallest fragments were not visible (possibly due to the movement of the EtBr front or due to too little DNA being loaded), but it was still possible to obtain conclusive results. In a few cases, there were unexpected fragments present and in others there were fragments absent that were expected to be present. This was also experienced in a previous study using human blood which was attributed to the genetic variability among various individuals. It may also be possible that these were indeed common SNPs in most individuals, but that they had not yet been updated to databases such as Mitomap. Figures 4.8 a-e were studied and compared to Table 3.4 (Section 3.9.1) in order to determine the haplogroup for each patient using the processes of elimination and deduction. Table C1 in Appendix C shows these results for each patient, where all patients, except for one, were found to have the expected haplogroup.

Patient SA39 fell in the Others Dde- category based on the RFLP gel photos, but according to the NGS, the haplogroup should be H3+73. The PCR-RFLP process was repeated on patient SA39, using fresh cybrid cells, but the same result was obtained. The SNP for AluI on fragment D should not have been present for patient SA39, but it was found to be positive. This may be due to the sub-haplogroup of this patient (which differed to all other haplogroup H patients), which cannot be detected with the PCR-RFLP qualitative approach - compared to the sensitive and quantitative NGS approach - and thus provided a false result.

The PCR-RFLP approach was used as a less expensive way of confirming the macro haplogroup, during the procedures used in this study. All the haplogroups of the subjects in this

study were known from NGS, but since these PCR-RFLP results corresponded with previous sequencing data, it could be concluded that the mtDNA from the patient's blood platelets was indeed successfully transferred to the ρ^0 cells during cybrid cell development. As mentioned before (Section 4.3.2), this finding was further validated by the full mtDNA NGS of four cybrid cell lines, which also confirmed exact transfer of mtDNA from blood platelets to ρ^0 cells.

4.5. RMCN determination using real-time PCR C_T values – *Objective 4*

As discussed in Section 3.10, triplicate C_T values were obtained for each gene (β-globin and MT-ND2) of every subject cybrid cell line at multiple time intervals. These values were then entered into the $2^{-\Delta\Delta CT}$ formula and the coefficient of variance (CV) for the RMCN calculated according to the formula (Miller *et al.*, 2003): $\sqrt{CV_{MT-ND2}{}^2 + CV_{\beta-globin}{}^2}$. As mentioned, multiple RMCN values were obtained for each patient, since each patient was analysed on more than one XF analyser microplate and at two separate time intervals. At each time interval, two out of the three plates analysed used the same patient cybrid cell line. This was due to the plate layout where essentially three subject groups were compared across the three plates, namely: ME patients with haplogroup U, ME patients with non-U haplogroups and healthy controls. Duplicate plates had identical RMCNs because they were seeded simultaneously using the same cybrid cell dilutions. Figures 4.9a-c depict four RMCN results ± CV (CV% of RMCN) for each subject (for each of the two plates at week 3 and 6). The y-axis ranges for all graphs were kept identical, to allow for a non-biased comparison between the three graphs, which resulted in one data point in Figure 4.9c lying outside of this range. In Figure 4.9b, identical RMCN results were obtained for plates 1 and 3, since the same dilution of ME patient cybrid cells was used to seed both of these plates at week 3.

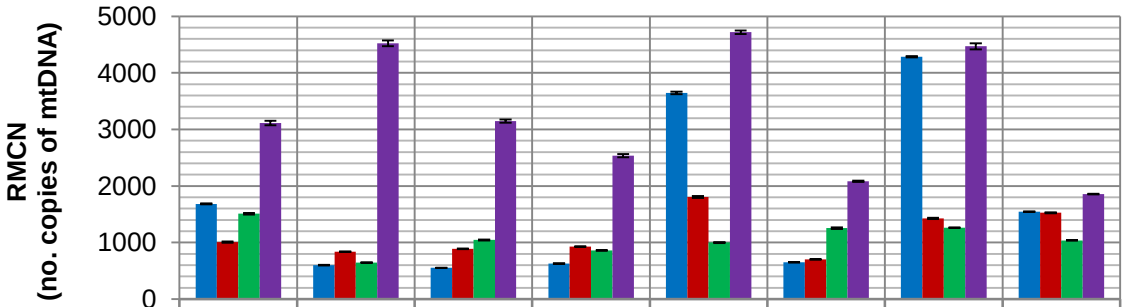

	SA5	SA6	SA11	SA25	SA26	SA36	SA1	SA19
Plate 1 - Week 3	1683	602	554	628	3647	652	4284	1544
Plate 2 - Week 3	1006	838	890	930	1804	701	1425	1526
Plate 1 - Week 6	1509	647	1045	860	1000	1255	1264	1039
Plate 2 - Week 6	3113	4523	3148	2534	4719	2084	4471	1857

Figure 4.9a: Histogram, showing ME patients with haplogroup U, of the RMCN ± CV% for Plates 1 and 2 at week 3 and 6.

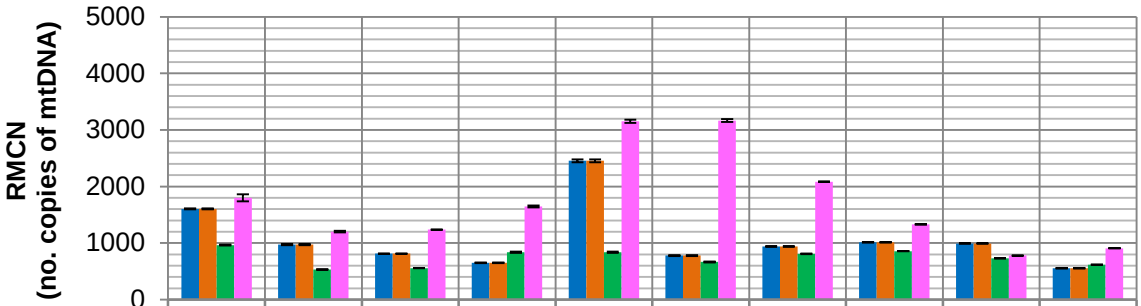

	SA16	SA35	SA31	SA7	SA9	SA12	SA39	SA20	SA23	SA24
Plate 1 - Week 3	1605	973	813	652	2455	779	940	1013	993	555
Plate 3 - Week 3	1605	973	813	652	2455	779	940	1013	993	555
Plate 1 - Week 6	965	531	557	837	838	668	809	857	730	617
Plate 3 - Week 6	1800	1202	1239	1645	3151	3166	2084	1330	779	908

Figure 4.9b: Histogram, showing ME patients with non-U haplogroups, of the RMCN ± CV% for Plates 1 and 3 at week 3 and 6. The same ME patient cybrid cells were used to seed plates 1 and 3 at week 3, thus, an identical RMCN was obtained for those two plates.

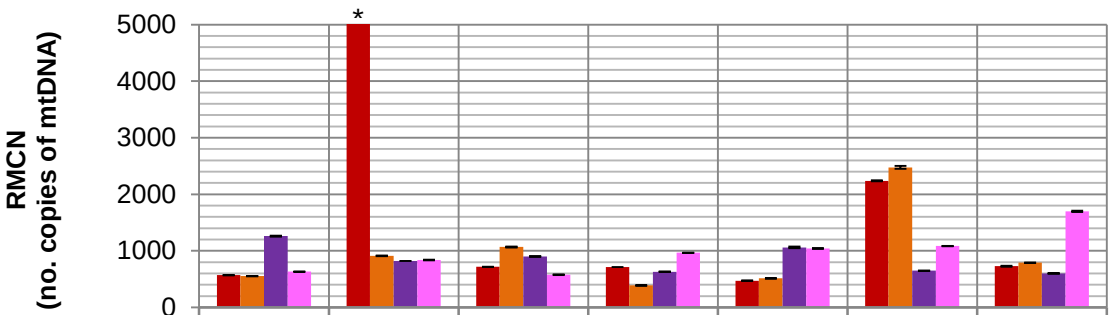

	HC1	HC2	HC3	HC4	HC5	HC6	HC7
Plate 2 - Week 3	569	7865	718	714	472	2237	729
Plate 3 - Week 3	555	911	1068	389	513	2476	792
Plate 2 - Week 6	1261	821	899	629	1061	649	601
Plate 3 - Week 6	634	838	577	966	1042	1086	1700

Figure 4.9c: Histogram, showing healthy controls, of the RMCN ± CV% for Plates 2 and 3 at week 3 and 6.
* Patient HC2 had a RMCN of 7865 which was outside of the range shown here.

A factorial ANOVA was performed to compare the main effects of week, plate and subject group, as well as their interactions, with the RMCN. The duplicate RMCN results shown in Figure 4.9b for plate 3 at week 3 were excluded from the analysis.

4.5.1. Comparison between the RMCN at Week 3 and Week 6

No significant differences were seen between week 3 and week 6 ($p = 0.595$), but significant effects were seen for the interaction between week and plate ($p = 0.001$), as well as between week and subject group ($p = 0.0002$). It was not known whether or not any changes in the RMCN would occur with three weeks of additional cell culture, but since the ρ^0 cells were

completely depleted of mtDNA at the time of cybrid cell creation, it was possible that the RMCN would increase the longer the newly developed cybrid cells were cultured. Since no significant difference was seen in the main effect of week, it appeared that the cybrid cells did not undergo any significant RMCN increase after week 3. However, the significant interactions seen between week and plate, as well as between week and subject group, indicated that the amount of time that the cells were cultured did indeed have an effect in certain subject groups and on different plates. This can also be seen in Figures 4.9a-c where values varied widely for individual subjects, not only between week 3 and week 6, but also between plates analysed on the same day. When studying the means for each plate at week 3 and 6 to investigate the interaction seen between week and plate, the expected increase in RMCN from week 3 to week 6 could be seen in Plates 2 and 3, while for Plate 1 the opposite was true.

In a similar study using 143B cybrids, authors indicated that they only observed steady-state levels of the RMCN in the cybrid cells at passage numbers of 20 and higher (Gómez-Durán *et al.*, 2010), while in this study the RMCN of each subject cybrid cell line was at passage 11 at week 6. More consistent and reliable results would possibly have been obtained if the cybrid cells had been cultured for a longer period of time and the RMCN had been calculated every few weeks until passage 20 or higher was reached. This would also have allowed one to see whether or not the RMCN truly did stabilize after 20 passages. However, it is typical to see changes over time in cell culture studies, due to the constant changes in culture conditions.

Up to 2-3 weeks after cybrid cell development, there was an increase in the RMCN of the cybrid cells since this was the period during which selection for cybrid cells occurred (using uridine-free media), with apparent increased cell death and decreased cell growth. Thereafter, cell growth increased and cell death was no longer evident, thus indicating that the minimal mtDNA level required for cell survival was reached after 2-3 weeks, as also discussed in Section 4.7.

4.5.2. Comparison between the RMCN of each plate

Approximately four days before the XF analysis, each patient cybrid cell line was divided from one flask into two flasks (one flask for each of the two plates that used the same subject group). It was thus expected that the RMCN, obtained from cybrid cells isolated from each of these two flasks on the day of XF analysis, should be very similar (since the only difference was four days cultured in separate flasks). Since the main effect for plates showed a significant difference ($p = 0.039$), this was not the case. Tukey's HSD post-hoc test was performed and found no significant differences between any of the plates at week 3 (p-values between 0.5 and 0.9), but at week 6, significant differences were seen between all three plates. This was investigated further using dependent-means *t*-tests, as shown in Table 4.6.

Table 4.6: Dependent-means *t*-test results showing differences between the RMCN of each plate at week 6.

Subject Group	Group 1	Group 2	Mean difference (Group 1 – Group 2)	SEM	df	*t*	p
Haplogroup U ME patients	Plate 1	Plate 2	-2228.75	434.14	7	-5.134	**0.001***
Non-U haplogroup ME patients	Plate 1	Plate 3	-989.50	258.22	9	-3.832	**0.004***
Healthy controls	Plate 2	Plate 3	-131.71	212.04	6	-0.621	0.557

* Indicates significant p-values of <0.05. SEM = standard error of the mean; df = degrees of freedom; t = test statistic.

The *t*-tests showed that Plates 2 and 3 had a significantly larger RMCN than plate 1. These significant differences seen between the plates at week 6 were believed to be caused by cell confluency. When the cybrid cells were divided into two flasks, it resulted in the cells being split into one old flask (up to two weeks old) and one new flask. When trypsinizing cells in the old flask, some cells remained attached to the plastic and could immediately continue with growth and division, without requiring additional time for attachment or stabilization. Residual growth factors may also have remained in the old flask which could also have influenced the re-plated cells by allowing them to divide and grow at an increased rate, since they did not require additional time to produce their own growth factors. Thus, despite the same ratio of cells being split into both flasks, the older flask had more cells (over confluent) compared to the new one at the time of cell seeding for the XF analysis. As seen by the significantly decreased RMCN of Plate 1 (which was seeded using the older flasks for each cell line), the cells were over confluent resulting in decreased cell growth, increased cell death, and thus a decreased RMCN compared to the other two plates that had been seeded using the new flasks. This effect was not seen at week 3 since the cells were analysed one day earlier than those at week 6 and were thus not yet over confluent.

4.5.3. Comparison between the RMCN of each subject group

Significant differences were found between the three different subject groups ($p = 0.05$), whilst no significant effects were seen for the interaction between subject group and plate ($p = 0.124$), an indication that the data was robust. To investigate the significant difference seen between the subject groups, as well as the significant effect seen between week and subject group (Section 4.5.1), Tukey's HSD post-hoc test was performed, as shown in Table 4.7.

Table 4.7: Tukey's HSD post-hoc test showing differences between the RMCN of each plate at week 6.

Group 1	Group 2	Mean difference (Group 1 – Group 2)	SEM	p
Haplogroup U ME patients (N = 32)	Non-U haplogroup ME patients (N = 30)	622.65	261.00	**0.050***
Haplogroup U ME patients (N = 32)	Healthy controls (N = 28)	635.26	265.77	**0.050***
Non-U haplogroup ME patients (N = 30)	Healthy controls (N = 28)	12.60	269.87	0.999

* Indicates significant p-values of <0.05. SEM = standard error of the mean.

This post-hoc test showed that the haplogroup U ME patients had a significantly higher RMCN than the non-U haplogroup ME patients and the healthy controls. A similar study (mentioned Section 4.5.1) using 143B cybrids found that subjects with haplogroup UK (the parent haplogroup of haplogroups U and K) had significantly less mtDNA than those with haplogroup H, contrary to the results shown here. However, the authors also indicated that they only observed steady-state levels of the RMCN in the cybrid cells at passage numbers of 20 and higher (Gómez-Durán *et al.*, 2010). In a recent study performed using ME patients and healthy controls, differentiated myotubes obtained from muscle biopsies were analysed at passage 7, rather than later passages, to increase the probability that effects seen within cultures were due to retained genetic or epigenetic factors (Brown *et al.*, 2015). Thus, culturing the cells to higher passage numbers (contrary to passage 11 used here) may provide more stable and consistent results, but changes in the genetic basis of the cultured cells may also occur, making differences between patients and healthy controls harder to detect.

Independent-means *t*-tests were used to compare the RMCN between *all* ME patients and healthy controls at week 3 and week 6. No significant difference was seen at week 3 ($p = 0.613$), but at week 6 the ME patients (mean = 1660.58; SEM = 197.47) had a significantly increased RMCN compared to the healthy controls (mean = 911.71; SEM = 83.35), $t(48) = 2.320$ ($p = 0.025$). This also emphasizes the interaction effect that was seen between week and group where differences between these subject groups were only evident at week 6. This increased RMCN could indicate increased ROS in the ME patients compared to healthy controls since it has been previously reported that higher ROS levels improved mtDNA replication (Achanta *et al.*, 2005).

4.6. Determination of bioenergetics parameters using respiratory rates obtained from the Seahorse XF^{e}96 analyser – *Objective 5*

4.6.1. Introduction

Raw bioenergetics data for each well, obtained from each plate analysed using the Seahorse XF^{e}96 analyser (as described in Section 3.11), was sorted according to patient and measurement number. The Tukey method was used to identify outlier wells, and these wells were then removed from the data set used in the Seahorse Wave software. After outlier wells had been removed, the data was exported into Microsoft Excel 2007. Seahorse Bioscience has XF Mito Stress Test and BHI report generators (www.seahorsebio.com) which are capable of automatically calculating the Mito Stress test parameters and the BHI for each plate using the Wave bioenergetics data that had been exported to Excel (as shown in Table 4.8). The report generator also allowed the normalization data to be entered. All raw data obtained from the Mito Stress report generator for each plate is shown in Appendix D.

Table 4.8: Equations used by the Seahorse Wave software for XF Mito Stress and BHI Report Generators

Bioenergetic Parameter	Measurement Number and Equations used by Report Generators
Non-mitochondrial respiration	Minimum OCR measurement after rotenone and antimycin A injection.
Basal respiration	Measurement #3 – Non-mitochondrial respiration
ATP production	Measurement #3 – Minimum OCR measurement after oligomycin injection
Proton leak	Minimum OCR measurement after oligomycin injection – Non-mitochondrial respiration
Maximal respiration	Maximum OCR measurement after FCCP injection – Non-mitochondrial respiration
Spare respiratory capacity	Maximal respiration – Basal respiration
Spare respiratory capacity (%)	$\frac{\text{Maximal respiration}}{\text{Basal respiration}} \times 100$
Coupling efficiency (%)	$\frac{\text{ATP production}}{\text{Basal respiration}} \times 100$
*BHI**	$\frac{(\text{Spare respiratory capacity}) \times (\text{ATP production})}{(\text{Non-mitochondrial respiration}) \times (\text{Proton leak})}$

* All exponents for the BHI are set to 1.
Table adapted from XF Stress Test Report Generator User Guide (103247-400, Rev. B).

As mentioned in Section 3.11, three plates were analysed in duplicate at two time intervals, resulting in twelve plates in total. Plates were run in duplicate in case of any error that may occur during an XF analysis. An error did occur for two of the 12 plates, where poor quality data was obtained, most likely due to poor loading of the injection ports which resulted in a volume of the injection compounds remaining behind in the injection port. The plate layout used was

shown in Figures 3.4 - 3.6 and the total number of plates for which data was obtained is shown in Table 4.9 (where the two plates that had errors were excluded).

Table 4.9: Total number of plates for which data was obtained

	Plate 1	**Plate 2**	**Plate 3**	**Total**
Week 3	One plate	Duplicate plates	Duplicate plates	
Week 6	Duplicate plates	Duplicate plates	One plate	
Total no. of plates:	3	4	3	*= 10*

Various intrinsic factors, such as cell number/mass, mitochondrial number/mass and mitochondrial complex activity, may influence mitochondrial bioenergetics. As also recommended by Seahorse Bioscience, it is thus essential to normalize data according to such factors in order to compensate for the intrinsic changes that may occur within cells during an experimental treatment. One form of normalization utilized by the XF analyser was the blank wells included in the 96-well plate layout, which acted as temperature controls in each XF analysis, allowing the Seahorse Wave software to automatically correct the data to account for any temperature drifts (Dranka *et al.*, 2011). As described in Section 3.12, the bioenergetics data obtained in this study was normalized according to the total DNA content per well, and since the DNA content of cells is tightly regulated, these CyQUANT assays can be used as a measure of cell number (Jones *et al.*, 2001; Steketee *et al.*, 2012). The normalized data (according to cell number) was thus used for all further statistical analyses and data interpretation.

4.6.2. Repeatability between duplicate plates

Seahorse Bioscience reports CV values of <20% between individual wells, different experiments and inter-day experiments (Dranka *et al.*, 2011). To assess the repeatability between duplicate plates, Pearson's correlation coefficient and the corresponding p-values were determined for the four pairs of duplicate plates (Table 4.9) for each of the bioenergetics parameters (Table 4.8). Basal respiration, ATP production and maximal respiration showed Pearson correlation coefficients of 0.707 to 0.910 with $p < 0.001$, for all four duplicate plates, thus indicating excellent repeatability for these three bioenergetic parameters. Inconsistent results were seen for all the other bioenergetics parameters, where some duplicate plates showed significant correlations, but others did not. For proton leak and non-mitochondrial respiration this was most likely since they were measured at very low levels, below the level of sensitivity for the instrument. All the other bioenergetic parameters were ratios and were thus influenced by more than one bioenergetic parameter. The percentage of total Pearson correlation coefficients that were not significant was 22%, thus concurring with the variability observed by Seahorse Bioscience.

4.6.3. Comparison of nine bioenergetics parameters between subject groups

The plate layout was initially designed to allow for a comparison between ME patients suspected to harbour the known pathogenic mtDNA variants and all other ME patients and healthy controls, but after verifying that the mtDNA variants in the U5 haplogroup were not present, this plate design was no longer relevant. However, in this plate layout essentially three groups were compared (as also mentioned in Section 4.5), namely: ME patients with haplogroup U (N = 8), ME patients with non-U haplogroups (N = 10) and healthy controls (N = 7). The data obtained for each of the bioenergetics parameters was sorted into these three groups for week 3 and week 6, and duplicate plates were included where possible (Table 4.9). Boxplots were constructed for each of the nine bioenergetics parameters, as shown in Figures 4.10a-i, where a fourth group was also included showing all ME patients (data from haplogroup U and non-U haplogroup ME patients combined; N = 18). Significant differences between subject groups were indicated with hashes.

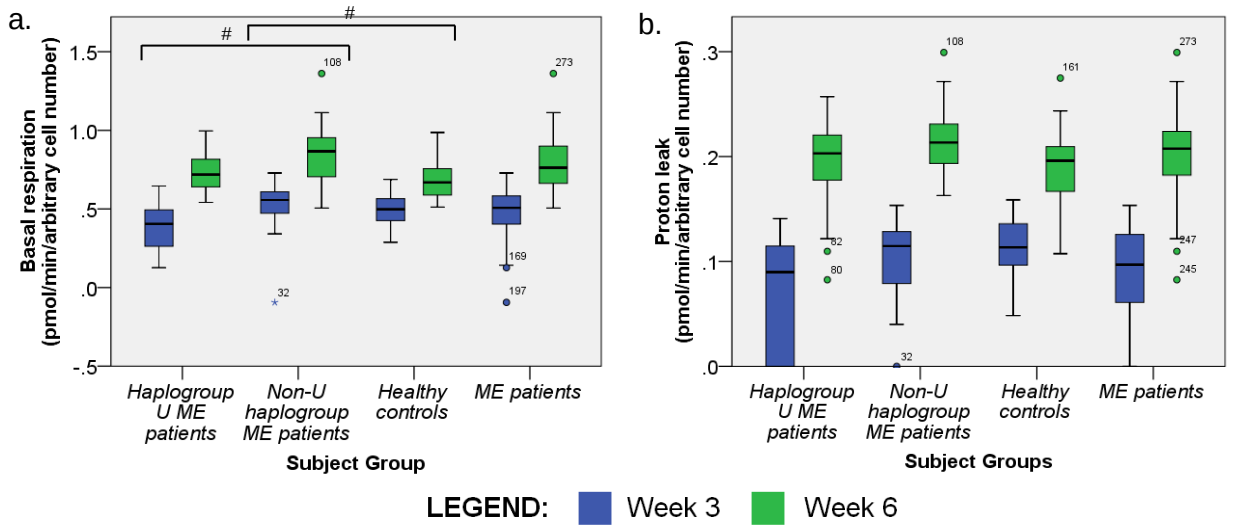

Figure 4.10a-b: Boxplots at week 3 and 6 for four subject groups: Haplogroup U ME patients (N = 56), non-U haplogroup ME patients (N = 60), healthy controls (N = 49) and ME patients (haplogroup U and non-U combined, N = 116); for **(a)** basal respiration and **(b)** proton leak. Circles represent outliers, asterisks represent extreme outliers and the numbers associated with these outliers are the case numbers in the data set. Hashes indicate significant differences between subject groups (# $p<0.05$; ## $p<0.01$; ### $p<0.001$).

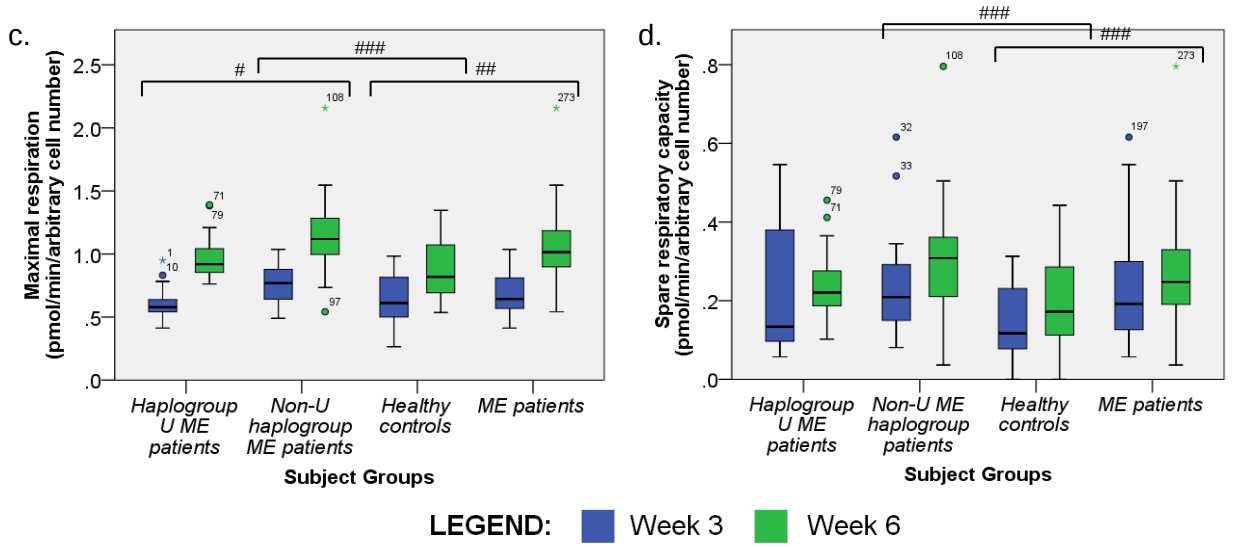

Figure 4.10c-d: Boxplots at week 3 and 6 for four subject groups: Haplogroup U ME patients (N = 56), non-U haplogroup ME patients (N = 60), healthy controls (N = 49) and ME patients (haplogroup U and non-U combined, N = 116); for **(c)** maximal respiration and **(d)** spare respiratory capacity. Circles represent outliers, asterisks represent extreme outliers and the numbers associated with these outliers are the case numbers in the data set. Hashes indicate significant differences between subject groups (# p<0.05; ## p<0.01; ### p<0.001).

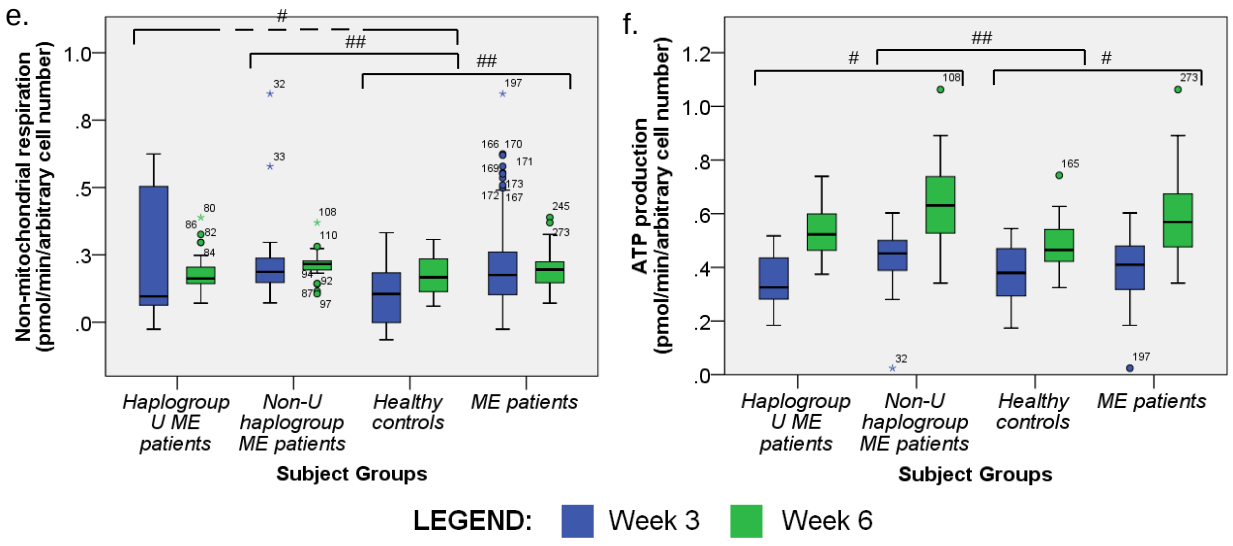

Figure 4.10e-f: Boxplots at week 3 and 6 for four subject groups: Haplogroup U ME patients (N = 56), non-U haplogroup ME patients (N = 60), healthy controls (N = 49) and ME patients (haplogroup U and non-U combined, N = 116); for **(e)** non-mitochondrial respiration and **(f)** ATP production. Circles represent outliers, asterisks represent extreme outliers and the numbers associated with these outliers are the case numbers in the data set. Hashes indicate significant differences between subject groups (# p<0.05; ## p<0.01; ### p<0.001).

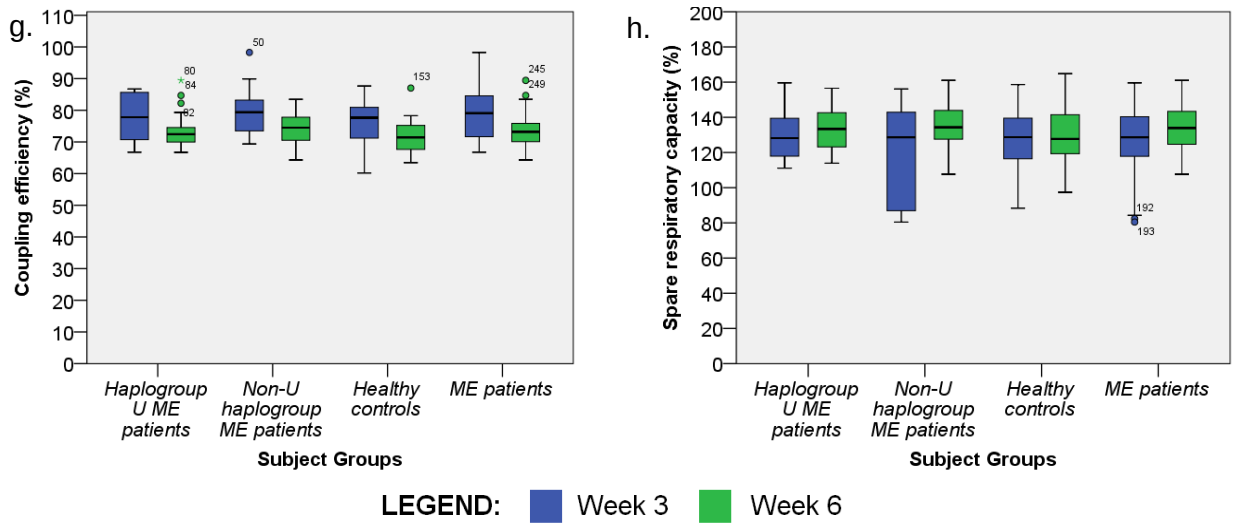

Figure 4.10g-h: Boxplots at week 3 and 6 for four subject groups: Haplogroup U ME patients (N = 56), non-U haplogroup ME patients (N = 60), healthy controls (N = 49) and ME patients (haplogroup U and non-U combined, N = 116); for **(g)** coupling efficiency and **(h)** spare respiratory capacity (%). Circles represent outliers, asterisks represent extreme outliers and the numbers associated with these outliers are the case numbers in the data set. There were numerous outliers present outside of the y-axis ranges shown here, which will be discussed later.

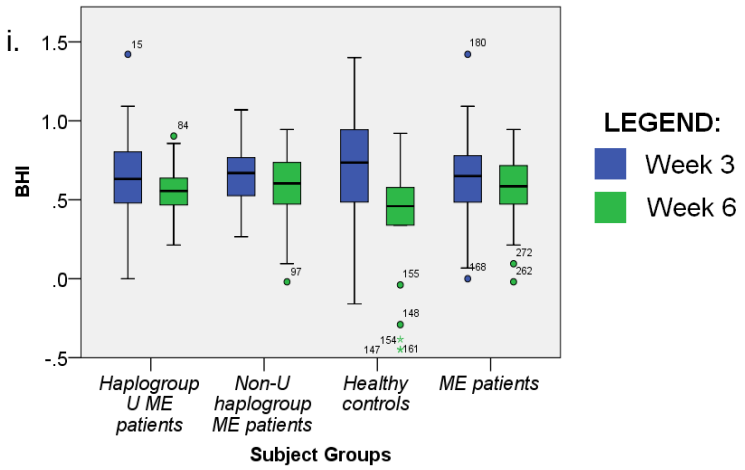

Figure 4.10i: Boxplots of the BHI at week 3 and 6 for four subject groups: Haplogroup U ME patients, non-U haplogroup ME patients, healthy controls and ME patients. Circles represent outliers, asterisks represent extreme outliers and the numbers associated with these outliers are the case numbers in the data set.

COMPARISON BETWEEN WEEK 3 AND WEEK 6

The OCR values for basal respiration, proton leak, maximal respiration, spare respiratory capacity and ATP production (Figures 4.10a, b, c, d and f, respectively) at week 3 were significantly lower for all the subject groups compared to week 6, as confirmed by an independent-means *t*-test ($p < 0.01$). In contrast, the BHI (Figure 4.10i) was significantly higher

at week 3 than week 6 for all subject groups ($p = 0.002$). No significant differences were obtained between week 3 and 6 for non-mitochondrial respiration, coupling efficiency and percentage spare respiratory capacity, as can be seen by the similar OCR values in Figures 4.10e, g and h.

These differences between week 3 and week 6 were thought to be due to an increase in RMCN over the time interval, but no significant difference was seen in the main effect of RMCN between week 3 and 6 (Section 4.5.1). However, significant differences were seen in the interaction between week and plate as well as between week and group, and the RMCN appeared to be increased at week 6 compared to week 3 for two of the three plates. The interaction between week and group was investigated by comparing the means of each subject group at week 3 and week 6, and this showed that haplogroup U and non-U haplogroup ME patients had an increased RMCN at week 6 compared to week 3, while the opposite was seen for the healthy controls. In Figures 4.10a, b, c, d and f increased respiration is seen at week 6 compared to week 3 for all of the subject groups, including the healthy controls. This indicates that the RMCN may be partially responsible for the difference seen in respiration at week 3 and week 6, but that other factors were also involved.

The BHI is a measure of the overall bioenergetic health status of cells, so a decrease in BHI from week 3 to week 6 could indicate a deteriorating phenotype with increased length of cell culture. However, this decrease was seen in both ME patients and healthy controls indicating that the decrease was more likely due to a change in overall cell culture conditions than a worsening phenotype in the ME patients.

Another possible explanation was a difference between experimental conditions at week 3 and week 6. The number of cells seeded at week 3 could have been consistently less than those seeded at week 6 due to a technical discrepancy in the Sceptor 2.0 handheld cell counter, but it was unlikely that this would have an effect since the data had been normalized to account for such differences. The two different batches of injectable compound stocks used at each time interval may have been diluted with slight differences, thus resulting in less/more of a compound being injected compared to the optimized concentration. However, this would then be seen in relative bioenergetics parameters such as the percentage spare respiratory capacity and coupling efficiency as well, but as can be seen from the corresponding figures, small to no differences were seen in these relative bioenergetic parameters between week 3 and 6.

It may thus be plausible to say that the 143B cybrid cells, in general, had increased overall respiration six weeks after cybrid cell development compared to three weeks after cybrid cell

development. The increase in respiration from week 3 to week 6 for each of the bioenergetic parameters appeared to be proportional since no differences were seen in the relative bioenergetic parameters (percentage spare respiratory capacity and coupling efficiency) between the two time intervals compared to all the other absolute bioenergetics parameters. The RMCN appeared to play a role to some extent, but it is possible that the respiration rate may also only stabilize once cells have been cultured for a certain period of time (as discussed in Section 4.5).

In general, the spread for all subject groups at week 6 appeared to be smaller than week 3, thus indicating less variability in week 6 than week 3. Since the analyses performed at week 6 were identical to those performed at week 3, the improvement in the variability at week 6 could be attributed to the experience and practice obtained at week 3, thus allowing for less human error and more accurate practical execution at week 6.

COMPARISON BETWEEN SUBJECT GROUPS

The spread of the data, as indicated by the inter-quartile range, was relatively similar in most cases, except for the haplogroup U ME patients. This subject group, at week 3, showed a very wide spread for proton leak, spare respiratory capacity and non-mitochondrial respiration, and a very narrow spread for maximal respiration; compared to all other subject groups. The non-U haplogroup ME patients also showed a wide spread at week 3 for the percentage spare respiratory capacity. Since this variability in haplogroup U ME patients was not seen at week 6, it was most likely due to human error, or possibly due to the confluency of the cells prior to cell seeding for the XF analyser, as also discussed in Section 4.5.2.

When comparing the first three subject groups in Figure 4.10, there appeared to be a general trend at both week 3 and 6 for basal respiration, maximal respiration, spare respiratory capacity, and ATP production (all absolute parameters), where for each of these bioenergetic parameters the non-U haplogroup ME patients had the highest OCR medians followed by the healthy controls and then the haplogroup U ME patients, with the lowest OCR medians. A one-way ANOVA was performed to determine the effects of subject group on each bioenergetic parameter, and these results showed significant differences for basal respiration ($p = 0.015$), maximal respiration ($p = 0.0002$), spare respiratory capacity ($p = 0.0002$), non-mitochondrial respiration ($p = 0.003$) and ATP production ($p = 0.001$). Tukey's HSD post-hoc test was then performed, as shown in Table E1 (Appendix E), and the results confirmed the trend seen for these parameters in Figure 4.10, where non-U haplogroup ME patients had significantly increased OCR values compared to haplogroup U ME patients and healthy controls ($p < 0.043$).

The difference seen between the haplogroup U and non-haplogroup U ME patients corresponded with other studies using 143B cybrids where it was found that haplogroups UK and J had decreased basal respiration, ATP production and maximal respiration compared to haplogroup H (Gómez-Durán *et al.*, 2010; Gómez-Durán *et al.*, 2012). Since seven of the ten patients in the non-U haplogroup ME patient group had haplogroup H, the comparisons being made in the current study were effectively also between haplogroup U and haplogroup H. However, in these studies by Gómez-Durán et al. they also found a decreased RMCN in haplogroup U patients which they associated with impaired energy production due to decreased mitochondrial protein synthesis and complex IV activity, contrary to the haplogroup U ME patients here who had an increased RMCN compared to the non-U haplogroup ME patients (Section 4.5.3).

A statistical comparison could not be made between the haplogroups of the healthy controls and the ME patients due to the small sample sizes of the haplogroups within the healthy controls. But comparisons could be made between the ME patients and healthy controls as a whole using the one-way ANOVA and Tukey's HSD post-hoc tests described above. The ME patients showed significantly increased OCR values compared to healthy controls for maximal respiration, spare respiratory capacity, non-mitochondrial respiration and ATP production. This increased ATP production in ME patients was contrary to the decreased ATP levels seen in other *in vivo* studies (as discussed in Section 2.4.2). The increased ETS capacity, ATP production and spare respiratory capacity seen in the ME patients was contrary to the mitochondrial dysfunction that was expected to be seen, but it may possibly indicate that ME patient cybrid cells had a higher energy demand when placed under stress (since no differences were seen between ME patients and healthy controls for basal respiration) and that additional compensatory mechanisms were activated in the ME patient cybrids to account for this. Non-mitochondrial respiration is believed to be a negative indicator of bioenergetic health and since this was increased in the ME patients, it could indicate that these cells were indeed more stressed than the healthy controls.

In Figure 4.10, it appeared that the differences seen between ME patients and healthy controls were more apparent at week 6 than week 3. This may indicate that differences between the patient and healthy control groups were enhanced the longer the cybrid cells were cultured, but further analyses would need to be performed at later time intervals to confirm this observation.

Proton leak and non-mitochondrial respiration, in general, showed wide ranges and numerous outliers. This was most likely since these two bioenergetic parameters were measured at very low OCR levels where the instruments sensitivity was not optimal and thus resulted in more

inaccurate readings compared to the other bioenergetic parameters. Numerous outliers were also present, but not shown, in Figures 4.10g and h. These outliers were only present at week 3 for haplogroup U ME patients, non-U haplogroup ME patients and ME patients and ranged between -1158% and 786%. Since the coupling efficiency and spare respiratory capacity were percentages measured by dividing ATP production and maximal respiration, respectively, by the basal respiration, the variation seen in each of these three bioenergetic parameters was compounded in the coupling efficiency and percentage spare respiratory capacity. The improvement in variation seen at week 6 may thus also be attributed to improved technique and thus less human error.

4.6.4. Correlation between RMCN and bioenergetics parameters

In order to determine whether or not there was any correlation between the RMCN and each of the nine bioenergetics parameters, Pearson's correlation coefficient (r) was determined along with the corresponding p-value for each subject group, as shown in Table 4.10. Significant p-values of <0.05 were highlighted in bold and marked with an asterisk.

With a p-value of 5% and a total of 72 correlations, one would expect approximately four statistically significant correlations to occur by chance in this data. In total, only five statistically significant correlations were obtained and after correcting for multiple testing, none of these values would remain significant. A correlation between any of the bioenergetic parameters and the RMCN could thus not be found. The lack of any correlation between the RMCN and bioenergetics parameters of the cells may have been an indication that the RMCN was not directly linked to the respiration in these cells, or that RMCN changes could occur within the cybrid cells in a short period of time (<24 hours). The cells that were used to determine the RMCN were obtained at the time that the cells were seeded for XF analysis. It was thus possible that at the time of the XF analysis (24 hours later), changes may have occurred in the RMCN since the sample had been obtained.

Repeating the analyses once the cybrid cells had reached passage 20 and the RMCN had reached stable levels (as discussed in Section 4.5) could possibly provide a better correlation between the RMCN and bioenergetics parameters. The RMCN could also be more accurately determined by isolating DNA from cybrid cells obtained directly after the XF analysis, although the injectable compounds may also have an effect on the RMCN. It is known that mtDNA is constantly being turned over in cells and that an entire mtDNA molecule can be replicated in less than 90 minutes (Clayton, 1982; Elson *et al.*, 2001). The 24 hour incubation period after the cybrid cells were obtained for RMCN analyses, as well as the duration of an XF analysis (approximately two hours), is thus ample time for changes in the RMCN to occur.

Table 4.10: Pearson's correlation coefficient and p-values for four subject groups, at week 3 and week 6, testing the correlation between each bioenergetic parameter and the RMCN.

Bioenergetic parameter	Statistic	Haplogroup U ME patients		Non-U haplogroup ME patients		Healthy controls		ME patients	
		Week 3	*Week 6*	*Week 3*	*Week 6*	*Week 3*	*Week 6*	*Week 3*	*Week 6*
Basal respiration	*r*	-0.204	-0.237	-0.150	-0.140	0.084	0.295	-0.214	-0.309
	p-value	0.338	0.192	0.429	0.460	0.671	0.194	0.120	**0.014***
Proton leak	*r*	-0.267	-0.341	-0.115	0.069	-0.095	0.136	-0.246	-0.310
	p-value	0.207	0.056	0.546	0.718	0.629	0.557	0.073	**0.014***
Maximal respiration	*r*	0.256	-0.059	-0.412	-0.015	0.026	0.263	-0.122	-0.197
	p-value	0.227	0.747	**0.024***	0.936	0.896	0.249	0.378	0.124
Spare respiratory capacity	*r*	0.377	0.234	-0.355	0.148	-0.050	0.181	0.116	0.005
	p-value	0.069	0.198	0.054	0.436	0.799	0.433	0.402	0.970
Non-mitochondrial respiration	*r*	0.345	0.067	-0.147	0.178	-0.106	0.134	0.188	-0.036
	p-value	0.099	0.717	0.439	0.347	0.593	0.561	0.174	0.779
ATP production	*r*	0.032	-0.157	-0.169	-0.167	0.112	0.286	-0.107	-0.272
	p-value	0.883	0.392	0.373	0.377	0.571	0.209	0.442	**0.032***
Coupling efficiency (%)	*r*	-0.030	0.231	-0.033	-0.184	0.161	0.072	-0.027	0.057
	p-value	0.889	0.203	0.862	0.331	0.414	0.756	0.847	0.658
Spare respiratory capacity (%)	*r*	-0.068	0.339	0.199	0.327	-0.044	0.075	-0.011	0.229
	p-value	0.752	0.058	0.292	0.078	0.823	0.747	0.939	0.074
BHI	*r*	0.132	0.468	-0.176	-0.034	0.085	0.243	0.038	0.184
	p-value	0.538	**0.007***	0.352	0.860	0.669	0.289	0.783	0.152

* Indicates significant p-values of <0.05.

4.7. 143B and RD ρ^0 cells – *Objective 6*

4.7.1. 143B cybrids

When blood was collected from all the subjects, enough isolated blood platelets were stored for two batches of cybrid cells to be created per patient (initially intended to be used for two different ρ^0 cell lines). The first batch of 143B cybrid cells were created in three batches, one batch per week. The cybrid cells of all subjects were then analysed using the XF analyser, two weeks after the last batch was created. From these bioenergetics results, major batch effects could be seen, where the last batch had significantly lower OCR measurements for all bioenergetics parameters compared to the first two batches. The RMCN results obtained for these cells confirmed and possibly explained this observation since the last batch had significantly lower RMCN results compared to the previous two batches.

4.7.2. RD ρ^0 cell development

The RD cell line was selected for determining the effect of a different nuclear background (compared to 143B) on the cybrid cells. This cell line was selected since it was obtained from muscle tissue and was thus expected to be more reliant on OXPHOS than the 143B cell line. A different cell line was selected since the nuclear background influences the genotype-phenotype relationship and previous cybrid studies have shown that different nuclear backgrounds can cause cells to shift away from, or towards variant mtDNA (Wilkins *et al.*, 2014). To develop the RD ρ^0 cell line, RD cells were treated with 50 ng/mL EtBr (and supplemented with 1 mM pyruvate and 50 µg/mL uridine) over a prolonged period of time. As expected, the RMCN of the RD cells decreased with continued exposure to EtBr (shown in Figure 4.11), but after approximately three weeks, the RMCN began to increase again (despite continued EtBr exposure). The only author with published data on RD ρ^0 cells (Vergani *et al.*, 2000; Vergani *et al.*, 2004; Vergani *et al.*, 2007) was contacted for advice. This experiment was then repeated three times, each time altering a different experimental condition such as: increased FBS concentration from 10% to 30% (w/v) and increased glutamine concentration from 2 mM to 6 mM; replenishing the culture media at more regular intervals; and splitting the cells at 70-80% confluency. Exactly the same result was obtained for all three replicated experiments, where one of these experiments is shown in Figure 4.11.

The only difference between the protocol followed and the advice provided by Prof. Vergani was the FBS that was used. At the time of these experiments, FBS from Gibco (as was used by Prof. Vergani's laboratory) was not available in South Africa. It is thus possible that the FBS (Biochrom) used in this study did not contain the necessary growth factors for RD ρ^0 cell development that is ordinarily found in FBS from Gibco.

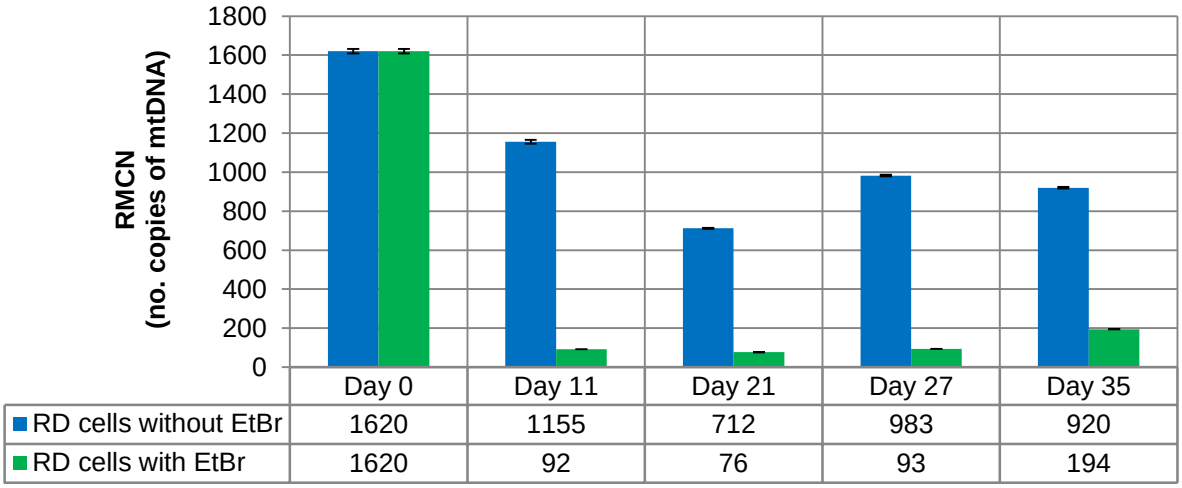

	Day 0	Day 11	Day 21	Day 27	Day 35
RD cells without EtBr	1620	1155	712	983	920
RD cells with EtBr	1620	92	76	93	194

Figure 4.11: Histogram showing the RMCN ± CV% for control RD cells and RD cells treated with EtBr over a certain time period.

4.7.3. RD cybrids

The next approach was to obtain the cells from the only author with published data using RD ρ^0 cells (Vergani *et al.*, 2000; Vergani *et al.*, 2004; Vergani *et al.*, 2007). Prof. Lodovica Vergani (University of Padova, Department of Neurosciences, Padova, Italy) generously donated RD ρ^0 cells to our laboratory. These cells were found to be mycoplasma-free and true ρ^0 cells with an RMCN of 0.4. They were cultured for approximately two weeks to test their sustainability and the cells were found to grow sustainably in the culture media (despite using Biochrom FBS). The RMCN also remained constant during this time.

Blood platelets from a test subject were then used in a test run to develop a cybrid cell line using the RD ρ^0 cells. During selection, 143B cybrids were cultured in media containing BrdU and lacking uridine since the only cells able to survive under those conditions were blood platelets that had fused with the 143B ρ^0 cells (which were thymidine kinase negative, TK^-). Any residual white blood cells, unfused blood platelets, unfused ρ^0 cells, or white blood cells fused with ρ^0 cells, were unable to survive under these conditions (Chomyn, 1994). Unlike the 143B ρ^0 cells, the RD ρ^0 cells were not TK^-, so BrdU could not be used for this selection procedure. The RD cybrids were thus only cultured in uridine-free media causing any residual unfused RD ρ^0 cells to die, but white blood cells, unfused blood platelets and white blood cells fused with ρ^0 cells, could not be eliminated. The RD cybrids grew very slowly compared to the 143B cells, and after two weeks, the RMCN was found to be 22, compared to an RMCN of at least 100 normally seen in the 143B cybrids at the same time interval. This test RD cybrid cell line was also analysed after two weeks using the XF analyser and results obtained were normally seen in a ρ^0 cell line where all OCR readings were near to 0 pmol/min.

Based on these results, the lack of any literature for non-differentiated RD cybrids, and the apparent lack of RD cells being a recognised ρ^0 cell line (Wilkins *et al.*, 2014), it was thus decided that the RD cell line was not a suitable cell line for developing cybrid cells to be analysed using an XF analyser. The remaining blood platelets for all of the patients were then used to create a second batch of 143B cybrids where all cybrids were created on the same day to eliminate the batch effects seen previously. This batch of 143B cell lines were then analysed as discussed in Sections 3.11 and 4.6.

4.8. Pathogenicity and the mutational load hypothesis – *Objective 7*

Since the absence of the three mtDNA variants (m.7497G>A, m.9185T>C and m.10197G>A) had been verified in the ME patients, the first question proposed in the problem statement (Section 2.7.1), which asked whether these known pathogenic mtDNA variants (at low allele frequencies) had a functional effect on energy metabolism, was no longer applicable. Despite successful transfer of mtDNA from patient blood platelets to cybrid cells, as required by the mtDNA pathogenicity point mutation criteria (Section 2.5.1), no assessment of the pathogenicity of these mtDNA variants could thus be carried out.

The second question that was proposed in the problem statement, which asked whether the combination of rare non-synonymous variants (the mutational load hypothesis) in the mtDNA of patients could have a functional effect on energy metabolism, was however still relevant. The whole mtDNA genome adjusted MutPred scores indicated in Table 4.3 (Section 4.3.2) were correlated to each of the nine bioenergetic parameters discussed in Section 4.6.3. The Pearson correlation coefficients (r) and corresponding p-values are shown in Table 4.11, where significant p-values (<0.05) were highlighted in bold and marked with an asterisk.

Compared to the five significantly correlated bioenergetic parameters obtained for the RMCN (Section 4.6.4), 15 significantly correlated bioenergetic parameters were obtained for the MutPred scores, thus indicating a possible link between certain bioenergetic parameters and the MutPred scores, which was unlikely to have occurred by chance. Since variation was also seen between plates (Section 4.6.2), this strengthened any significant correlations that were seen across different plates. Of the nine bioenergetic parameters, eight were significantly correlated at week 6 for non-U haplogroup ME patients, while at week 3 only maximal respiration and ATP production had negative significant correlations. Week 6 of the haplogroup U ME patients showed the same pattern where maximal respiration and ATP production had negative significant correlations. The BHI was significantly correlated for the non-U haplogroup ME patients at week 6, and the healthy controls at both week 3 and week 6. Since all of these

significant correlations were negative, they possibly indicated that an increase in MutPred score led to a decrease in the OCR of the relevant bioenergetic parameter.

The fact that significant correlations were not seen in all bioenergetic parameters was understandable since one would expect certain bioenergetic parameters to correlate more closely with the MutPred scores than others. Where significant correlations were seen for a specific bioenergetic parameter, but not in all subject groups, it may be possible that other mtDNA variants or factors played a role in compensating for (or exaggerating) the effects from the non-synonymous variants. In this study, the type or position of the variants seen in patients and healthy controls was not studied; rather averages of the MutPred scores for all of these variants in a patient were determined. Individual SNPs could thus also have played a role. The interaction between the 143B nuclear background and each patient's mtDNA and the effect thereof was also not known and most likely played a significant role, since it is well-known that the nuclear background of the ρ^0 cell line used has a major influence on mitochondrial genotype-phenotype relationships and can lead to shift in the proportion of variant mtDNA or wild-type mtDNA (Dunbar *et al.*, 1995).

The bioenergetic parameters of most interest were maximal respiration and ATP production since significant correlations were seen at both week 3 and week 6 for the non-U haplogroup ME patients and at week 6 for the haplogroup U ME patients, as shown in Figures 4.12 and 4.13 respectively. Significant correlations were thus expected to be seen in ME patients as a whole, but as seen in Table 4.11, this was not the case. The reason for this was discussed in Section 4.3.2, where significant differences were seen between the MutPred scores of haplogroup U ME patients and non-U haplogroup ME patients. This can also be seen in Figures 4.12 and 4.13 where the haplogroup U ME patients had MutPred scores ranging from 0.30 to 0.37, while the non-U haplogroup ME patients had MutPred scores ranging from 0.36 to 0.50. The haplogroup of the ME patients thus appeared to be an important genetic background that should be taken into account when investigating the effect of rare non-synonymous variants in a patient group.

The BHI was also significantly correlated for the healthy controls at week 3 and week 6, as well as for the non-U haplogroup ME patients at week 6. Since none of the other bioenergetics parameters were significantly correlated for the healthy controls, and since the p-values were very close to 0.05, the BHI correlation was not investigated further.

Table 4.11: Pearson correlation coefficients and p-values for four subject groups, at week 3 and week 6, showing the correlation between each bioenergetic parameter and the whole mtDNA genome adjusted MutPred scores.

Bioenergetic parameter	Statistic	Haplogroup U ME patients		Non-U haplogroup ME patients		Healthy controls		ME patients	
		Week 3	*Week 6*	*Week 3*	*Week 6*	*Week 3*	*Week 6*	*Week 3*	*Week 6*
Basal respiration	*r*	-0.207	-0.377	-0.355	-0.508	-0.290	-0.273	0.160	0.008
	p-value	0.332	**0.033***	0.054	**0.004***	0.135	0.231	0.248	0.950
Proton leak	*r*	0.066	-0.245	-0.288	-0.186	-0.101	-0.003	0.166	0.087
	p-value	0.758	0.177	0.123	0.326	0.610	0.991	0.231	0.503
Maximal respiration	*r*	-0.256	-0.372	-0.384	-0.544	-0.305	-0.344	0.186	-0.005
	p-value	0.227	**0.036***	**0.036***	**0.002***	0.115	0.127	0.178	0.972
Spare respiratory capacity	*r*	-0.001	-0.184	-0.045	-0.492	-0.256	-0.314	0.024	-0.021
	p-value	0.998	0.314	0.812	**0.006***	0.189	0.166	0.864	0.871
Non-mitochondrial respiration	*r*	-0.006	-0.084	0.110	-0.453	-0.057	-0.060	0.022	0.036
	p-value	0.978	0.649	0.562	**0.012***	0.774	0.797	0.875	0.783
ATP production	*r*	-0.375	-0.370	-0.370	-0.518	-0.279	-0.312	0.082	-0.014
	p-value	0.071	**0.037***	**0.044***	**0.003***	0.151	0.168	0.556	0.916
Coupling efficiency (%)	*r*	0.095	-0.056	-0.116	-0.469	-0.252	-0.274	-0.028	-0.140
	p-value	0.658	0.761	0.543	**0.009***	0.195	0.229	0.842	0.277
Spare respiratory capacity (%)	*r*	0.234	0.057	0.010	-0.401	-0.331	-0.295	0.161	-0.071
	p-value	0.272	0.758	0.959	**0.028***	0.085	0.195	0.245	0.586
BHI	*r*	-0.369	-0.301	-0.184	-0.465	-0.384	-0.433	-0.153	-0.229
	p-value	0.076	0.094	0.331	**0.010***	**0.044***	**0.050***	0.271	0.073

* Indicates significant p-values of <0.05.

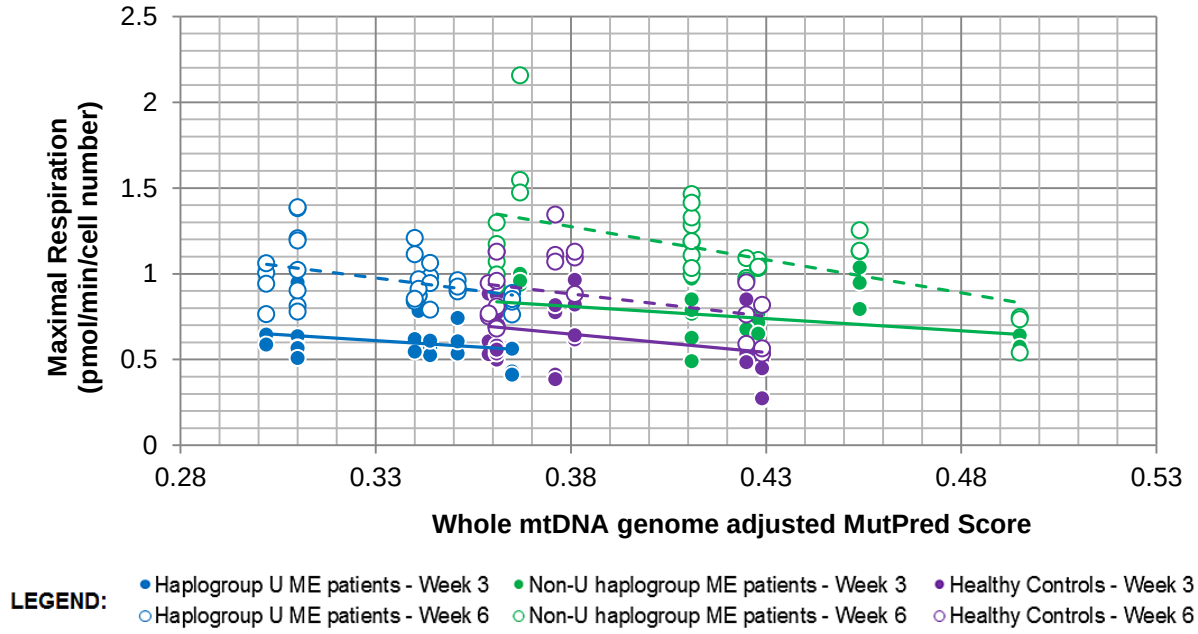

Figure 4.12: Scatter plot depicting the correlation between maximal respiration and the whole mtDNA genome adjusted MutPred scores for haplogroup U ME patients, non-U haplogroup ME patients and healthy controls at both week 3 and week 6. Trendlines for week 3 were depicted with a solid line, while those for week 6 were depicted with a broken line.

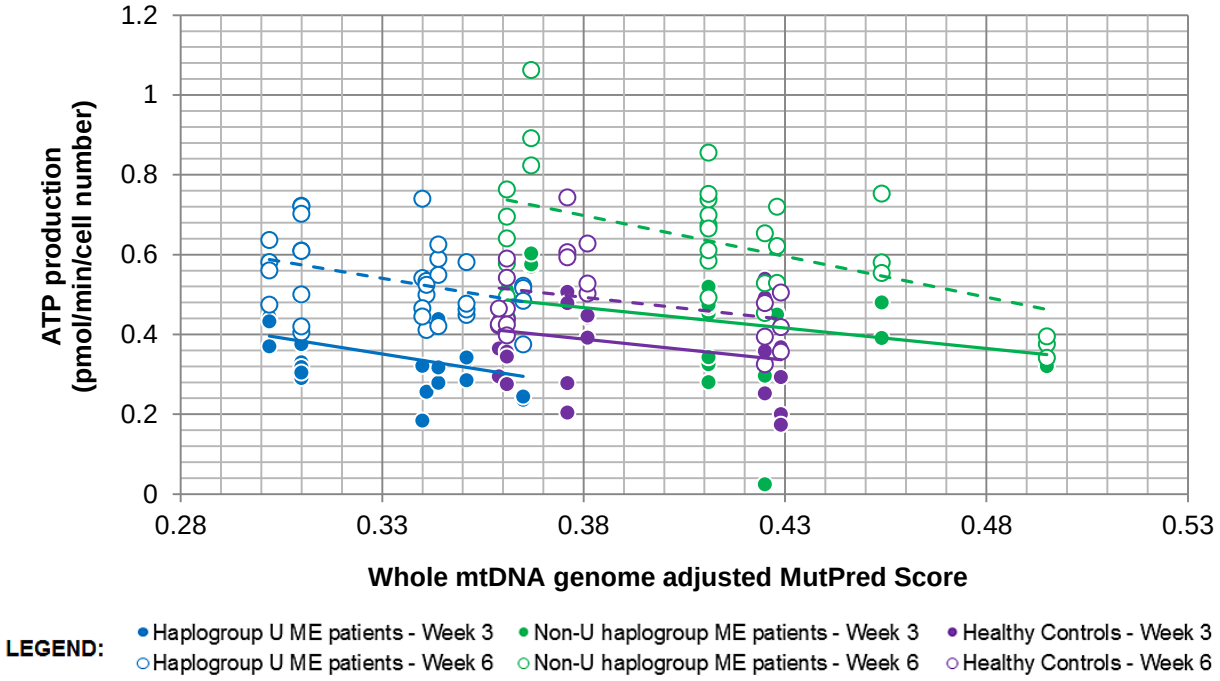

Figure 4.13: Scatter plot depicting the correlation between ATP production and the whole mtDNA genome adjusted MutPredscores for haplogroup U ME patients, non-U haplogroup ME patients and healthy controls at both week 3 and week 6. Trendlines for week 3 were depicted with a solid line, while those for week 6 were depicted with a broken line.

From Figures 4.12 and 4.13 it can be seen that there appeared to be a decrease in maximal respiration and ATP production with increasing whole mtDNA genome adjusted MutPred scores. Since these correlations were only significant for the haplogroup U ME and non-U haplogroup ME patients, and not for the healthy controls, this could indicate a possible premise for the mutational load hypothesis. The presence of certain rare non-synonymous mtDNA variants may lead to decreased synthesis of specific OXPHOS subunits, which in turn would lead to decreased OXPHOS activity and thus place the cell in a vulnerable state. The occurrence of other non-synonymous mtDNA variants would then be more likely to be harmful. Specific non-synonymous mtDNA variants were not investigated here, however, depending on the gene in which the variant occurred, certain OXPHOS complexes may be more affected than others and may lead to a decreased OXPHOS rate or increased ROS production (Raule *et al.*, 2014). Increased ROS could then lead to further damage of various ETS complexes, and thus cause impaired OXPHOS. Numerous rare non-synonymous mtDNA variants may thus have had a cumulative effect in increasing the risk for ME, as seen by decreased ATP synthesis and decreased ETS capacity.

CHAPTER 5: Conclusions

5.1. Rationale and aim of the study

This study was initiated due to a recognized necessity to develop functional *in vitro* tools to investigate mtDNA variants detected in diseases. The initial aim of this study was to investigate the bioenergetic effect of three known pathogenic mtDNA variants (m.7497G>A, m.9185T>C and m.10197G>A) found at low allele frequencies in patients with ME, using the Seahorse XF^{e}96 analyser (Jaksch *et al.*, 1998; Kirby *et al.*, 2004; Moslemi *et al.*, 2005). In order to do this, the protocols and techniques required to operate the XF analyser, needed to be developed and optimized using various selected cell lines. The model used to investigate this effect was cybrid cells, comprising of each patient's mtDNA against the same nDNA background. NGS was also performed using blood obtained from the ME patients who were previously shown to harbour one or more of the three known pathogenic mtDNA variants. Verification of these mtDNA variants had proved problematic prior to this study, and the NGS performed during this study provided the final evidence that these variants were in fact not present in any of the patients, and had most likely been sequencing artefacts. The aim was thus shifted to focus more on developing and evaluating the cybrid and respirometry techniques and, with regard to the role of mtDNA variants in ME, to investigate the effect of homozygous rare non-synonymous variants in ME patients that could possibly individually or collectively affect bioenergetics parameters – the so-called mutational load hypothesis. The conclusions made for each objective will be discussed here.

5.2. Objective 1 – Development of techniques and protocols for the Seahorse XF^{e}96 analyser

The cell seeding density, oligomycin and FCCP concentrations, and pyruvate and glucose concentrations in the assay media were successfully optimized for six cell lines (143B, RD, SH-SY5Y, HEPG2, A549 and C2C12), using the XF analyser, as shown in Table 4.1, Section 4.2.5. Of these six cell lines, only two were used for further objectives of this study, but it was still considered essential to evaluate and report the optimization of the XF conditions for these other cell lines that are frequently used in bioenergetics investigations. The experience and skills gained were used to develop the standard assay template shown in Appendix A, and to analyse the cybrid cells which were later developed.

Cell seeding density varied greatly between cell lines, presumably due to cell diameter, the growth doubling time and the metabolism of different cell lines. The optimized oligomycin concentration that provided maximal ATP synthase inhibition was found to be constant for all

cell lines at 1 µM and it was thus concluded that oligomycin was not a condition that needed to be optimized for future cell lines, unless otherwise specified in literature. Optimized FCCP concentrations were found to vary between 0.5 and 1 µM, thus depicting that very specific optimization of FCCP should always be carried out. Glucose and pyruvate concentrations were shown to influence both basal respiration and maximal respiration, thus indicating that optimized concentrations should be selected, based on the purpose of individual experiments. In general, 1 mM pyruvate and 5 mM glucose in the assay medium should prove sufficient for typical XF analyses, where basic OXPHOS parameters/mitochondrial function are the aim of the experiment.

As also advised by the supplier, it was concluded from these initial optimization experiments that a thorough optimization of reaction conditions for bioenergetics investigations is essential, even if conditions are reported in literature, and will greatly improve the outcomes of subsequent investigations.

5.3. Objective 2 – Next-generation sequencing and MutPred scores

As mentioned above, three known pathogenic mtDNA variants (m.7497G>A, m.9185T>C and m.10197G>A) were detected in six ME patients, at low allele frequencies (~5-20%), in a previous study done by the CHM, NWU. NGS using the Ion Torrent PGM and MiSeq both successfully detected the mtDNA variants, but at inconsistent levels, while pyrosequencing and real-time PCR proved unsuccessful for detecting these mtDNA variants. Sequencing performed during this study, using fresh blood, once again made use of the Ion Torrent PGM, but deeper coverage was obtained and more recent Ion Torrent software tools were used. Results showed unsuccessful detection of these mtDNA variants in any of the ME patients and it was thus concluded that the mtDNA variants originally seen were more likely sequencing artefacts, that were not detected during this study (or using pyrosequencing and real-time PCR), due to the improved accuracy of updated software tools.

From the NGS results obtained from this study and a prior study using the selected subjects, mtDNA sup-haplogroups and MutPred scores could be determined. MutPred scores are computed scores which compare non-synonymous protein variants with known wild-type protein sequences to predict what effect such a variant may have on protein structure and function. Other models, such as SIFT, can also be used to predict the effect of non-synonymous variants, but this was beyond the scope of this study. ME patients with non-U haplogroups were found to have increased MutPred scores compared to haplogroup U ME patients. A spot check was performed where randomly selected patient cybrid cell lines were also sequenced and these results confirmed that the patient mtDNA along with mtDNA variants were successfully

transferred to the ρ^0 cells, since the mtDNA sub-haplogroup and MutPred scores obtained from patient's blood and cybrid cells were identical.

5.4. Objective 3 – Cybrid cell development and mtDNA transfer confirmation using PCR-RFLP haplogroup analysis

Due to the cost of NGS, it could not be used to confirm mtDNA transfer from the blood platelets to the ρ^0 cells for *all* patient cybrid cell lines. The PCR-RFLP approach was used instead to determine the mtDNA haplogroup of all cybrid cells. From the gel electrophoresis results the haplogroups for all patients were successfully determined and for all patients (except one) these haplogroups corresponded to the haplogroups obtained from NGS results in a previous study that used the patient's blood. The one patient that differed had an mtDNA sub-haplogroup unlike all the other patients and it was concluded that this sub-haplogroup possibly skewed the results of the main haplogroup when using the PCR-RFLP approach. Taken together, it was concluded after completing this objective that the transfer procedures were effective and accurate in the transfer of mtDNA from blood platelets to ρ^0 cells and that cybrids were thus effectively formed.

5.5. Objective 4 – RMCN determination of cybrid cells using real-time PCR

The RMCN of each patient cybrid cell line was tested numerous times, each time providing different results, but still confirming successful mtDNA transfer from blood platelets to ρ^0 cells for all patients. An increase in RMCN between week 3 and week 6 (as was expected) could not be directly determined, but when looking at the interaction between week and plate, this increase could be seen in two out of three plates. Based on cell growth versus cell death during the cybrid selection process, it appeared that the RMCN reached the stable minimal level that was required for cell survival, after 2-3 weeks.

The cell confluency was found to have a significant impact on the RMCN. Flasks of the same patient cybrid cell lines that were over confluent resulted in a significantly decreased RMCN compared to the cells obtained from flasks that were not as confluent, presumably due to the decreased cell growth and increased cell death normally seen in over confluent cells. Gómez-Durán et al. (2010) indicated that 143B cybrids only reached steady-state levels of RMCN at passage 20 and higher, where cells in this study were only cultured until passage 11. This reference, which was unfortunately only noted after completion of this study, may explain the large variability seen in the RMCN values obtained for patients at different time intervals and on different plates. However, as mentioned by Brown *et al.* (2015), the risk for genetic or epigenetic changes in the cultured cells may increase, the longer they are cultured.

Haplogroup U ME patients were found to have a significantly higher RMCN than the non-U haplogroup ME patients and the healthy controls, while ME patients (haplogroup U and non-U combined) had an increased RMCN compared to healthy controls. This increased RMCN in ME patients could be an indication of increased ROS since higher ROS levels have been found to increase mtDNA replication (Achanta *et al.*, 2005).

As also experienced during this study, despite the great amount of literature available for studies investigating mtDNA content, many inconsistencies exist, in many cases data cannot be compared between studies due to the methodologies used, and there is a lack of consensus regarding the actual mtDNA copy numbers in specific cell lines (Malik & Czajka, 2013).

5.6. Objective 5 – Determination of bioenergetics parameters using the XF analyser

Nine bioenergetic parameters were measured in four subject groups: haplogroup U ME patients, non-U haplogroup ME patients, healthy controls and ME patients (as a whole). As shown by boxplots, for almost all of the bioenergetic parameters (except non-mitochondrial respiration, coupling efficiency, percentage spare respiratory capacity and BHI) and in all subject groups, there was significantly increased respiration at week 6 compared to week 3, which appeared to be partially due to an increased RMCN at week 6. The non-U haplogroup ME patients had significantly higher OCR values than haplogroup U ME patients for basal respiration, maximal respiration and ATP production. This corresponded to Gómez-Durán et al. (2010) who found 143B cybrids with haplogroups UK to have decreased basal respiration, ATP production and maximal respiration compared to those cybrids with haplogroup H.

Compared to the healthy controls, ME patients were shown to have significantly higher OCR values for maximal respiration, spare respiratory capacity, non-mitochondrial respiration and ATP production. Thus, no obvious bioenergetic irregularities or mitochondrial dysfunction were observed in the *in vitro* bioenergetics data obtained from these ME patients compared to healthy controls, contrary to the major mitochondrial abnormalities that have been reported from in vivo studies on ME (Section 2.4.2). The increased respiration seen in these ME patients could be an indication that the cells were under more stress and that compensatory mechanisms had been activated. Since cancer cells tend to lean more towards glycolysis than OXPHOS, cultivating the cells in galactose media lacking glucose may increase respiration and thus more clearly distinguish differences in OXPHOS between patients by forcing the cells to rely more heavily on mitochondrial respiration (Mueller et al., 2012). Since ME appears to be a systemic disease and manifests differently and to varying degrees in various patients, more information could be gathered from future studies by using a whole organ systemic approach (Hollingsworth *et al.*, 2010).

No significant correlation was found between the bioenergetic parameters for each subject group (at week 3 and 6) and the RMCN. This may have been attributed to the unstable RMCN levels seen at lower passage numbers, or due to RMCN changes in the 24 hours from when the cybrid cell samples were obtained for RMCN analysis and when they were actually analysed in the XF analyser. The relationship between the RMCN results and bioenergetics parameters could be more accurately tested in the future by possibly isolating the DNA from the cells in the XF cell culture plate directly after the XF analysis (to then be used for RMCN analyses). It was not possible to do this during this study due to the number of plates analysed and the time and cost that would be associated with determining the RMCN for each well on a plate. Future studies should also culture the cybrid cells for longer time periods to allow the RMCN to reach steady-state levels and thus possibly provide more accurate results.

5.7. Objective 6 – Effect of a different nuclear background when using a different ρ^0 cell line

Due to the effect that a different nuclear background (of a different ρ^0 cell line) is known to have on the genotype-phenotype relationships of cybrid cells, all experiments were initially intended to be repeated using a more OXPHOS-dependent RD ρ^0 cell line. Attempts were made to develop an RD ρ^0 cell line using EtBr, but proved unsuccessful, possibly due to the FBS available for this study. After contacting the only author to have developed these cells, ready-made RD ρ^0 cells were obtained. These RD ρ^0 cells were used in a test run to develop cybrid cells. Selection against white blood cells and unfused blood platelets could not be performed using BrdU (as was done for the 143B cells) since RD cells were not TK^-. This, combined with slow cell growth, a low RMCN and a lack of any literature using non-differentiated RD cybrids resulted in the conclusion that RD ρ^0 cells were not a suitable cell line for testing the effect of a different nuclear background. For future studies, the use of a different ρ^0 cell line such as NT2 (teratocarcinoma), A549 or SH-SY5Y cells, which have been well documented in cybrid cell development (Wilkins *et al.*, 2014), would be imperative for investigating the effect of a different nuclear background on the mitochondrial genotype-phenotype relationship.

5.8. Objective 7 – Pathogenicity and mutational load hypothesis

After verifying that the three mtDNA variants were not present in the selected ME patients, the pathogenicity of these variants could no longer be assessed. Focus was thus placed on the mutational load hypothesis where the combined effect of rare non-synonymous mtDNA variants on the energy metabolism of patients was examined. Significant correlations were seen for certain subject groups or bioenergetic parameters, whilst not for others. This was believed to be due to the unknown positive or negative effects of other mtDNA variants or factors when combined with the influence of the non-synonymous variants, since individual SNPs were not

directly investigated in this study. The interaction between the patient mtDNA and the nuclear background of the ρ^0 cell line was also expected to influence the mitochondrial genotype-phenotype relationship within the cells.

Maximal respiration and ATP production were significantly correlated for haplogroup U ME patients at week 6, and for non-U haplogroup ME patients at both week 3 and 6. The haplogroup of the ME patients was seen to have an effect on the relationship between these bioenergetic parameters and the adjusted MutPred scores. There seemed to be possible evidence for the occurrence of the mutational load hypothesis since increased adjusted MutPred scores (and thus a greater cumulative effect of rare non-synonymous variants) appeared to be associated with decreased ATP synthesis and ETS capacity in the ME patients. Certain rare non-synonymous variants may lead to decreased OXPHOS subunit synthesis and thus decreased OXPHOS activity, causing the cells to be more susceptible to the effects of other non-synonymous variants occurring simultaneously. The cumulative effect of these mtDNA variants could thus be harmful to the cell, leading to the decreased ATP synthesis and ETS capacity seen here. This impaired bioenergetic function could in turn cause the fatigue, post-exertional malaise and neurological abnormalities that have been observed in ME patients.

5.9. Final conclusion and future prospects

Optimization of the selected cell lines for the XF analyser provided essential information for further experiments using the instrument, as well as invaluable experience on the techniques required for optimal utilization of the instrument. Ideally, all respirometry results should have been verified using an alternative method (such as the OROBOROS O2k) and future studies would obtain a more holistic view of mitochondrial dysfunction in ME patients by including such alternative methods in conjunction with mitochondrial membrane potential analyses. Future prospects for the XF analyses in this, and other laboratories, include many different research areas and the utilisation of different cell lines, isolated mitochondria and even small organisms such as nematodes. In addition, numerous different types of analyses such as assessing glycolytic function and the metabolic phenotype of cells can, and have been, assessed. The optimizations of the XF protocols in general also led to the direct contribution of the author to many other studies. Three of these studies have led to publications which are in process, or have been submitted for publication. These are:

1. “Altered mitochondrial respiration and other features of mitochondrial dysfunction in parkin-mutant fibroblasts from South African Parkinson’s disease patients”. Authors: Haylett, W.; Swart, C.; van der Westhuizen, F.H.; van Dyk, H.C.; van der Merwe, L.; van der Merwe, C.; Loos, B.; Carr, J.; Kinnear, C.; Bardien, S. (published in *Parkinson’s disease,* Volume 2016);

2. “Curcumin rescues a PINK1 knock down SH-SY5Y cellular model of Parkinson’s disease from mitochondrial dysfunction and cell death”. Authors: van der Merwe, C.; van Dyk, H.C.; Engelbrecht, L.; van der Westhuizen, F.H.; Kinnear, C.; Loos, B.; Bardien, S. (accepted for publication in *Molecular Neurobiology*);
3. “Oxygen consumption rates with reference to two Meloidogyne species using the polarographic oxygen and fibre optic oxygen sensors”. Authors: van Aardt, W.J.; Fourie, H.; Louw, R.; van Dyk, H.C. (submitted to *Nematology*).

Although disappointing, the unsuccessful verification of the three mtDNA variants (m.7497G>A, m.9185T>C and m.10197G>A) may aid future mitochondrial researchers in focusing on other possible pathogenic mtDNA variants that may be linked to ME. The NGS results obtained in this study along with the evaluation of the effect of MutPred scores may provide a basis, as pilot study, for future research into the relationship between mtDNA haplogroups, mtDNA variants and ME.

The protocol for cybrid cell development was successfully established in this laboratory with overwhelming evidence for its success based on the PCR-RFLP haplogroup, RMCN and NGS results. Future cybrid studies within this laboratory - using the 143B cell line - can thus be carried out with confidence, taking into consideration some of the valuable lessons learnt from it. The use of other ρ^0 cell lines for cybrid cell development should be restricted to those that have been well established in literature and that have preferably been analysed using an XF analyser in previous research. To assess the effect of aneuploidy in cancer ρ^0 cell lines, cybrids could also be karyotyped to ensure similar chromosomal numbers between cybrid cell lines (Gómez-Durán *et al.*, 2010).

Ideally, more patients and healthy controls should be included to allow for more advanced statistical procedures to be performed, but since this was only a pilot study, it was adequate for this investigation. The data from this study could be used to calculate the numbers required to do a well-powered study in the future. Since it was necessary to culture all cybrid cells simultaneously, increasing the number of patients and controls in the study would also have proved practically difficult to maintain and would have led to increased risk of contamination or infection. A shortfall of this study was the lack of availability of a positive control harbouring a well-known pathogenic mtDNA variant or mtDNA deletion known to have a strong negative bioenergetic impact. Future studies would greatly benefit from the inclusion of such patients when analysing the XF analyser data.

In conclusion, the aims set out in the beginning of this study were met by successfully optimizing the techniques and protocols required for investigating the bioenergetics of several cell lines using the Seahorse XF^{e}96 analyser, and by successfully developing cybrid cells (using blood platelets obtained from ME patients and healthy controls) to investigate the effect of known pathogenic mtDNA variants at sub-clinical levels, as well as the cumulative effect of rare non-synonymous mtDNA variants, on the energy metabolism of these cybrid cells. During this study various techniques and instruments were mastered, such as: cell culture and aseptic techniques, cybrid cell development, PCR, RFLP, real-time PCR and the Seahorse XF^{e}96 analyser.

As described in the title of this study, the influence of mtDNA variants (both known pathogenic mtDNA variants and rare non-synonymous mtDNA variants) were investigated in ME patients. While the known pathogenic mtDNA variants proved to be sequencing artefacts, the presence of other possible known pathogenic mtDNA variants should not be excluded and future investigations could aim to identify any pathogenic or compensatory mtDNA variants that may be present in ME patients. The decreased ATP production and ETS capacity that was correlated to increased adjusted MutPred scores in the ME patients provided a possible premise for the mutational load hypothesis. The higher respiratory values seen in ME patients (compared to healthy controls) for numerous bioenergetic parameters were contrary to the bioenergetic irregularities that were expected to be seen. As discussed in Section 2.3.1, the mutation rate in mtDNA is approximately ten times greater than in nDNA (Brown et al., 1979), which indicates that the cell must consist of numerous compensatory mechanisms capable of counteracting mtDNA-associated variation, for example, by increasing the RMCN (as was seen in this study by the increased RMCN in ME patients compared to healthy controls). The maintenance of wild type mtDNA hypothesis (Section 2.3.3) further supports this by indicating that molecular defects can lead to a compensatory response where both variant and wild type mtDNA proliferation increases. Much information can be gained from future studies by focusing on the compensatory and physiological mechanisms that function in the mitochondria of these patients, as well as by investigating oxidative stress, ETS enzyme activity, protein expression levels of relevant mitochondrial proteins, etc.

Promising data was obtained in this pilot study, with much potential for other researchers as well as the possibility of publication (since novel findings were obtained), which serves as justification for the use of a larger cohort and thus a well-powered study in future investigations.

REFERENCES

ACHANTA, G., SASAKI, R., FENG, L., CAREW, J.S., LU, W., PELICANO, H., KEATING, M.J. & HUANG, P. 2005. Novel role of p53 in maintaining mitochondrial genetic stability through interaction with DNA pol gamma. *The EMBO journal,* 24(19):3482-3492.

AINSCOW, E.K. & BRAND, M.D. 1999. Top-down control analysis of ATP turnover, glycolysis and oxidative phosphorylation in rat hepatocytes. *European journal of biochemistry,* 263(3):671-685.

ANDERSON, S., BANKIER, A.T., BARRELL, B.G., DE BRUIJN, M., COULSON, A.R., DROUIN, J., EPERON, I., NIERLICH, D., ROE, B.A. & SANGER, F. 1981. Sequence and organization of the human mitochondrial genome. *Nature,* 290(5806):457-465.

ANDREWS, R.M., KUBACKA, I., CHINNERY, P.F., LIGHTOWLERS, R.N., TURNBULL, D.M. & HOWELL, N. 1999. Reanalysis and revision of the cambridge reference sequence for human mitochondrial DNA. *Nature genetics,* 23(2):147.

ANKEL-SIMONS, F. & CUMMINS, J.M. 1996. Misconceptions about mitochondria and mammalian fertilization: Implications for theories on human evolution. *Proceedings of the national academy of sciences of the united states of america,* 93(24):13859-13863.

BEHAN, W., MORE, I. & BEHAN, P. 1991. Mitochondrial abnormalities in the postviral fatigue syndrome. *Acta neuropathologica,* 83(1):61-65.

BERG, H. 1988. Electrofusion of cells. New York: Marcel Dekker inc. p. 365-389.

BLAIR, R.C. & HIGGINS, J.J. 1980. A comparison of the power of wilcoxon's rank-sum statistic to that of student'st statistic under various nonnormal distributions. *Journal of educational and behavioral statistics,* 5(4):309-335.

BRAND, M. & NICHOLLS, D. 2011. Assessing mitochondrial dysfunction in cells. *Biochem.J,* 435:297-312.

BROOKES, A.J. 1999. The essence of SNPs. *Gene,* 234(2):177-186.

BROWN, G.C., LAKIN-THOMAS, P.L. & BRAND, M.D. 1990. Control of respiration and oxidative phosphorylation in isolated rat liver cells. *European journal of biochemistry,* 192(2):355-362.

BROWN, A.E., JONES, D.E., WALKER, M. & NEWTON, J.L. 2015. Abnormalities of AMPK activation and glucose uptake in cultured skeletal muscle cells from individuals with chronic fatigue syndrome. *PloS one,* 10(4).

BROWN, W.M., GEORGE, M.,JR & WILSON, A.C. 1979. Rapid evolution of animal mitochondrial DNA. *Proceedings of the national academy of sciences of the united states of america,* 76(4):1967-1971.

BROWNLEE, M. 2001. Biochemistry and molecular cell biology of diabetic complications. *Nature,* 414(6865):813-820.

BUSTIN, S.A., BENES, V., GARSON, J.A., HELLEMANS, J., HUGGETT, J., KUBISTA, M., MUELLER, R., NOLAN, T., PFAFFL, M.W. & SHIPLEY, G.L. 2009. The MIQE guidelines: Minimum information for publication of quantitative real-time PCR experiments. *Clinical chemistry,* 55(4):611-622.

CANN, R.L., STONEKING, M. & WILSON, A.C. 1987. Mitochondrial DNA and human evolution. *Nature,* 325(6099):31-36.

CARRUTHERS, B.M., VAN DE SANDE, MARJORIE I, DE MEIRLEIR, K.L., KLIMAS, N.G., BRODERICK, G., MITCHELL, T., STAINES, D., POWLES, A.P., SPEIGHT, N. & VALLINGS, R. 2011. Myalgic encephalomyelitis: International consensus criteria. *Journal of internal medicine,* 270(4):327-338.

CASTAGNA, A.E., ADDIS, J., MCINNES, R.R., CLARKE, J.T., ASHBY, P., BLASER, S. & ROBINSON, B.H. 2007. Late onset leigh syndrome and ataxia due to a T to C mutation at bp 9,185 of mitochondrial DNA. *American journal of medical genetics part A,* 143(8):808-816.

CHACKO, B.K., KRAMER, P.A., RAVI, S., BENAVIDES, G.A., MITCHELL, T., DRANKA, B.P., FERRICK, D., SINGAL, A.K., BALLINGER, S.W., BAILEY, S.M., HARDY, R.W., ZHANG, J., ZHI, D. & DARLEY-USMAR, V.M. 2014. The bioenergetic health index: A new concept in mitochondrial translational research. *Clinical science,* 127(6):367-373.

CHAE, J.H., LEE, J.S., KIM, K.J., HWANG, Y.S., BONILLA, E., TANJI, K. & HIRANO, M. 2007. A novel ND3 mitochondrial DNA mutation in three korean children with basal ganglia lesions and complex I deficiency. *Pediatric research,* 61:622-624.

CHANCE, B. & WILLIAMS, G.R. 1955. Respiratory enzymes in oxidative phosphorylation. III. the steady state. *The journal of biological chemistry,* 217(1):409-427.

CHILDS, A., HUTCHIN, T., PYSDEN, K., HIGHET, L., BAMFORD, J., LIVINGSTON, J. & CROW, Y. 2007. Variable phenotype including leigh syndrome with a 9185T> C mutation in the MTATP6 gene. *Neuropediatrics,* 38(06):313-316.

CHINNERY, P.F. & SAMUELS, D.C. 1999. Relaxed replication of mtDNA: A model with implications for the expression of disease. *The american journal of human genetics,* 64(4):1158-1165.

CHINNERY, P.F. & HUDSON, G. 2013. Mitochondrial genetics. *British medical bulletin,* 106(1):135-159.

CHOMYN, A., MEOLA, G., BRESOLIN, N., LAI, S.T., SCARLATO, G. & ATTARDI, G. 1991. In vitro genetic transfer of protein synthesis and respiration defects to mitochondrial DNA-less cells with myopathy-patient mitochondria. *Molecular and cellular biology,* 11(4):2236-2244.

CHOMYN, A. 1994. [29] platelet-mediated transformation of human mitochondrial DNA-less cells. (In Anon. Methods in enzymology. Academic Press. p. 334-339.) (Mitochondrial Biogenesis and Genetics Part B.).

CLARK JR, L. 1956. Monitor and control of blood and tissue oxygen tensions. *ASAIO journal,* 2(1):41-48.

CLAYTON, D.A. 1982. Replication of animal mitochondrial DNA. *Cell,* 28(4):693-705.

CLAYTON, E.W. 2015. Beyond myalgic encephalomyelitis/chronic fatigue syndrome: An IOM report on redefining an illness. *JAMA,* 313(11):1101-1102.

COCCO, S., SECONDO, A., DEL VISCOVO, A., PROCACCINI, C., FORMISANO, L., FRANCO, C., ESPOSITO, A., SCORZIELLO, A., MATARESE, G. & DI RENZO, G. 2015. Polychlorinated biphenyls induce mitochondrial dysfunction in SH-SY5Y neuroblastoma cells. *PloS one,* 10(6).

COLLER, H.A., KHRAPKO, K., BODYAK, N.D., NEKHAEVA, E., HERRERO-JIMENEZ, P. & THILLY, W.G. 2001. High frequency of homoplasmic mitochondrial DNA mutations in human tumors can be explained without selection. *Nature genetics,* 28(2):147-150.

COLLINS, F.S., BROOKS, L.D. & CHAKRAVARTI, A. 1998. A DNA polymorphism discovery resource for research on human genetic variation. *Genome research,* 8(12):1229-1231.

CROUCH, S., KOZLOWSKI, R., SLATER, K. & FLETCHER, J. 1993. The use of ATP bioluminescence as a measure of cell proliferation and cytotoxicity. *Journal of immunological methods,* 160(1):81-88.

DEN HOLLANDER, B., SUNDSTROM, M., PELANDER, A., SILTANEN, A., OJANPERA, I., MERVAALA, E., KORPI, E.R. & KANKURI, E. 2015. Mitochondrial respiratory dysfunction due to the conversion of substituted cathinones to methylbenzamides in SH-SY5Y cells. *Scientific reports,* 5:14924.

DEPRISTO, M.A., BANKS, E., POPLIN, R., GARIMELLA, K.V., MAGUIRE, J.R., HARTL, C., PHILIPPAKIS, A.A., DEL ANGEL, G., RIVAS, M.A. & HANNA, M. 2011. A framework for variation discovery and genotyping using next-generation DNA sequencing data. *Nature genetics,* 43(5):491-498.

DIMAURO, S. & SCHON, E.A. 2003. Mitochondrial respiratory-chain diseases. *New england journal of medicine,* 348(26):2656-2668.

DIMAURO, S. & SCHON, E.A. 2001. Mitochondrial DNA mutations in human disease. *American journal of medical genetics,* 106(1):18-26.

DIMAURO, S., SCHON, E.A., CARELLI, V. & HIRANO, M. 2013. The clinical maze of mitochondrial neurology. *Nature reviews neurology,* 9(8):429-444.

DRANKA, B.P., BENAVIDES, G.A., DIERS, A.R., GIORDANO, S., ZELICKSON, B.R., REILY, C., ZOU, L., CHATHAM, J.C., HILL, B.G. & ZHANG, J. 2011. Assessing bioenergetic function in response to oxidative stress by metabolic profiling. *Free radical biology and medicine,* 51(9):1621-1635.

DUNBAR, D.R., MOONIE, P.A., JACOBS, H.T. & HOLT, I.J. 1995. Different cellular backgrounds confer a marked advantage to either mutant or wild-type mitochondrial genomes. *Proceedings of the national academy of sciences of the united states of america,* 92(14):6562-6566.

ELLIOTT, H.R., SAMUELS, D.C., EDEN, J.A., RELTON, C.L. & CHINNERY, P.F. 2008. Pathogenic mitochondrial DNA mutations are common in the general population. *The american journal of human genetics,* 83(2):254-260.

ELSON, J., SAMUELS, D., TURNBULL, D. & CHINNERY, P. 2001. Random intracellular drift explains the clonal expansion of mitochondrial DNA mutations with age. *The american journal of human genetics,* 68(3):802-806.

ELSON, J., TURNBULL, D. & HOWELL, N. 2004. Comparative genomics and the evolution of human mitochondrial DNA: Assessing the effects of selection. *The american journal of human genetics,* 74(2):229-238.

ELSON, J.L., HERRNSTADT, C., PRESTON, G., THAL, L., MORRIS, C.M., EDWARDSON, J., BEAL, M.F., TURNBULL, D.M. & HOWELL, N. 2006. Does the mitochondrial genome play a role in the etiology of Alzheimer's disease? *Human genetics,* 119(3):241-254.

EVENGÅRD, B. & KLIMAS, N. 2002. Chronic fatigue syndrome. *Drugs,* 62(17):2433-2446.

FERRICK, D.A., NEILSON, A. & BEESON, C. 2008. Advances in measuring cellular bioenergetics using extracellular flux. *Drug discovery today,* 13(5):268-274.

FIELD, A. 2009. Discovering Statistics using SPSS. London: Sage Publications. p. 821.

FLIER, J.S., UNDERHILL, L.H. & JOHNS, D.R. 1995. Mitochondrial DNA and disease. *New england journal of medicine,* 333(10):638-644.

FUKUDA, K., STRAUS, S.E., HICKIE, I., SHARPE, M.C., DOBBINS, J.G. & KOMAROFF, A. 1994. The chronic fatigue syndrome: A comprehensive approach to its definition and study. *Annals of internal medicine,* 121(12):953-959.

GERENCSER, A.A., NEILSON, A., CHOI, S.W., EDMAN, U., YADAVA, N., OH, R.J., FERRICK, D.A., NICHOLLS, D.G. & BRAND, M.D. 2009. Quantitative microplate-based respirometry with correction for oxygen diffusion. *Analytical chemistry,* 81(16):6868-6878.

GHEZZI, D., MARELLI, C., ACHILLI, A., GOLDWURM, S., PEZZOLI, G., BARONE, P., PELLECCHIA, M.T., STANZIONE, P., BRUSA, L. & BENTIVOGLIO, A.R. 2005. Mitochondrial DNA haplogroup K is associated with a lower risk of parkinson's disease in italians. *European journal of human genetics,* 13(6):748-752.

GIBCO. 2015. Cell culture basics handbook.
www.thermofisher.com/za/en/home/references/gibco-cell-culture-basics.html.
Date of access: 12 Oct. 2015.

GILES, R.E., BLANC, H., CANN, H.M. & WALLACE, D.C. 1980. Maternal inheritance of human mitochondrial DNA. *Proceedings of the national academy of sciences of the united states of america,* 77(11):6715-6719.

GNAIGER, E. 2014. Mitochondrial Pathways and Respiratory Control. Introduction to OXPHOS Analysis. 4th ed. Innsbruck, Austria: OROBOROS MiPNet Publications. 1-80p.

GNAIGER, E. & FASCHING, M. 2014. Oxygraph-2k and O2k-MultiSensor system: Specifications for respirometry and comprehensive OXPHOS analysis. *Mitochondrial physiology network 18.10(04),* 1-8.

GÓMEZ-DURÁN, A., PACHEU-GRAU, D., MARTÍNEZ-ROMERO, Í., LÓPEZ-GALLARDO, E., LÓPEZ-PÉREZ, M.J., MONTOYA, J. & RUIZ-PESINI, E. 2012. Oxidative phosphorylation differences between mitochondrial DNA haplogroups modify the risk of leber's hereditary optic neuropathy. *Biochimica et biophysica acta (BBA)-molecular basis of disease,* 1822(8):1216-1222.

GÓMEZ-DURÁN, A., PACHEU-GRAU, D., LÓPEZ-GALLARDO, E., DIEZ-SANCHEZ, C., MONTOYA, J., LÓPEZ-PÉREZ, M.J. & RUIZ-PESINI, E. 2010. Unmasking the causes of multifactorial disorders: OXPHOS differences between mitochondrial haplogroups. *Human molecular genetics,* 19(17):3343-3353.

GONG, S., PENG, Y., JIANG, P., WANG, M., FAN, M., WANG, X., ZHOU, H., LI, H., YAN, Q., HUANG, T. & GUAN, M.X. 2014. A deafness-associated tRNAHis mutation alters the mitochondrial function, ROS production and membrane potential. *Nucleic acids research,* 42(12):8039-8048.

GRAZIEWICZ, M.A., DAY, B.J. & COPELAND, W.C. 2002. The mitochondrial DNA polymerase as a target of oxidative damage. *Nucleic acids research,* 30(13):2817-2824.

GUTMAN, M., COLES, C., SINGER, T. & CASIDA, J. 1971. On the functional organization of the respiratory chain at the dehydrogenase-coenzyme Q junction. *Biochemistry,* 10(11):2036-2043.

HATEFI, Y., HAAVIK, A., FOWLER, L. & GRIFFITHS, D. 1962. Studies on the electron transfer system XLII. reconstitution of the electron transfer system. *Journal of biological chemistry,* 237(8):2661-2669.

HATEFI, Y. 1985. The mitochondrial electron transport and oxidative phosphorylation system. *Annual review of biochemistry,* 54(1):1015-1069.

HERRNSTADT, C., ELSON, J.L., FAHY, E., PRESTON, G., TURNBULL, D.M., ANDERSON, C., GHOSH, S.S., OLEFSKY, J.M., BEAL, M.F. & DAVIS, R.E. 2002. Reduced-median-network analysis of complete mitochondrial DNA coding-region sequences for the major african, asian, and european haplogroups. *The american journal of human genetics,* 70(5):1152-1171.

HERRNSTADT, C. & HOWELL, N. 2004. An evolutionary perspective on pathogenic mtDNA mutations: Haplogroup associations of clinical disorders. *Mitochondrion,* 4(5–6):791-798.

HOLLINGSWORTH, K.G., JONES, D.E., TAYLOR, R., BLAMIRE, A.M. & NEWTON, J.L. 2010. Impaired cardiovascular response to standing in chronic fatigue syndrome. *European journal of clinical investigation,* 40(7):608-615.

HOLT, I., HARDING, A. & MORGAN-HUGHES, J. 1988. Deletions of muscle mitochondrial DNA in patients with mitochondrial myopathies. *Nature*, 331(6158):717-719.

HOWELL, N., ELSON, J.L., CHINNERY, P.F. & TURNBULL, D.M. 2005. mtDNA mutations and common neurodegenerative disorders. *Trends in genetics,* 21(11):583-586.

HUDSON, G., GOMEZ-DURAN, A., WILSON, I.J. & CHINNERY, P.F. 2014. Recent mitochondrial DNA mutations increase the risk of developing common late-onset human diseases. *PLoS genetics,* 10(5).

INOUE, K., TAKAI, D., HOSAKA, H., ITO, S., SHITARA, H., ISOBE, K., LEPECQ, J., SEGAL-BENDIRDJIAN, E. & HAYASHI, J. 1997. Isolation and characterization of mitochondrial DNA-less lines from various mammalian cell lines by application of an anticancer drug, ditercalinium. *Biochemical and biophysical research communications,* 239(1):257-260.

ISHIYAMA, M., TOMINAGA, H., SHIGA, M., SASAMOTO, K., OHKURA, Y. & UENO, K. 1996. A combined assay of cell viability and in vitro cytotoxicity with a highly water-soluble tetrazolium salt, neutral red and crystal violet. *Biological and pharmaceutical bulletin,* 19(11):1518-1520.

JAKSCH, M., KLOPSTOCK, T., KURLEMANN, G., DÖRNER, M., HOFMANN, S., KLEINLE, S., HEGEMANN, S., WEISSERT, M., MÜLLER-HÖCKER, J. & PONGRATZ, D. 1998. Progressive myoclonus epilepsy and mitochondrial myopathy associated with mutations in the tRNASer (UCN) gene. *Annals of neurology,* 44(4):635-640.

JAZAYERI, M., ANDREYEV, A., WILL, Y., WARD, M., ANDERSON, C.M. & CLEVENGER, W. 2003. Inducible expression of a dominant negative DNA polymerase-gamma depletes mitochondrial DNA and produces a rho0 phenotype. *The journal of biological chemistry,* 278(11):9823-9830.

JONES, L.J., GRAY, M., YUE, S.T., HAUGLAND, R.P. & SINGER, V.L. 2001. Sensitive determination of cell number using the CyQUANT® cell proliferation assay. *Journal of immunological methods,* 254(1):85-98.

KENOSI, M. 2014. Optimizing the conditions of the A549 cell line and bioenergetics assays for use on the Seahorse XFe96 analyser. Potchefstroom: North-West University: (Mini-dissertation - Honours).

KING, M.P. & ATTARDI, G. 1989. Human cells lacking mtDNA: Repopulation with exogenous mitochondria by complementation. *Science,* 246(4929):500-503.

KING, M.P. & ATTARDI, G. 1996. [27] isolation of human cell lines lacking mitochondrial DNA. (In Anon. Methods in enzymology. Academic Press. p. 304-313.) (Mitochondrial Biogenesis and Genetics Part B.).

KIRBY, D.M., SALEMI, R., SUGIANA, C., OHTAKE, A., PARRY, L., BELL, K.M., KIRK, E.P., BONEH, A., TAYLOR, R.W., DAHL, H.H., RYAN, M.T. & THORBURN, D.R. 2004. NDUFS6 mutations are a novel cause of lethal neonatal mitochondrial complex I deficiency. *The journal of clinical investigation,* 114(6):837-845.

KIVISILD, T., SHEN, P., WALL, D.P., DO, B., SUNG, R., DAVIS, K., PASSARINO, G., UNDERHILL, P.A., SCHARFE, C., TORRONI, A., SCOZZARI, R., MODIANO, D., COPPA, A., DE KNIJFF, P., FELDMAN, M., CAVALLI-SFORZA, L.L. & OEFNER, P.J. 2006. The role of selection in the evolution of human mitochondrial genomes. *Genetics,* 172(1):373-387.

KRAMER, P.A., CHACKO, B.K., GEORGE, D.J., ZHI, D., WEI, C.C., DELL'ITALIA, L.J., MELBY, S.J., GEORGE, J.F. & DARLEY-USMAR, V.M. 2015. Decreased bioenergetic health index in monocytes isolated from the pericardial fluid and blood of post-operative cardiac surgery patients. *Bioscience reports,* 35(4):10.

KUKAT, A., KUKAT, C., BROCHER, J., SCHÄFER, I., KROHNE, G., TROUNCE, I.A., VILLANI, G. & SEIBEL, P. 2008. Generation of ρ0 cells utilizing a mitochondrially targeted restriction endonuclease and comparative analyses. *Nucleic acids research,* 36(7).

LENGERT, N. & DROSSEL, B. 2015. In silico analysis of exercise intolerance in myalgic encephalomyelitis/chronic fatigue syndrome. *Biophysical chemistry,* 202:21-31.

LENTZ, B.R. 1994. Polymer-induced membrane fusion: Potential mechanism and relation to cell fusion events. *Chemistry and physics of lipids,* 73(1):91-106.

LENTZ, B.R. & LEE, J. 1999. Poly (ethylene glycol)(PEG)-mediated fusion between pure lipid bilayers: A mechanism in common with viral fusion and secretory vesicle release?(review). *Molecular membrane biology,* 16(4):279-296.

LI, B., KRISHNAN, V.G., MORT, M.E., XIN, F., KAMATI, K.K., COOPER, D.N., MOONEY, S.D. & RADIVOJAC, P. 2009. Automated inference of molecular mechanisms of disease from amino acid substitutions. *Bioinformatics (oxford, england),* 25(21):2744-2750.

LIN, T.K., LIN, H.Y., CHEN, S.D., CHUANG, Y.C., CHUANG, J.H., WANG, P.W., HUANG, S.T., TIAO, M.M., CHEN, J.B. & LIOU, C.W. 2011. The creation of cybrids harboring mitochondrial haplogroups in the taiwanese population of ethnic chinese background: An extensive in vitro tool for the study of mitochondrial genomic variations. *Oxidative medicine and cellular longevity,* 2012:824275.

LIU, M., WATSON, L.T. & ZHANG, L. 2015. Predicting the combined effect of multiple genetic variants. *Human genomics,* 9(1):1-7.

LIVAK, K.J. & SCHMITTGEN, T.D. 2001. Analysis of relative gene expression data using real-time quantitative PCR and the 2(-delta delta C(T)) method. *Methods,* 25(4):402-408.

LOEB, K.R. & LOEB, L.A. 2000. Significance of multiple mutations in cancer. *Carcinogenesis,* 21(3):379-385.

LOTT, M.T., LEIPZIG, J.N., DERBENEVA, O., XIE, H.M., CHALKIA, D., SARMADY, M., PROCACCIO, V. & WALLACE, D.C. 2013. mtDNA variation and analysis using MITOMAP and MITOMASTER. *Current protocols in bioinformatics,* 1(123):1-23.

MALIK, A.N. & CZAJKA, A. 2013. Is mitochondrial DNA content a potential biomarker of mitochondrial dysfunction? *Mitochondrion,* 13(5):481-492.

MCFARLAND, R., ELSON, J.L., TAYLOR, R.W., HOWELL, N. & TURNBULL, D.M. 2004. Assigning pathogenicity to mitochondrial tRNA mutations: When ‘definitely maybe’is not good enough. *Trends in genetics,* 20(12):591-596.

MCINNIS, O.A., MATHESON, K. & ANISMAN, H. 2014. Living with the unexplained: Coping, distress, and depression among women with chronic fatigue syndrome (CFS) and/or fibromyalgia comparedto an autoimmune disorder. *Anxiety, stress & coping,* 27(6):601-618.

MEISSNER-ROLOFF, M. 2009. The occurrence of mitochondrial DNA polymerase gamma gene mutations in mitochondrial deficiencies, in a selection of South African paediatric patients. Potchefstroom: North-West University. (Dissertation - Masters).

MEREIS, M. 2014. Optimizing the bioenergetic assay of the RD cell line for use on the Seahorse XFe96 Extracellular Flux analyser. Potchefstroom: North-West University: (Mini-dissertation - Honours).

MILLER, F.J., ROSENFELDT, F.L., ZHANG, C., LINNANE, A.W. & NAGLEY, P. 2003. Precise determination of mitochondrial DNA copy number in human skeletal and cardiac muscle by a PCR-based assay: Lack of change of copy number with age. *Nucleic acids research,* 31(11):e61-e67.

MITCHELL, P. 1961. Coupling of phosphorylation to electron and hydrogen transfer by a chemi-osmotic type of mechanism. *Nature,* 191(4784):144-148.

MOLLERS, M., MANIURA-WEBER, K., KISELJAKOVIC, E., BUST, M., HAYRAPETYAN, A., JAKSCH, M., HELM, M., WIESNER, R.J. & VON KLEIST-RETZOW, J.C. 2005. A new mechanism for mtDNA pathogenesis: Impairment of post-transcriptional maturation leads to severe depletion of mitochondrial tRNASer(UCN) caused by T7512C and G7497A point mutations. *Nucleic acids research,* 33(17):5647-5658.

MONTOYA, J., LOPEZ-GALLARDO, E., DIEZ-SANCHEZ, C., LOPEZ-PEREZ, M.J. & RUIZ-PESINI, E. 2009. 20 years of human mtDNA pathologic point mutations: Carefully reading the pathogenicity criteria. *Biochimica et biophysica acta,* 1787(5):476-483.

MORRIS, G. & MAES, M. 2013. Mitochondrial dysfunctions in myalgic Encephalomyelitis/chronic fatigue syndrome explained by activated immuno-inflammatory, oxidative and nitrosative stress pathways. *Metabolic brain disease,* 29(1):19-36.

MOSLEMI, A.R., DARIN, N., TULINIUS, M., OLDFORS, A. & HOLME, E. 2005. Two new mutations in the MTATP6 gene associated with leigh syndrome. *Neuropediatrics,* 36(5):314-318.

MUELLER, E.E., BRUNNER, S.M., MAYR, J.A., STANGER, O., SPERL, W. & KOFLER, B. 2012. Functional differences between mitochondrial haplogroup T and haplogroup H in HEK293 cybrid cells. *PLoS ONE*, 7(12).

MYHILL, S., BOOTH, N.E. & MCLAREN-HOWARD, J. 2009. Chronic fatigue syndrome and mitochondrial dysfunction. *International journal of clinical and experimental medicine,* 2(1):1-16.

NELSON, I., HANNA, M.G., WOOD, N.W. & HARDING, A. 1997. Depletion of mitochondrial DNA by ddC in untransformed human cell lines. *Somatic cell and molecular genetics,* 23(4):287-290.

NICHOLLS, D.G. & FERGUSON, S.J. 2013a. 12 - Mitochondria in physiology and pathology. (In Nicholls, D.G. & Ferguson, S.J., eds. Bioenergetics (fourth edition). Boston: Academic Press. p. 345-386.).

NICHOLLS, D.G. & FERGUSON, S.J. 2013b. 4 - The chemiosmotic proton circuit in isolated organelles: Theory and practice. (In Nicholls, D.G. & Ferguson, S.J., eds. Bioenergetics (fourth edition). Boston: Academic Press. p. 53-87.).

NICHOLLS, D.G. & FERGUSON, S.J. 2013c. 5 - Respiratory chains. (In Nicholls, D.G. & Ferguson, S.J., eds. Bioenergetics (fourth edition). Boston: Academic Press. p. 91-157.).

NICHOLLS, D.G. & FERGUSON, S.J. 2013d. Introduction to part 1. (In Nicholls, D.G. & Ferguson, S.J., eds. Bioenergetics (fourth edition). Boston: Academic Press. p. 1-2.).

PAUL LEE, W., WAHJUDI, P.N., XU, J. & GO, V.L. 2010. Tracer-based metabolomics: Concepts and practices. *Clinical biochemistry,* 43(16):1269-1277.

PAUL, L., WOOD, L., BEHAN, W.M. & MACLAREN, W.M. 1999. Demonstration of delayed recovery from fatiguing exercise in chronic fatigue syndrome. *European journal of neurology,* 6(1):63-69.

PEREIRA, L., SOARES, P., RADIVOJAC, P., LI, B. & SAMUELS, D.C. 2011. Comparing phylogeny and the predicted pathogenicity of protein variations reveals equal purifying selection across the global human mtDNA diversity. *The american journal of human genetics,* 88(4):433-439.

PFAFFL, M.W., HORGAN, G.W. & DEMPFLE, L. 2002. Relative expression software tool (REST©) for group-wise comparison and statistical analysis of relative expression results in real-time PCR. *Nucleic acids research,* 30(9):e36.

PITCEATHLY, R.D., MURPHY, S.M., COTTENIE, E., CHALASANI, A., SWEENEY, M.G., WOODWARD, C., MUDANOHWO, E.E., HARGREAVES, I., HEALES, S., LAND, J., HOLTON, J.L., HOULDEN, H., BLAKE, J., CHAMPION, M., FLINTER, F., ROBB, S.A., PAGE, R., ROSE, M., PALACE, J., CROWE, C., LONGMAN, C., LUNN, M.P., RAHMAN, S., REILLY, M.M. & HANNA, M.G. 2012. Genetic dysfunction of MT-ATP6 causes axonal charcot-marie-tooth disease. *Neurology,* 79(11):1145-1154.

POULTON, J., DEADMAN, M. & GARDINER, R.M. 1989. Duplications of mitochondrial DNA in mitochondrial myopathy. *The lancet,* 333(8632):236-240.

PRITCHARD, J.K. & COX, N.J. 2002. The allelic architecture of human disease genes: Common disease-common variant...or not? *Human molecular genetics,* 11(20):2417-2423.

PYLE, A., HUDSON, G., WILSON, I.J., COXHEAD, J., SMERTENKO, T., HERBERT, M., SANTIBANEZ-KOREF, M. & CHINNERY, P.F. 2015. Extreme-depth re-sequencing of mitochondrial DNA finds no evidence of paternal transmission in humans. *PLoS Genetics*, 11(5).

RADOMSKA, H.S. & ECKHARDT, L.A. 1995. Mammalian cell fusion in an electroporation device. *Journal of immunological methods,* 188(2):209-217.

RAULE, N., SEVINI, F., LI, S., BARBIERI, A., TALLARO, F., LOMARTIRE, L., VIANELLO, D., MONTESANTO, A., MOILANEN, J.S. & BEZRUKOV, V. 2014. The co-occurrence of mtDNA mutations on different oxidative phosphorylation subunits, not detected by haplogroup analysis, affects human longevity and is population specific. *Aging cell,* 13(3):401-407.

RICHARDS, M., CORTE-REAL, H., FORSTER, P., MACAULAY, V., WILKINSON-HERBOTS, H., DEMAINE, A., PAPIHA, S., HEDGES, R., BANDELT, H.J. & SYKES, B. 1996. Paleolithic and neolithic lineages in the european mitochondrial gene pool. *American journal of human genetics,* 59(1):185-203.

RICHTER, C., PARK, J. & AMES, B.N. 1988. Normal oxidative damage to mitochondrial and nuclear DNA is extensive. *Proceedings of the national academy of sciences,* 85(17):6465-6467.

ROOSTALU, U., KUTUEV, I., LOOGVALI, E.L., METSPALU, E., TAMBETS, K., REIDLA, M., KHUSNUTDINOVA, E.K., USANGA, E., KIVISILD, T. & VILLEMS, R. 2007. Origin and expansion of haplogroup H, the dominant human mitochondrial DNA lineage in west eurasia: The near eastern and caucasian perspective. *Molecular biology and evolution,* 24(2):436-448.

ROSSIGNOL, R., FAUSTIN, B., ROCHER, C., MALGAT, M., MAZAT, J. & LETELLIER, T. 2003. Mitochondrial threshold effects. *Biochem.J,* 370:751-762.

ROSSIGNOL, R., MALGAT, M., MAZAT, J. & LETELLIER, T. 1999. Threshold effect and tissue specificity implication for mitochondrial cytopathies. *Journal of biological chemistry,* 274(47):33426-33432.

SALAS, A. & ELSON, J.L. 2015. Mitochondrial DNA as a risk factor for false positives in case-control association studies. *Journal of genetics and genomics,* 42(4):169-172.

SAMUELS, D.C., CAROTHERS, A.D., HORTON, R. & CHINNERY, P.F. 2006. The power to detect disease associations with mitochondrial DNA haplogroups. *The american journal of human genetics,* 78(4):713-720.

SANETO, R.P. & SINGH, K.K. 2010. Illness-induced exacerbation of leigh syndrome in a patient with the< i> MTATP6</i> mutation, m. 9185 T> C. *Mitochondrion,* 10(5):567-572.

SARZI, E., BROWN, M.D., LEBON, S., CHRETIEN, D., MUNNICH, A., ROTIG, A. & PROCACCIO, V. 2007. A novel recurrent mitochondrial DNA mutation in ND3 gene is associated with isolated complex I deficiency causing leigh syndrome and dystonia. *American journal of medical genetics part A,* 143(1):33-41.

SCADUTO JR, R.C. & GROTYOHANN, L.W. 1999. Measurement of mitochondrial membrane potential using fluorescent rhodamine derivatives. *Biophysical journal,* 76(1):469-477.

SCHEFFLER, I.E. 1999. Structure and morphology. (In Anon. Mitochondria. John Wiley & Sons, Inc. p. 15-47.).

SCHON, E.A., DIMAURO, S. & HIRANO, M. 2012. Human mitochondrial DNA: Roles of inherited and somatic mutations. *Nature reviews genetics,* 13(12):878-890.

SHADEL, G.S. & CLAYTON, D.A. 1997. Mitochondrial DNA maintenance in vertebrates. *Annual review of biochemistry,* 66(1):409-435.

SHEPHARD, R.J. 2001. Chronic fatigue syndrome. *Sports medicine,* 31(3):167-194.

SMIT, L. 2009. Mitochondrial DNA haplotype analysis in paediatric patients with mitochondrial disorders. Potchefstroom: North-West University. (Mini-dissertation - Honours).

SMITS, B., VAN DEN HEUVEL, L., KNOOP, H., KÜSTERS, B., JANSSEN, A., BORM, G., BLEIJENBERG, G., RODENBURG, R. & VAN ENGELEN, B. 2011. Mitochondrial enzymes discriminate between mitochondrial disorders and chronic fatigue syndrome. *Mitochondrion,* 11(5):735-738.

SOARES, P., ABRANTES, D., RITO, T., THOMSON, N., RADIVOJAC, P., LI, B., MACAULAY, V., SAMUELS, D.C. & PEREIRA, L. 2013. Evaluating purifying selection in the mitochondrial DNA of various mammalian species. *PloS one,* 8(3).

STEKETEE, M.B., MOYSIDIS, S.N., WEINSTEIN, J.E., KREYMERMAN, A., SILVA, J.P., IQBAL, S. & GOLDBERG, J.L. 2012. Mitochondrial dynamics regulate growth cone motility, guidance, and neurite growth rate in perinatal retinal ganglion cells in vitro. *Investigative ophthalmology & visual science,* 53(11):7402-7411.

SUTOVSKY, P. 2003. Ubiquitin-dependent proteolysis in mammalian spermatogenesis, fertilization, and sperm quality control: Killing three birds with one stone. *Microscopy research and technique,* 61(1):88-102.

SWERDLOW, R.H. 2007. Mitochondria in cybrids containing mtDNA from persons with mitochondriopathies. *Journal of neuroscience research,* 85(15):3416-3428.

TAYLOR, R.W., TAYLOR, G.A., DURHAM, S.E. & TURNBULL, D.M. 2001. The determination of complete human mitochondrial DNA sequences in single cells: Implications for the study of somatic mitochondrial DNA point mutations. *Nucleic acids research,* 29(15):e74.

TAYLOR, R.W. & TURNBULL, D.M. 2005. Mitochondrial DNA mutations in human disease. *Nature reviews genetics,* 6(5):389-402.

TORPY, D.J., BACHMANN, A.W., GARTSIDE, M., GRICE, J., HARRIS, J.M., CLIFTON, P., EASTEAL, S., JACKSON, R. & WHITWORTH, J. 2004. Association between chronic fatigue syndrome and the corticosteroid-binding globulin gene ALA SER224 polymorphism. *Endocrine research,* 30(3):417-429.

TUKEY, J.W. 1977. Exploratory data analysis. p. 2-3.

TUPPEN, H.A., BLAKELY, E.L., TURNBULL, D.M. & TAYLOR, R.W. 2010. Mitochondrial DNA mutations and human disease. *Biochimica et biophysica acta,* 1797(2):113-128.

VAN DER WALT, E. 2012. Molecular genetic characterization of mitochondrial DNA in a cohort of South African patients with mitochondrial disorders. Potchefstroom: North-West University. (Thesis - PhD).

VAN DYK, H.C. 2013. Development of cytoplasmic hybrid cells to evaluate mitochondrial DNA mutation pathogenicity. Potchefstroom: North-West University. (Mini-dissertation - Honours).

VAN HEERDEN, L.M. 2013. Development of a real-time PCR assay for the detection of mitochondrial DNA mutations associated with chronic fatigue syndrome. Potchefstroom: North-West University: (Mini-dissertation - Honours).

VAN OVEN, M. & KAYSER, M. 2009. Updated comprehensive phylogenetic tree of global human mitochondrial DNA variation. *Human mutation,* 30(2):E386-E394.

VAUGHAN, R.A., GARCIA-SMITH, R., GANNON, N.P., BISOFFI, M., TRUJILLO, K.A. & CONN, C.A. 2013. Leucine treatment enhances oxidative capacity through complete carbohydrate oxidation and increased mitochondrial density in skeletal muscle cells. *Amino acids,* 45(4):901-911.

VERGANI, L., FLOREANI, M., RUSSELL, A., CECCON, M., NAPOLI, E., CABRELLE, A., VALENTE, L., BRAGANTINI, F., LEGER, B. & DABBENI-SALA, F. 2004. Antioxidant defences and homeostasis of reactive oxygen species in different human mitochondrial DNA-depleted cell lines. *European journal of biochemistry,* 271(18):3646-3656.

VERGANI, L., PRESCOTT, A.R. & HOLT, I.J. 2000. Rhabdomyosarcoma ρ 0 cells: Isolation and characterization of a mitochondrial DNA depleted cell line with 'muscle-like'properties. *Neuromuscular disorders,* 10(6):454-459.

VERGANI, L., MALENA, A., SABATELLI, P., LORO, E., CAVALLINI, L., MAGALHAES, P., VALENTE, L., BRAGANTINI, F., CARRARA, F., LEGER, B., POULTON, J., RUSSELL, A.P. & HOLT, I.J. 2007. Cultured muscle cells display defects of mitochondrial myopathy ameliorated by anti-oxidants. *Brain : A journal of neurology,* 130(10):2715-2724.

VERMEULEN, R.C., KURK, R.M., VISSER, F.C., SLUITER, W. & SCHOLTE, H.R. 2010. Patients with chronic fatigue syndrome performed worse than controls in a controlled repeated exercise study despite a normal oxidative phosphorylation capacity. *J transl med,* 8(93).

VERNON, S.D., WHISTLER, T., CAMERON, B., HICKIE, I.B., REEVES, W.C. & LLOYD, A. 2006. Preliminary evidence of mitochondrial dysfunction associated with post-infective fatigue after acute infection with epstein barr virus. *BMC infectious diseases,* 6(1):15.

VIHINEN, M. 2015. Muddled genetic terms miss and mess the message. *Trends in genetics,* 31(8):423-425.

VILLANI, G. & ATTARDI, G. 1997. In vivo control of respiration by cytochrome c oxidase in wild-type and mitochondrial DNA mutation-carrying human cells. *Proceedings of the national academy of sciences of the united states of america,* 94(4):1166-1171.

VUNJAK-NOVAKOVIC, G. & FRESHNEY, R.I. 2006. Culture of Cells for Tissue Engineering. John Wiley & Sons.

WALLACE, D.C., SINGH, G., LOTT, M.T., HODGE, J.A., SCHURR, T.G., LEZZA, A.M., ELSAS, L.J.,2ND & NIKOSKELAINEN, E.K. 1988. Mitochondrial DNA mutation associated with leber's hereditary optic neuropathy. *Science (new york, N.Y.),* 242(4884):1427-1430.

WANG, K., TAKAHASHI, Y., GAO, Z., WANG, G., CHEN, X., GOTO, J., LOU, J. & TSUJI, S. 2009. Mitochondrial ND3 as the novel causative gene for leber hereditary optic neuropathy and dystonia. *Neurogenetics,* 10(4):337-345.

WANG, Y. & BOGENHAGEN, D.F. 2006. Human mitochondrial DNA nucleoids are linked to protein folding machinery and metabolic enzymes at the mitochondrial inner membrane. *The journal of biological chemistry,* 281(35):25791-25802.

WILKINS, H.M., CARL, S.M. & SWERDLOW, R.H. 2014. Cytoplasmic hybrid (cybrid) cell lines as a practical model for mitochondriopathies. *Redox biology,* 2:619-631.

WILLIAMS, A.J., MURRELL, M., BRAMMAH, S., MINCHENKO, J. & CHRISTODOULOU, J. 1999. A novel system for assigning the mode of inheritance in mitochondrial disorders using cybrids and rhodamine 6G. *Human molecular genetics,* 8(9):1691-1697.

YARHAM, J.W., AL-DOSARY, M., BLAKELY, E.L., ALSTON, C.L., TAYLOR, R.W., ELSON, J.L. & MCFARLAND, R. 2011. A comparative analysis approach to determining the pathogenicity of mitochondrial tRNA mutations. *Human mutation,* 32(11):1319-1325.

YE, K., LU, J., MA, F., KEINAN, A. & GU, Z. 2014. Extensive pathogenicity of mitochondrial heteroplasmy in healthy human individuals. *Proceedings of the national academy of sciences of the united states of america,* 111(29):10654-10659.

ZEVIANI, M. & DI DONATO, S. 2004. Mitochondrial disorders. *Brain : A journal of neurology,* 127(10):2153-2172.

ZHANG, C., BAUMER, A., MACKAY, I.R., LINNANE, A.W. & NAGLEY, P. 1995. Unusual pattern of mitochondrial DNA deletions in skeletal muscle of an adult human with chronic fatigue syndrome. *Human molecular genetics,* 4(4):751-754.

ZHANG, J., NUEBEL, E., WISIDAGAMA, D.R., SETOGUCHI, K., HONG, J.S., VAN HORN, C.M., IMAM, S.S., VERGNES, L., MALONE, C.S. & KOEHLER, C.M. 2012. Measuring energy metabolism in cultured cells, including human pluripotent stem cells and differentiated cells. *Nature protocols,* 7(6):1068-1085.

APPENDIX A: Seahorse XF^{e}96 assay template

DAY 1

1. Create a protocol for the assay using the Seahorse Bioscience software

Turn on instrument and start XF software to allow instrument to stabilize at 37°C 3-24 hours before analysis.

	1	2	3	4	5	6	7	8	9	10	11	12
A	BLANK											BLANK
B												
C												
D												
E												
F												
G												
H	BLANK											BLANK

2. Seed Cells in XF^{e}96 Cell Culture Plate

- Harvest cells by trypsinization. Add _____ mL media to _____ flask/well.
- Mix well and place all cells into a 15 mL centrifuge tube
- Place 900 µL PBS into a 1.5 mL epi and add 100 µL of the cells to this. Count the cells using the Sceptor 2.0 Handheld cell counter. Multiply the answer by 10 and enter the values into the excel spreadsheet.

Sample				
Number of cells per mL				
Desired cell seeding density (cells/well)				
Final volume of cells to be added to master mix				
Final volume of medium to be added to mastermix				

- Make up master mixes and seed 80 µL cells/well using a multichannel pipette and sterile reservoir or using a single-channel pipette.
- Allow the plate to stand at room temperature for 1 hour in the laminar flow cabinet before placing in the 5% CO_2 incubator at 37°C for _____ hours.

Time that cells were placed in incubator: _____

3. Prepare Sensor Cartridge for the XF96 Assay

Add 200 µL of Seahorse XF Calibrant into each well of the sensor cartridge utility plate. Place in a non-CO_2 37 °C incubator for 24 hours. Wrap the cartridge in parafilm if it is incubated for more than 24 hours to prevent evaporation.

DAY 2 – MITO STRESS TEST

1. Prepare unbuffered assay medium - _____ mL in total

- Pyruvate (_____ mM) - _____ mL
- Glucose (_____ mM) - _____ mL
- Assay medium - _____ mL
- Warm assay medium to 37°C and adjust pH to 7.4 with _____ µL 0.5M NaOH
- Set aside _____ mL assay medium for injectable compounds.
- Adjust buffering capacity on Wave software, accordingly - _____

2. Replace cell culture medium with assay medium and incubate in non-CO_2 incubator for 1 hour

- Time to begin washing cells: _____
- Check cells under microscope
- XF Prep Station requires approximately 140 mL assay medium, 300 mL ddH_2O and 200 mL 70% ethanol ("Clean") per 96 well plate.
- Prime Manifold – First prime with "Clean" then prime with "H_2O".
- Media Change – Select "Do Prime" and "Do Rinse" and the final volume _175_ µL.
- Check cells under microscope and incubate in non-CO_2 incubator for 1 hour.
- Maintenance tab – Empty all media from the media bottle and re-attach it. Choose "Long Shutdown". Rinse all bottles, including waste bottle, and caps with 70% ethanol and then ddH_2O.

3. Prepare injectable compounds using unbuffered assay medium

- Calculate all volumes and concentrations using the excel spreadsheet
- Make up the compounds:
- A – Oligomycin (_____ µM) → _____ µL oligomycin (2.5 mM) + _____ µL assay medium
- B – FCCP (_____µM) → _____ µL FCCP (2.5 mM) + _____ µL assay medium
- C – Rotenone (1 µM) and antimycin A (1 µM) → _____ µL each for rotenone (2.5 mM) and antimycin A (2.5 mM) + _____ µL assay medium
- Load 25 µL of each compound into the respective wells (including blanks) using the loading guides

4. Place cartridge & utility plate with calibration buffer into XF Analyser. Run protocol from template to calibrate cartridge. Check cells under microscope. Upon completion of cartridge calibration, load cell culture plate into instrument. Continue to run assay protocol.

APPENDIX B: MutPred scores

Table B1: Adjusted MutPred scores for each mitochondrial gene and complex of each patient

Subject	MT-ATP6	MT-ATP8	MT-CO1	MT-CO3	MT-CYB*	MT-ND1	MT-ND2	MT-ND3	MT-ND4	MT-ND5	MT-CI	MT-CIV	MT-CV
SA5	0.369	0.320		0.249	0.309							0.249	0.345
SA6	0.369		0.629	0.249	0.309							0.439	0.369
SA11	0.369			0.249	0.309	0.661	0.292				0.477	0.249	0.369
SA25	0.369			0.249	0.360							0.249	0.369
SA26	0.369			0.249	0.362							0.249	0.369
SA36	0.369			0.249	0.362							0.249	0.369
SA1	0.369			0.255	0.309							0.255	0.369
SA19	0.286				0.282				0.394		0.394		0.286
SA16	0.492	0.514			0.309		0.628			0.724	0.676		0.498
SA35	0.369				0.331	0.611		0.170		0.390	0.390		0.369
SA31	0.369			0.249	0.238	0.611	0.628				0.620	0.249	0.369
SA7	0.369				0.452								0.369
SA9	0.369				0.452	0.463					0.463		0.369
SA12	0.369				0.452								0.369
SA20	0.369				0.452								0.369
SA23	0.369				0.452					0.454	0.454		0.369
SA24	0.369				0.452	0.540					0.540		0.369
SA39	0.369		0.353		0.452					0.270	0.270	0.353	0.369
HC1	0.369			0.255	0.452							0.249	0.369
HC2	0.369			0.249	0.362					0.600	0.600	0.255	0.369
HC3	0.369			0.249	0.309	0.645				0.517	0.549	0.249	0.369
HC4	0.369				0.331	0.611		0.170		0.390	0.390		0.369
HC5	0.369				0.331	0.611		0.170		0.390	0.390		0.369
HC6	0.369				0.452					0.454	0.454		0.369
HC7	0.369				0.452				0.306		0.306		0.369

* MT-CYTB was the only gene in complex III that had non-synonymous variants.

APPENDIX C: Haplogroup identification

Table C1: Results from RFLP gel photos and haplogroup identification

Subject	B – NlaIII	D – AluI	F – DdeI	G – HinfI	H – BstNI	Haplogroup
SA5	No	Yes	No	Yes	Yes	U
SA6	No	Yes	No	Yes	Yes	U
SA11	No	Yes	No	Yes	Yes	U
SA25	No	Yes	No	Yes	Yes	U
SA26	No	Yes	No	Yes	Yes	U
SA36	No	Yes	No	Yes	Yes	U
SA1	No	Yes	No	Yes	Yes	U
SA19	No	Yes	No	Yes	Yes	U
SA16	No	Yes	No	No	Yes	Others DdeI-
SA35	Yes	Yes	Yes	No	No	J
SA31	Yes	Yes	No	No	Yes	T
SA7	No	No	No	No	Yes	H
SA9	No	No	No	No	Yes	H
SA12	No	No	No	No	Yes	H
SA39	No	*Yes*	No	No	Yes	*Others DdeI-*
SA20	No	No	No	No	Yes	H
SA23	No	No	No	No	Yes	H
SA24	No	No	No	No	Yes	H
HC1	No	Yes	No	Yes	Yes	U
HC2	No	Yes	No	Yes	Yes	U
HC3	No	Yes	No	Yes	Yes	U
HC4	Yes	Yes	Yes	No	No	J
HC5	Yes	Yes	Yes	No	No	J
HC6	No	No	No	No	Yes	H
HC7	No	No	No	No	Yes	H

APPENDIX D: Bioenergetics Results

The results obtained from the Mito Stress report generator for each of the plates shown in Table 4.9 (Section 4.6.1) are shown here, where A and B denote duplicate plates.

PLATE 1

WEEK 3

Table D1: Non-normalized bioenergetics results for Plate 1A at week 3

Subject	Basal respiration*		Proton leak*		Maximal respiration*		Spare respiratory capacity*		Non-mitochondrial respiration*		ATP production*	
	Value	SD	Value	SD	Value	SD	Value	SD	Value	SD	Value	SD
SA5	27.6	15.7	0.0	0.0	66.3	2.0	38.7	14.8	44.6	23.1	34.8	1.8
SA6	13.1	17.9	0.0	0.0	42.2	3.3	29.1	15.4	37.2	29.1	18.3	2.2
SA11	11.6	17.0	0.0	0.0	38.5	1.7	26.8	16.9	35.6	31.5	16.8	1.3
SA25	8.1	15.1	0.0	0.0	40.0	2.8	31.8	13.8	40.0	27.8	13.3	3.8
SA26	12.8	19.8	0.0	0.0	49.2	3.8	36.4	18.1	42.9	31.6	22.3	4.4
SA36	9.5	18.5	0.0	0.0	41.3	4.2	31.8	20.5	41.9	34.7	20.3	2.5
SA1	16.7	18.9	0.0	0.0	43.6	4.3	26.9	18.8	35.8	30.0	22.5	4.1
SA19	20.1	13.8	0.0	0.0	47.7	4.1	27.6	12.6	41.8	21.5	27.4	3.8
SA16	24.6	4.2	3.6	2.8	37.9	4.4	13.3	6.2	18.6	10.3	21.0	2.3
SA31	48.5	4.7	8.3	2.6	70.5	5.7	22.0	3.3	18.2	4.0	40.2	4.1
SA35	42.1	5.1	6.2	4.8	63.1	5.8	21.1	6.3	20.4	5.2	35.9	9.1
SA7	39.3	4.1	6.9	1.8	54.9	4.7	15.6	5.1	16.7	6.0	32.4	4.0
SA9	38.3	4.1	7.6	1.8	52.6	4.5	14.3	5.5	13.5	2.6	30.7	2.6
SA12	41.7	4.8	6.2	2.0	60.5	7.3	18.8	5.0	12.6	7.0	35.5	4.7
SA20	23.7	2.7	4.3	3.5	34.0	3.0	10.3	2.6	14.3	3.7	19.4	3.5
SA23	-6.2	8.1	0.0	0.0	34.1	1.8	40.3	6.6	55.5	8.1	1.6	13.3
SA24	29.4	8.5	2.8	1.4	65.1	5.6	35.8	5.8	40.2	9.4	26.6	9.5
SA39	35.4	1.0	7.8	0.5	54.7	2.7	19.3	2.4	13.5	4.6	27.6	0.7

* Units in pmol/min

Table D1N: Normalized bioenergetics results for Plate 1A at week 3

Subject	Basal respiration*		Proton leak*		Maximal respiration*		Spare respiratory capacity*		Non-mitochondrial respiration*		ATP production*	
	Value	SD	Value	SD	Value	SD	Value	SD	Value	SD	Value	SD
SA5	0.40	0.24	0.00	0.00	0.95	0.05	0.55	0.19	0.62	0.30	0.50	0.04
SA6	0.20	0.25	0.00	0.00	0.59	0.08	0.40	0.19	0.50	0.36	0.26	0.04
SA11	0.19	0.25	0.00	0.00	0.56	0.04	0.38	0.21	0.49	0.41	0.25	0.03
SA25	0.13	0.21	0.00	0.00	0.56	0.06	0.43	0.16	0.54	0.34	0.18	0.05
SA26	0.21	0.30	0.00	0.00	0.74	0.08	0.53	0.23	0.62	0.43	0.34	0.07
SA36	0.14	0.26	0.00	0.00	0.57	0.05	0.42	0.26	0.56	0.44	0.28	0.02
SA1	0.25	0.28	0.00	0.00	0.64	0.06	0.38	0.26	0.51	0.42	0.33	0.07
SA19	0.27	0.19	0.00	0.00	0.64	0.08	0.37	0.16	0.55	0.26	0.37	0.07
SA16	0.37	0.06	0.05	0.04	0.58	0.07	0.21	0.10	0.29	0.17	0.32	0.03
SA31	0.69	0.04	0.12	0.04	1.00	0.06	0.31	0.05	0.26	0.07	0.57	0.04
SA35	0.60	0.06	0.09	0.07	0.90	0.04	0.30	0.08	0.30	0.09	0.51	0.12
SA7	0.55	0.04	0.10	0.02	0.77	0.05	0.22	0.07	0.24	0.09	0.45	0.04
SA9	0.56	0.06	0.11	0.03	0.77	0.11	0.21	0.09	0.20	0.04	0.45	0.04
SA12	0.59	0.04	0.09	0.03	0.85	0.08	0.27	0.07	0.18	0.10	0.50	0.05
SA20	0.34	0.04	0.06	0.05	0.49	0.04	0.15	0.04	0.21	0.05	0.28	0.05
SA23	-0.09	0.12	0.00	0.00	0.52	0.03	0.62	0.10	0.85	0.12	0.02	0.20
SA24	0.43	0.13	0.04	0.02	0.95	0.11	0.52	0.07	0.58	0.11	0.39	0.15
SA39	0.54	0.02	0.12	0.01	0.83	0.05	0.29	0.04	0.21	0.08	0.42	0.02

* Units in pmol/min/cell number

Table D2: Coupling efficiency, spare respiratory capacity (%) and BHI for Plate 1A at week 3

Subject	Coupling Efficiency (%)		Spare respiratory capacity (%)		BHI	
	Value	SD	Value	SD	Value	SD
SA5	276.4	319.8	539.1	637.0	0.701	0.120
SA6	-114.6	269.1	-268.5	668.3	0.361	0.205
SA11	-490.5	1038.7	-1158.1	2432.4	0.489	0.169
SA25	-76.2	202.8	-146.3	524.2	0.266	0.160
SA26	-43.6	157.0	-88.4	359.4	0.717	0.270
SA36	-24.7	123.5	-35.1	243.4	0.540	0.117
SA1	-258.6	564.2	-622.7	1273.8	0.626	0.134
SA19	419.7	582.2	785.8	1131.7	0.410	0.056
SA16	86.8	9.4	159.6	35.4	0.879	0.686
SA31	83.0	4.9	145.9	9.0	0.796	0.263
SA35	84.3	11.6	151.5	17.9	0.625	0.206
SA7	82.3	4.1	140.7	15.0	0.662	0.328
SA9	80.5	2.9	138.8	17.2	0.620	0.165
SA12	85.0	4.9	145.6	11.8	0.827	0.329
SA20	82.3	15.5	144.6	13.4	0.471	0.334
SA23	-155.8	530.7	-808.3	1674.5	0.000	0.000
SA24	87.0	12.4	250.3	99.1	0.988	0.605
SA39	78.1	1.1	154.5	6.7	0.732	0.196

WEEK 6

Table D3: Non-normalized bioenergetics results for Plate 1A at week 6

Subject	Basal respiration*		Proton leak*		Maximal respiration*		Spare respiratory capacity*		Non-mitochondrial respiration*		ATP production*	
	Value	SD	Value	SD	Value	SD	Value	SD	Value	SD	Value	SD
SA5	56.9	2.8	15.7	1.2	81.6	4.8	24.7	2.3	15.2	1.1	41.2	2.2
SA6	42.9	6.3	14.3	2.5	61.0	11.9	18.1	7.3	12.5	4.7	28.6	4.3
SA11	36.1	5.1	11.1	1.6	50.8	4.1	14.7	4.4	10.7	5.9	25.0	5.0
SA25	56.5	1.2	16.3	1.3	82.9	5.2	26.4	5.4	15.4	3.3	40.2	1.4
SA26	41.7	0.9	12.8	1.2	58.9	3.8	17.2	3.9	11.1	2.0	28.9	1.4
SA36	41.6	3.2	12.6	1.4	54.8	2.1	13.2	3.3	8.9	2.2	29.1	2.0
SA1	39.6	5.5	12.5	1.2	54.2	3.2	14.6	3.5	9.2	5.7	27.0	4.8
SA19	54.6	1.7	16.3	0.7	66.0	5.0	11.4	4.6	10.9	0.9	38.3	1.6
SA16	31.2	3.9	11.3	3.6	39.8	3.1	8.7	2.2	7.6	3.3	19.9	2.5
SA31	76.4	2.4	16.1	1.0	113.6	3.6	37.2	4.4	16.6	2.9	60.3	2.4
SA35	51.4	5.4	13.1	3.1	75.1	2.8	23.7	3.4	15.0	3.0	38.4	3.6
SA7	44.8	6.7	12.1	2.3	66.0	6.8	21.2	3.5	12.7	6.9	32.8	4.9
SA9	59.7	2.4	14.6	0.9	74.8	6.5	15.1	6.1	14.2	3.6	45.0	2.2
SA12	57.9	7.4	14.4	6.9	76.4	8.1	18.5	2.1	7.7	5.7	43.5	8.1
SA20	53.0	2.9	15.6	3.1	71.0	3.7	18.0	1.3	12.9	1.9	37.4	2.2
SA23	54.5	2.6	16.9	1.2	69.5	3.5	15.0	1.8	10.3	3.9	37.6	1.6
SA24	50.3	1.2	13.5	0.3	72.0	3.6	21.7	2.8	14.4	1.7	36.8	1.1
SA39	50.7	4.8	13.5	0.8	68.6	2.1	17.9	4.8	11.6	4.7	37.2	4.7

* Units in pmol/min

Table D3N: Normalized bioenergetics results for Plate 1A at week 6

Subject	Basal respiration*		Proton leak*		Maximal respiration*		Spare respiratory capacity*		Non-mitochondrial respiration*		ATP production*	
	Value	SD	Value	SD	Value	SD	Value	SD	Value	SD	Value	SD
SA5	0.84	0.07	0.23	0.03	1.21	0.10	0.37	0.03	0.22	0.02	0.61	0.04
SA6	0.62	0.09	0.21	0.04	0.88	0.16	0.26	0.10	0.18	0.07	0.41	0.06
SA11	0.54	0.07	0.17	0.03	0.76	0.05	0.22	0.07	0.16	0.09	0.38	0.07
SA25	0.76	0.02	0.22	0.02	1.11	0.07	0.35	0.07	0.21	0.04	0.54	0.02
SA26	0.65	0.04	0.20	0.01	0.91	0.04	0.27	0.05	0.17	0.03	0.45	0.04
SA36	0.60	0.07	0.18	0.03	0.79	0.04	0.19	0.04	0.13	0.03	0.42	0.05
SA1	0.59	0.06	0.19	0.01	0.81	0.03	0.22	0.06	0.14	0.09	0.40	0.06
SA19	0.83	0.09	0.25	0.02	1.01	0.18	0.18	0.09	0.17	0.03	0.58	0.07
SA16	0.59	0.09	0.21	0.07	0.75	0.08	0.16	0.04	0.14	0.06	0.38	0.07
SA31	1.04	0.08	0.22	0.01	1.55	0.09	0.51	0.05	0.23	0.05	0.82	0.08
SA35	0.77	0.10	0.19	0.04	1.13	0.11	0.36	0.06	0.23	0.05	0.58	0.08
SA7	0.67	0.12	0.18	0.03	0.99	0.16	0.32	0.08	0.19	0.12	0.49	0.09
SA9	0.82	0.04	0.20	0.02	1.03	0.11	0.21	0.09	0.20	0.05	0.62	0.03
SA12	0.90	0.15	0.23	0.12	1.19	0.16	0.29	0.02	0.12	0.08	0.67	0.13
SA20	0.83	0.04	0.24	0.05	1.11	0.04	0.28	0.01	0.20	0.04	0.58	0.02
SA23	0.77	0.05	0.24	0.02	0.98	0.06	0.21	0.02	0.14	0.05	0.53	0.03
SA24	0.79	0.06	0.21	0.02	1.13	0.06	0.34	0.03	0.23	0.01	0.58	0.04
SA39	0.87	0.17	0.23	0.03	1.17	0.16	0.30	0.08	0.19	0.07	0.64	0.15

* Units in pmol/min/cell number

Table D4: Non-normalized bioenergetics results for Plate 1B at week 6

Subject	Basal respiration*		Proton leak*		Maximal respiration*		Spare respiratory capacity*		Non-mitochondrial respiration*		ATP production*	
	Value	SD	Value	SD	Value	SD	Value	SD	Value	SD	Value	SD
SA5	67.7	4.0	16.4	1.5	84.9	4.1	17.1	1.7	13.5	0.6	51.4	2.6
SA6	49.2	1.6	13.6	1.3	58.3	3.0	9.1	3.2	9.3	2.8	35.6	0.9
SA11	47.0	1.2	13.7	0.9	53.5	2.3	6.5	2.5	9.2	2.1	33.3	0.4
SA25	67.3	1.6	17.3	0.8	81.8	5.3	14.5	5.7	13.6	2.6	49.9	1.0
SA26	51.1	3.1	14.2	1.7	61.2	4.6	10.1	3.3	9.3	1.2	36.9	1.6
SA36	47.4	1.8	12.4	1.5	58.5	2.3	11.0	1.4	8.9	1.0	35.1	0.8
SA1	50.7	1.0	13.5	0.9	62.4	3.9	11.7	2.9	9.5	0.9	37.2	1.4
SA19	62.9	2.0	15.9	0.8	78.3	2.8	15.4	3.3	11.5	2.2	46.9	1.7
SA16	33.4	2.7	10.9	1.8	35.9	2.1	2.4	2.3	7.0	2.6	22.6	1.3
SA31	78.1	3.1	15.5	1.4	103.3	4.7	25.3	4.6	19.1	4.8	62.6	2.6
SA35	62.3	6.1	12.9	8.1	76.1	7.5	13.8	9.1	15.6	10.4	49.4	11.1
SA7	54.3	4.7	10.3	2.1	65.0	4.3	10.7	5.0	11.6	2.6	44.0	5.4
SA9	62.8	4.0	13.4	2.3	74.3	8.7	11.5	7.2	13.4	3.5	49.5	3.3
SA12	64.7	10.5	10.8	2.4	92.4	20.4	27.7	11.0	14.9	1.4	53.9	8.2
SA20	66.5	1.4	15.0	1.8	89.5	4.7	23.0	4.0	15.2	2.7	51.5	1.3
SA23	62.0	3.3	18.2	4.0	73.2	3.6	11.2	3.1	16.0	4.2	43.9	5.7
SA24	58.0	1.4	12.9	1.0	75.2	4.1	17.2	4.0	13.3	2.7	45.2	1.7
SA39	61.8	4.2	13.9	1.1	81.4	1.5	19.6	4.0	11.5	3.0	47.9	3.1

* Units in pmol/min

Table D4N: Normalized bioenergetics results for Plate 1B at week 6

Subject	Basal respiration*		Proton leak*		Maximal respiration*		Spare respiratory capacity*		Non-mitochondrial respiration*		ATP production*	
	Value	SD	Value	SD	Value	SD	Value	SD	Value	SD	Value	SD
SA5	0.95	0.05	0.23	0.02	1.19	0.08	0.24	0.04	0.19	0.01	0.72	0.03
SA6	0.74	0.05	0.20	0.03	0.87	0.06	0.14	0.05	0.14	0.04	0.53	0.02
SA11	0.74	0.02	0.21	0.02	0.84	0.04	0.10	0.04	0.15	0.03	0.52	0.01
SA25	1.00	0.04	0.26	0.02	1.21	0.06	0.21	0.08	0.20	0.04	0.74	0.02
SA26	0.80	0.08	0.22	0.04	0.96	0.10	0.16	0.05	0.15	0.02	0.58	0.04
SA36	0.80	0.05	0.21	0.03	0.98	0.07	0.19	0.03	0.15	0.02	0.59	0.02
SA1	0.83	0.03	0.22	0.02	1.02	0.05	0.19	0.04	0.16	0.02	0.61	0.02
SA19	0.85	0.03	0.22	0.01	1.06	0.04	0.21	0.04	0.16	0.03	0.64	0.03
SA16	0.51	0.03	0.16	0.02	0.54	0.02	0.04	0.03	0.11	0.04	0.34	0.02
SA31	1.11	0.04	0.22	0.02	1.47	0.09	0.36	0.07	0.27	0.07	0.89	0.04
SA35	0.88	0.09	0.18	0.12	1.07	0.09	0.19	0.12	0.22	0.15	0.69	0.15
SA7	0.86	0.08	0.16	0.03	1.03	0.09	0.17	0.08	0.18	0.04	0.70	0.09
SA9	0.91	0.06	0.19	0.04	1.08	0.12	0.17	0.10	0.19	0.05	0.72	0.05
SA12	1.03	0.18	0.17	0.04	1.47	0.33	0.44	0.18	0.24	0.02	0.86	0.14
SA20	0.95	0.03	0.22	0.03	1.28	0.07	0.33	0.06	0.22	0.03	0.74	0.03
SA23	0.92	0.05	0.27	0.06	1.09	0.04	0.17	0.05	0.24	0.07	0.65	0.08
SA24	0.97	0.04	0.21	0.01	1.25	0.10	0.29	0.07	0.22	0.04	0.75	0.04
SA39	0.99	0.07	0.22	0.02	1.30	0.06	0.31	0.07	0.18	0.05	0.76	0.05

* Units in pmol/min/cell number

Table D5: Coupling efficiency, spare respiratory capacity (%) and BHI for Plates 1A and 1B at week 6

	Plate 1A – Week 6						Plate 1B – Week 6					
Subject	Coupling Efficiency (%)		Spare respiratory capacity (%)		BHI		Coupling Efficiency (%)		Spare respiratory capacity (%)		BHI	
	Value	SD	Value	SD	Value	SD	Value	SD	Value	SD	Value	SD
SA5	72.5	1.6	143.4	2.6	0.632	0.068	75.9	1.0	125.4	3.1	0.599	0.075
SA6	66.7	3.0	142.2	14.4	0.475	0.181	72.4	2.0	118.6	6.7	0.406	0.159
SA11	68.7	6.4	142.5	17.5	0.382	0.122	70.9	1.3	113.9	5.6	0.213	0.249
SA25	71.2	2.1	146.7	9.7	0.630	0.191	74.2	0.7	121.6	8.6	0.454	0.260
SA26	69.3	2.8	141.3	9.6	0.540	0.118	72.3	1.8	119.8	6.8	0.424	0.230
SA36	69.9	1.3	132.5	10.0	0.532	0.085	74.0	2.2	123.2	2.9	0.546	0.091
SA1	68.0	3.3	138.6	13.8	0.649	0.417	73.3	2.0	123.1	5.3	0.520	0.114
SA19	70.1	1.3	120.9	8.4	0.359	0.182	74.7	1.0	124.7	5.8	0.595	0.142
SA16	64.3	7.7	128.9	10.0	0.366	0.146	67.6	3.4	107.7	7.4	-0.02	0.213
SA31	79.0	1.3	148.8	6.8	0.929	0.075	80.1	1.4	132.5	6.4	0.736	0.096
SA35	74.7	4.0	147.1	10.2	0.681	0.079	78.7	13.5	123.2	16.2	0.288	0.383
SA7	73.2	2.4	148.7	12.3	0.708	0.174	80.9	4.1	120.4	10.7	0.575	0.249
SA9	75.5	1.4	125.4	10.1	0.480	0.334	78.8	3.2	118.3	11.3	0.595	0.175
SA12	75.3	10.0	132.4	4.7	0.945	0.484	83.5	1.2	142.0	11.2	0.945	0.179
SA20	70.7	4.5	134.0	2.1	0.536	0.106	77.5	2.4	134.6	5.7	0.719	0.131
SA23	69.0	1.1	127.6	3.3	0.555	0.265	70.5	7.4	118.2	5.7	0.229	0.212
SA24	73.2	0.7	143.1	5.3	0.614	0.053	77.8	1.8	129.6	7.1	0.656	0.183
SA39	73.2	2.5	136.4	12.4	0.655	0.250	77.5	0.5	132.3	8.6	0.778	0.145

PLATE 2

WEEK 3

Table D6: Non-normalized bioenergetics results for Plate 2A at week 3

Subject	Basal respiration*		Proton leak*		Maximal respiration*		Spare respiratory capacity*		Non-mitochondrial respiration*		ATP production*	
	Value	SD	Value	SD	Value	SD	Value	SD	Value	SD	Value	SD
HC1	28.9	3.0	7.3	2.8	36.0	3.4	7.1	2.1	-1.7	4.8	21.6	1.8
HC2	33.3	1.6	6.1	1.2	37.9	3.3	4.6	3.1	3.0	1.4	27.1	1.6
HC3	18.4	2.2	6.4	2.4	16.1	1.7	0.0	0.0	-3.9	3.0	12.1	3.3
HC4	29.4	2.4	6.3	0.8	32.3	3.5	2.9	1.6	-0.6	2.1	23.1	1.8
HC5	28.2	1.3	6.6	1.3	35.1	2.2	7.0	1.5	-0.7	2.3	21.5	0.8
HC6	26.7	1.7	5.7	1.4	31.5	4.1	4.7	3.3	-2.7	2.7	21.0	2.0
HC7	18.6	2.9	2.7	2.7	23.6	3.3	5.0	4.5	-1.4	2.7	15.8	2.9
SA5	20.6	2.9	4.3	3.5	29.4	1.0	8.9	2.1	2.1	4.1	16.3	5.5
SA6	41.6	1.9	8.6	2.5	54.2	1.0	12.6	2.6	6.7	2.3	33.0	1.3
SA11	19.2	4.5	5.4	2.6	25.3	2.5	6.2	2.6	3.4	3.9	13.8	3.1
SA25	32.8	4.5	5.0	1.0	38.2	3.1	5.4	4.5	-0.8	5.7	27.8	4.4
SA26	26.5	5.0	7.8	3.0	35.0	3.4	8.5	2.6	2.5	5.2	18.7	7.4
SA36	27.7	5.2	6.1	2.0	35.9	4.1	8.2	3.1	6.1	5.9	21.6	5.7
SA1	30.5	1.6	6.7	1.5	36.1	3.4	5.7	2.8	-1.7	2.6	23.8	1.5
SA19	32.3	4.2	4.1	3.1	41.2	2.0	8.9	4.2	5.6	4.5	28.2	5.7

* Units in pmol/min

Table D6N: Normalized bioenergetics results for Plate 2A at week 3

Subject	Basal respiration*		Proton leak*		Maximal respiration*		Spare respiratory capacity*		Non-mitochondrial respiration*		ATP production*	
	Value	SD	Value	SD	Value	SD	Value	SD	Value	SD	Value	SD
HC1	0.49	0.05	0.12	0.04	0.61	0.05	0.12	0.03	-0.03	0.08	0.36	0.04
HC2	0.54	0.04	0.10	0.02	0.62	0.06	0.08	0.05	0.05	0.02	0.44	0.04
HC3	0.30	0.04	0.10	0.04	0.26	0.03	0.00	0.00	-0.07	0.05	0.20	0.06
HC4	0.45	0.03	0.10	0.01	0.50	0.05	0.05	0.03	-0.01	0.03	0.36	0.03
HC5	0.47	0.02	0.11	0.02	0.58	0.04	0.12	0.03	-0.01	0.04	0.36	0.02
HC6	0.45	0.02	0.10	0.02	0.53	0.06	0.08	0.05	-0.05	0.05	0.36	0.03
HC7	0.33	0.06	0.05	0.05	0.41	0.06	0.09	0.08	-0.03	0.05	0.28	0.05
SA5	0.37	0.05	0.08	0.06	0.53	0.02	0.16	0.04	0.04	0.07	0.29	0.10
SA6	0.64	0.04	0.13	0.04	0.83	0.04	0.19	0.04	0.10	0.04	0.51	0.02
SA11	0.33	0.08	0.09	0.05	0.43	0.05	0.10	0.04	0.06	0.07	0.24	0.05
SA25	0.53	0.08	0.08	0.02	0.62	0.05	0.09	0.07	-0.01	0.09	0.45	0.07
SA26	0.40	0.07	0.12	0.03	0.54	0.04	0.13	0.04	0.04	0.08	0.29	0.05
SA36	0.41	0.08	0.09	0.03	0.53	0.06	0.12	0.05	0.09	0.09	0.32	0.09
SA1	0.48	0.02	0.11	0.02	0.57	0.05	0.09	0.04	-0.03	0.04	0.38	0.03
SA19	0.51	0.07	0.06	0.05	0.64	0.03	0.14	0.06	0.09	0.07	0.44	0.11

* Units in pmol/min/cell number

Table D7: Non-normalized bioenergetics results for Plate 2B at week 3

Subject	Basal respiration*		Proton leak*		Maximal respiration*		Spare respiratory capacity*		Non-mitochondrial respiration*		ATP production*	
	Value	SD	Value	SD	Value	SD	Value	SD	Value	SD	Value	SD
HC1	27.9	2.0	8.3	0.9	35.4	1.8	7.6	2.4	5.5	4.2	19.6	2.1
HC2	34.2	5.1	7.7	2.4	43.5	5.2	9.3	2.3	2.3	7.9	26.5	4.4
HC3	19.1	1.9	7.6	1.0	18.2	1.1	0.0	0.0	-0.1	2.5	11.5	1.6
HC4	30.8	1.9	10.5	6.0	39.2	5.4	8.3	5.0	4.9	4.1	20.3	5.5
HC5	30.0	2.4	8.8	2.3	34.4	2.9	4.4	3.2	1.5	2.8	21.2	1.0
HC6	25.2	2.5	7.3	1.7	34.5	4.2	9.2	2.0	3.6	2.9	17.9	1.8
HC7	18.4	3.1	5.9	1.3	23.7	2.0	5.4	2.8	0.1	1.6	12.5	1.9
SA5	26.6	1.2	7.8	0.9	33.6	1.2	7.0	1.5	5.2	2.4	18.8	1.7
SA6	44.5	1.5	8.9	1.4	54.0	5.3	9.6	5.8	11.7	4.7	35.6	2.8
SA11	22.7	2.5	7.1	1.7	26.4	2.0	3.7	1.9	5.7	5.3	15.7	1.7
SA25	30.3	4.7	7.4	1.5	38.7	3.2	8.5	3.7	7.4	8.8	22.9	4.6
SA26	29.9	1.1	8.7	0.7	37.5	2.3	7.6	2.1	5.2	1.3	21.2	0.4
SA36	35.9	6.4	6.2	3.4	41.4	2.2	5.5	5.3	3.6	6.8	29.7	9.2
SA1	30.8	1.0	8.7	0.5	37.0	2.3	6.2	2.0	5.1	1.4	22.1	1.4
SA19	38.4	2.2	7.1	2.6	42.6	0.9	4.2	1.8	8.4	4.5	31.3	3.8

* Units in pmol/min

Table D7N: Normalized bioenergetics results for Plate 2B at week 3

Subject	Basal respiration*		Proton leak*		Maximal respiration*		Spare respiratory capacity*		Non-mitochondrial respiration*		ATP production*	
	Value	SD	Value	SD	Value	SD	Value	SD	Value	SD	Value	SD
HC1	0.42	0.04	0.12	0.01	0.53	0.03	0.11	0.04	0.08	0.06	0.29	0.04
HC2	0.51	0.08	0.11	0.04	0.64	0.08	0.14	0.03	0.03	0.11	0.39	0.07
HC3	0.29	0.04	0.11	0.02	0.27	0.02	0.00	0.00	0.00	0.04	0.17	0.03
HC4	0.42	0.04	0.15	0.09	0.54	0.09	0.12	0.07	0.07	0.06	0.27	0.07
HC5	0.49	0.04	0.14	0.04	0.56	0.06	0.07	0.05	0.02	0.05	0.34	0.02
HC6	0.36	0.04	0.10	0.03	0.48	0.06	0.13	0.03	0.05	0.04	0.25	0.02
HC7	0.30	0.06	0.10	0.03	0.39	0.05	0.09	0.04	0.00	0.03	0.20	0.04
SA5	0.45	0.03	0.13	0.01	0.57	0.04	0.12	0.03	0.09	0.04	0.32	0.04
SA6	0.65	0.04	0.13	0.02	0.78	0.06	0.14	0.08	0.17	0.07	0.52	0.05
SA11	0.35	0.04	0.11	0.03	0.41	0.03	0.06	0.03	0.09	0.08	0.24	0.03
SA25	0.43	0.05	0.10	0.02	0.55	0.04	0.12	0.06	0.11	0.13	0.32	0.05
SA26	0.48	0.02	0.14	0.01	0.61	0.04	0.12	0.03	0.08	0.02	0.34	0.01
SA36	0.53	0.09	0.09	0.05	0.61	0.02	0.08	0.08	0.05	0.10	0.44	0.13
SA1	0.42	0.01	0.12	0.01	0.51	0.03	0.09	0.03	0.07	0.02	0.30	0.02
SA19	0.53	0.04	0.10	0.03	0.59	0.03	0.06	0.02	0.11	0.05	0.43	0.06

* Units in pmol/min/cell number

Table D8: Coupling efficiency, spare respiratory capacity (%) and BHI for Plates 2A and 2B at week 3

Subject	Plate 2A – Week 3						Plate 2B – Week 3					
	Coupling Efficiency (%)		Spare respiratory capacity (%)		BHI		Coupling Efficiency (%)		Spare respiratory capacity (%)		BHI	
	Value	SD	Value	SD	Value	SD	Value	SD	Value	SD	Value	SD
HC1	75.2	7.4	125.1	9.0	1.145	0.660	70.3	3.4	127.6	10.1	0.506	0.361
HC2	81.6	3.5	114.1	9.7	0.765	0.677	77.8	6.1	128.1	9.1	0.719	0.247
HC3	64.7	15.4	88.3	13.8	0.000	0.000	60.2	4.2	96.1	5.8	0.000	0.000
HC4	78.6	1.7	109.6	5.2	1.059	0.336	66.3	17.9	127.1	15.5	0.419	0.220
HC5	76.6	3.7	124.7	5.2	1.215	0.112	71.1	5.8	115.2	12.0	0.953	0.666
HC6	78.6	5.1	117.6	11.6	1.400	0.613	71.3	5.1	136.2	5.7	0.929	0.444
HC7	86.1	15.5	130.3	29.9	0.432	0.613	68.3	3.1	131.7	16.6	1.273	0.329
SA5	77.5	17.5	145.6	17.9	0.779	0.356	70.6	3.8	126.7	6.7	0.551	0.344
SA6	79.5	5.1	130.7	7.3	0.895	0.259	80.0	3.8	121.7	13.3	0.431	0.396
SA11	74.1	14.1	140.1	35.6	0.757	0.478	69.2	5.8	117.2	10.1	0.068	0.197
SA25	84.6	3.2	117.8	13.4	1.029	0.217	75.1	6.8	130.4	19.1	0.707	0.674
SA26	66.8	23.0	135.8	19.3	0.484	1.090	70.8	1.5	125.6	6.8	0.552	0.191
SA36	77.0	10.2	132.3	16.1	0.639	0.379	81.1	10.6	118.0	16.7	0.476	0.204
SA1	78.1	4.3	118.6	8.7	1.421	0.129	71.6	2.3	120.2	6.3	0.485	0.226
SA19	86.7	9.4	129.6	17.3	1.093	0.597	81.4	7.1	111.1	5.2	0.386	0.262

WEEK 6

Table D9: Non-normalized bioenergetics results for Plate 2A at week 6

Subject	Basal respiration*		Proton leak*		Maximal respiration*		Spare respiratory capacity*		Non-mitochondrial respiration*		ATP production*	
	Value	SD	Value	SD	Value	SD	Value	SD	Value	SD	Value	SD
HC1	39.0	2.1	12.9	1.4	46.3	2.4	7.4	3.7	3.8	2.5	26.0	1.0
HC2	43.5	8.4	12.7	1.7	54.1	5.2	10.5	4.3	10.1	7.5	30.9	7.7
HC3	34.4	2.6	12.2	1.1	33.3	1.2	0.0	0.0	4.7	1.4	22.1	1.8
HC4	37.1	1.6	12.0	1.4	39.8	4.1	2.7	4.0	5.5	3.2	25.1	1.8
HC5	41.0	2.6	12.5	1.7	49.7	3.4	8.6	1.9	3.9	3.8	28.5	2.1
HC6	32.7	2.5	12.0	1.9	37.8	3.4	5.1	1.2	3.8	1.4	20.8	2.4
HC7	55.8	5.2	14.9	1.7	75.0	12.0	19.1	7.8	9.2	2.3	40.9	5.4
SA5	59.9	3.9	15.5	2.2	85.3	3.4	25.4	3.3	12.8	4.7	44.4	1.9
SA6	40.5	3.9	12.2	0.8	54.9	4.0	14.4	3.9	7.5	2.4	28.3	3.9
SA11	46.2	1.8	13.2	1.0	56.8	3.4	10.6	2.8	7.9	2.7	33.0	1.8
SA25	38.3	5.4	10.5	1.0	49.9	2.4	11.6	5.9	8.5	4.9	27.8	5.9
SA26	43.1	2.8	13.1	1.5	58.3	3.2	15.2	4.7	6.9	4.1	30.0	1.5
SA36	48.8	2.5	12.1	2.7	63.2	4.8	14.4	3.1	10.9	1.0	36.7	2.2
SA1	39.9	3.2	13.0	1.7	50.1	3.1	10.2	0.6	4.6	3.6	27.0	1.7
SA19	43.3	3.1	12.2	1.5	50.3	4.0	7.0	4.2	8.4	3.4	31.1	2.2

* Units in pmol/min

Table D9N: Normalized bioenergetics results for Plate 2A at week 6

Subject	Basal respiration*		Proton leak*		Maximal respiration*		Spare respiratory capacity*		Non-mitochondrial respiration*		ATP production*	
	Value	SD	Value	SD	Value	SD	Value	SD	Value	SD	Value	SD
HC1	0.63	0.05	0.21	0.02	0.75	0.07	0.12	0.06	0.06	0.04	0.42	0.03
HC2	0.71	0.14	0.21	0.03	0.88	0.08	0.17	0.07	0.17	0.13	0.50	0.13
HC3	0.55	0.05	0.20	0.02	0.54	0.03	0.00	0.00	0.08	0.02	0.36	0.03
HC4	0.65	0.04	0.21	0.02	0.69	0.07	0.05	0.07	0.10	0.06	0.44	0.04
HC5	0.67	0.06	0.20	0.03	0.81	0.08	0.14	0.03	0.06	0.06	0.46	0.05
HC6	0.51	0.04	0.19	0.03	0.59	0.06	0.08	0.02	0.06	0.02	0.32	0.04
HC7	0.83	0.07	0.22	0.03	1.11	0.17	0.28	0.12	0.14	0.03	0.61	0.08
SA5	0.97	0.06	0.25	0.03	1.38	0.06	0.41	0.06	0.21	0.08	0.72	0.03
SA6	0.72	0.06	0.22	0.02	0.97	0.05	0.25	0.07	0.13	0.05	0.50	0.06
SA11	0.72	0.01	0.21	0.01	0.89	0.05	0.17	0.04	0.12	0.04	0.52	0.02
SA25	0.64	0.07	0.18	0.02	0.84	0.05	0.20	0.11	0.14	0.09	0.47	0.09
SA26	0.66	0.05	0.20	0.03	0.90	0.06	0.23	0.07	0.11	0.06	0.46	0.03
SA36	0.73	0.05	0.18	0.04	0.95	0.09	0.22	0.05	0.16	0.01	0.55	0.04
SA1	0.62	0.05	0.20	0.03	0.78	0.05	0.16	0.01	0.07	0.06	0.42	0.03
SA19	0.66	0.06	0.19	0.03	0.76	0.04	0.10	0.06	0.13	0.05	0.47	0.03

* Units in pmol/min/cell number

Table D10: Non-normalized bioenergetics results for Plate 2B at week 6

Subject	Basal respiration*		Proton leak*		Maximal respiration*		Spare respiratory capacity*		Non-mitochondrial respiration*		ATP production*	
	Value	SD	Value	SD	Value	SD	Value	SD	Value	SD	Value	SD
HC1	38.9	1.6	11.3	1.7	50.0	2.1	11.1	2.9	9.4	3.1	27.6	1.3
HC2	43.3	7.0	6.2	4.5	64.7	6.5	21.4	2.1	18.4	8.3	37.1	4.0
HC3	39.6	5.1	11.5	3.6	38.2	2.4	0.0	0.0	7.7	4.1	28.1	7.3
HC4	35.9	6.6	9.5	4.8	43.1	4.4	7.2	5.2	9.7	12.3	26.4	2.9
HC5	36.7	2.4	9.5	2.0	46.6	2.2	10.0	3.0	10.4	3.3	27.2	0.7
HC6	34.1	1.7	8.5	2.0	49.5	2.4	15.4	1.3	14.1	4.4	25.6	1.3
HC7	51.6	4.0	11.3	2.9	72.8	8.8	21.2	8.2	16.1	6.4	40.3	3.2
SA5	61.4	4.8	15.2	2.8	91.4	6.9	29.9	3.8	16.3	4.9	46.2	5.3
SA6	36.6	7.3	4.7	10.4	55.1	4.3	18.5	6.7	23.7	6.8	31.9	9.5
SA11	48.5	2.7	13.1	3.0	62.5	3.6	14.0	2.2	12.8	5.4	35.3	1.2
SA25	36.0	5.7	7.0	4.8	55.6	5.3	19.6	3.5	19.6	7.6	29.0	2.4
SA26	42.4	2.0	10.9	1.5	61.4	3.6	19.0	2.6	13.2	2.5	31.5	1.6
SA36	49.2	9.2	8.0	4.3	70.1	7.5	20.9	6.0	19.6	10.6	41.2	6.0
SA1	41.2	4.7	10.5	2.6	55.6	4.4	14.4	1.5	8.9	5.7	30.7	5.0
SA19	41.7	5.7	8.9	3.6	55.1	4.5	13.4	4.6	19.0	7.8	32.7	2.7

* Units in pmol/min

Table D10N: Normalized bioenergetics results for Plate 2B at week 6

Subject	Basal respiration*		Proton leak*		Maximal respiration*		Spare respiratory capacity*		Non-mitochondrial respiration*		ATP production*	
	Value	SD	Value	SD	Value	SD	Value	SD	Value	SD	Value	SD
HC1	0.60	0.04	0.17	0.03	0.77	0.03	0.17	0.04	0.15	0.05	0.43	0.03
HC2	0.73	0.15	0.11	0.08	1.10	0.16	0.36	0.04	0.31	0.13	0.63	0.08
HC3	0.59	0.10	0.17	0.06	0.57	0.05	0.00	0.00	0.11	0.06	0.42	0.12
HC4	0.58	0.12	0.15	0.08	0.69	0.07	0.11	0.08	0.15	0.20	0.42	0.06
HC5	0.54	0.04	0.14	0.03	0.68	0.04	0.15	0.04	0.15	0.05	0.40	0.01
HC6	0.53	0.04	0.13	0.03	0.76	0.05	0.24	0.02	0.22	0.07	0.39	0.02
HC7	0.76	0.08	0.17	0.05	1.07	0.15	0.31	0.12	0.24	0.09	0.59	0.05
SA5	0.93	0.08	0.23	0.05	1.39	0.12	0.46	0.07	0.25	0.07	0.70	0.08
SA6	0.61	0.14	0.08	0.17	0.91	0.10	0.31	0.11	0.39	0.11	0.52	0.15
SA11	0.66	0.03	0.18	0.04	0.85	0.03	0.19	0.03	0.18	0.08	0.48	0.02
SA25	0.55	0.10	0.11	0.06	0.85	0.11	0.30	0.06	0.30	0.11	0.44	0.05
SA26	0.64	0.04	0.16	0.02	0.93	0.06	0.29	0.04	0.20	0.04	0.48	0.04
SA36	0.75	0.14	0.12	0.06	1.06	0.13	0.32	0.09	0.30	0.16	0.63	0.10
SA1	0.67	0.09	0.17	0.04	0.90	0.09	0.23	0.02	0.15	0.10	0.50	0.09
SA19	0.71	0.10	0.15	0.06	0.94	0.08	0.23	0.08	0.33	0.14	0.56	0.05

* Units in pmol/min/cell number

Table D11: Coupling efficiency, spare respiratory capacity (%) and BHI for Plates 2A and 2B at week 6

	Plate 2A – Week 6						Plate 2B – Week 6					
Subject	Coupling Efficiency (%)		Spare respiratory capacity (%)		BHI		Coupling Efficiency (%)		Spare respiratory capacity (%)		BHI	
	Value	SD	Value	SD	Value	SD	Value	SD	Value	SD	Value	SD
HC1	66.9	1.9	119.3	10.0	0.585	0.322	71.0	3.6	128.7	8.2	0.470	0.160
HC2	69.8	6.8	127.7	19.2	0.460	0.294	87.0	9.4	151.3	12.2	0.921	0.153
HC3	64.5	1.8	97.4	4.9	-0.45	0.199	70.2	9.8	97.7	11.3	-0.45	0.815
HC4	67.6	3.6	107.5	11.1	-0.29	0.813	75.3	12.2	123.2	19.9	-0.04	0.376
HC5	69.5	3.5	121.1	4.8	0.680	0.251	74.3	3.8	127.6	9.9	0.453	0.145
HC6	63.4	4.9	115.3	2.7	0.383	0.260	75.2	4.8	145.1	3.8	0.554	0.182
HC7	73.1	3.8	133.6	11.8	0.735	0.186	78.3	5.1	141.5	16.0	0.578	0.551
SA5	74.2	2.2	142.7	7.8	0.784	0.182	75.2	5.1	148.9	6.8	0.771	0.178
SA6	69.6	3.6	136.3	12.0	0.642	0.218	89.4	30.3	155.8	29.6	0.305	0.188
SA11	71.4	2.2	122.9	6.0	0.533	0.263	73.1	4.8	128.9	4.7	0.528	0.225
SA25	72.0	5.4	132.9	19.7	0.494	0.175	82.2	12.8	156.5	14.8	0.621	0.154
SA26	69.7	1.9	136.0	13.0	0.825	0.346	74.4	2.9	144.8	5.8	0.627	0.051
SA36	75.4	4.9	129.5	6.0	0.608	0.173	84.7	7.3	145.9	22.0	0.904	0.350
SA1	67.6	2.1	125.6	2.5	0.738	0.514	74.4	6.4	135.7	6.9	0.857	0.567
SA19	71.9	2.1	116.4	9.5	0.566	0.311	79.3	6.3	133.8	15.5	0.460	0.269

PLATE 3

WEEK 3

Table D12: Non-normalized bioenergetics results for Plate 3A at week 3

Subject	Basal respiration*		Proton leak*		Maximal respiration*		Spare respiratory capacity*		Non-mitochondrial respiration*		ATP production*	
	Value	SD	Value	SD	Value	SD	Value	SD	Value	SD	Value	SD
HC1	39.3	2.0	8.9	1.4	58.0	4.3	18.8	2.5	10.7	4.9	30.4	1.0
HC2	42.8	2.9	8.5	1.0	63.4	6.0	20.6	4.5	14.1	3.9	34.3	2.8
HC3	30.6	2.7	7.7	2.2	31.3	3.5	0.7	3.7	8.3	5.5	22.9	2.5
HC4	47.4	3.1	9.5	0.9	61.1	1.4	13.7	2.4	11.2	3.2	37.9	2.9
HC5	35.1	2.5	7.1	2.1	47.7	3.4	12.6	1.8	11.1	6.0	28.0	0.8
HC6	45.0	2.4	9.8	1.6	64.3	4.5	19.3	2.3	13.3	3.1	35.2	3.5
HC7	37.8	5.0	6.0	1.6	48.8	2.0	11.1	4.4	11.8	4.5	31.8	3.7
SA16	32.5	1.7	8.0	1.0	40.4	2.6	7.9	1.7	9.3	3.0	24.5	1.3
SA31	49.4	3.0	10.4	1.2	63.4	4.5	13.9	2.5	11.1	2.2	39.0	2.8
SA35	44.5	3.3	9.2	2.2	54.2	2.9	9.7	2.8	10.0	5.0	35.3	1.9
SA7	40.5	3.6	8.3	2.5	55.7	5.1	15.2	2.5	12.8	3.6	32.1	1.7
SA9	38.9	4.0	7.7	0.9	49.1	1.2	10.2	4.7	7.9	3.9	31.2	3.7
SA12	44.8	2.6	9.3	1.9	66.8	3.2	22.0	2.6	10.1	5.2	35.5	1.9
SA23	27.7	1.0	7.4	1.4	39.5	2.0	11.8	1.9	8.5	1.9	20.3	0.8
SA20	33.5	5.5	8.3	4.4	42.7	5.3	9.3	3.6	8.6	7.5	25.2	1.3
SA24	45.5	3.7	8.4	2.4	68.2	2.6	22.7	4.1	12.4	4.2	37.1	1.9
SA39	38.9	2.2	8.0	0.9	55.4	2.9	16.6	3.5	11.7	3.3	30.9	2.4

* Units in pmol/min

Table D12N: Normalized bioenergetics results for Plate 3A at week 3

Subject	Basal respiration*		Proton leak*		Maximal respiration*		Spare respiratory capacity*		Non-mitochondrial respiration*		ATP production*	
	Value	SD	Value	SD	Value	SD	Value	SD	Value	SD	Value	SD
HC1	0.60	0.03	0.14	0.02	0.88	0.07	0.29	0.04	0.16	0.07	0.46	0.02
HC2	0.65	0.04	0.13	0.02	0.97	0.07	0.31	0.06	0.22	0.07	0.52	0.04
HC3	0.49	0.05	0.12	0.04	0.50	0.06	0.01	0.06	0.13	0.08	0.37	0.04
HC4	0.68	0.05	0.14	0.02	0.88	0.03	0.20	0.03	0.16	0.05	0.55	0.04
HC5	0.57	0.03	0.11	0.03	0.77	0.05	0.20	0.03	0.18	0.10	0.45	0.02
HC6	0.69	0.04	0.15	0.02	0.98	0.07	0.29	0.03	0.20	0.05	0.54	0.05
HC7	0.60	0.09	0.09	0.03	0.78	0.05	0.18	0.07	0.19	0.07	0.51	0.07
SA16	0.52	0.04	0.13	0.02	0.64	0.06	0.13	0.03	0.15	0.05	0.39	0.03
SA31	0.73	0.03	0.15	0.02	0.93	0.05	0.21	0.03	0.16	0.03	0.58	0.04
SA35	0.58	0.03	0.12	0.03	0.71	0.02	0.13	0.04	0.13	0.07	0.46	0.02
SA7	0.59	0.05	0.12	0.04	0.81	0.07	0.22	0.03	0.19	0.05	0.47	0.03
SA9	0.56	0.05	0.11	0.01	0.71	0.03	0.15	0.07	0.12	0.06	0.45	0.04
SA12	0.65	0.03	0.14	0.02	0.97	0.03	0.32	0.04	0.15	0.08	0.52	0.03
SA23	0.44	0.02	0.12	0.02	0.63	0.04	0.19	0.03	0.14	0.03	0.33	0.01
SA20	0.53	0.09	0.13	0.07	0.68	0.09	0.15	0.06	0.14	0.12	0.40	0.03
SA24	0.69	0.06	0.13	0.04	1.04	0.02	0.34	0.06	0.19	0.06	0.56	0.02
SA39	0.62	0.03	0.13	0.01	0.88	0.06	0.26	0.06	0.19	0.05	0.49	0.04

* Units in pmol/min/cell number

Table D13: Non-normalized bioenergetics results for Plate 3B at week 3

Subject	Basal respiration*		Proton leak*		Maximal respiration*		Spare respiratory capacity*		Non-mitochondrial respiration*		ATP production*	
	Value	SD	Value	SD	Value	SD	Value	SD	Value	SD	Value	SD
HC1	42.1	2.7	11.2	1.1	55.2	2.7	13.1	2.3	9.8	3.0	30.8	2.0
HC2	38.3	6.5	5.9	2.0	59.7	5.3	21.4	4.8	24.1	4.7	32.4	5.2
HC3	29.5	3.3	9.5	1.5	30.8	1.8	1.3	3.8	8.8	5.0	20.1	3.2
HC4	42.5	5.7	5.6	3.8	62.9	5.9	20.4	5.4	20.4	5.9	36.9	3.2
HC5	37.2	2.9	9.0	1.0	44.5	2.6	7.2	4.7	8.6	1.9	28.2	3.5
HC6	41.4	4.3	5.4	3.1	62.3	5.1	20.9	4.2	21.0	5.6	36.0	2.5
HC7	38.3	5.6	5.5	2.6	55.9	3.2	17.6	4.6	12.8	5.2	32.8	8.2
SA16	31.6	3.6	5.2	0.8	40.3	2.6	8.7	3.9	16.3	2.5	26.4	3.9
SA31	47.8	8.7	6.4	3.9	65.7	6.7	17.9	6.0	19.4	7.7	41.4	6.0
SA35	46.9	2.3	10.0	0.9	59.3	4.7	12.5	3.2	12.6	2.9	36.9	2.7
SA7	42.7	1.6	9.8	1.8	54.8	2.0	12.1	2.6	8.8	3.0	32.9	1.1
SA9	36.5	3.5	4.2	6.1	46.7	3.6	10.2	3.6	12.9	6.0	32.2	3.1
SA12	40.7	7.1	2.9	10.0	61.9	4.2	21.3	3.3	17.3	7.7	37.8	3.2
SA23	32.1	3.6	8.9	2.0	42.7	2.4	10.5	4.7	8.1	3.6	23.3	1.9
SA20	27.9	2.2	8.5	0.4	33.2	2.1	5.3	0.7	4.7	1.7	19.4	2.2
SA24	41.4	3.6	6.6	3.4	57.8	2.6	16.4	2.4	15.6	3.9	34.8	2.2
SA39	36.1	6.7	5.4	3.3	50.0	1.7	13.9	7.3	16.6	4.6	30.7	5.3

* Units in pmol/min

Table D13N: Normalized bioenergetics results for Plate 3B at week 3

Subject	Basal respiration*		Proton leak*		Maximal respiration*		Spare respiratory capacity*		Non-mitochondrial respiration*		ATP production*	
	Value	SD	Value	SD	Value	SD	Value	SD	Value	SD	Value	SD
HC1	0.59	0.05	0.16	0.02	0.78	0.05	0.18	0.03	0.14	0.04	0.43	0.03
HC2	0.53	0.09	0.08	0.03	0.82	0.06	0.29	0.06	0.33	0.07	0.45	0.07
HC3	0.43	0.05	0.14	0.02	0.45	0.02	0.02	0.05	0.13	0.07	0.29	0.05
HC4	0.55	0.06	0.07	0.05	0.81	0.07	0.26	0.08	0.27	0.08	0.48	0.03
HC5	0.57	0.05	0.14	0.01	0.68	0.03	0.11	0.07	0.13	0.03	0.43	0.06
HC6	0.56	0.05	0.07	0.04	0.85	0.06	0.29	0.06	0.29	0.09	0.49	0.02
HC7	0.56	0.08	0.08	0.04	0.82	0.05	0.26	0.07	0.19	0.08	0.48	0.11
SA16	0.45	0.05	0.07	0.01	0.58	0.04	0.12	0.06	0.23	0.04	0.38	0.06
SA31	0.70	0.11	0.09	0.05	0.96	0.07	0.26	0.09	0.29	0.12	0.60	0.07
SA35	0.61	0.03	0.13	0.01	0.77	0.06	0.16	0.04	0.16	0.04	0.48	0.04
SA7	0.62	0.03	0.14	0.03	0.79	0.04	0.17	0.04	0.13	0.04	0.47	0.01
SA9	0.51	0.05	0.06	0.08	0.65	0.05	0.14	0.05	0.18	0.09	0.45	0.05
SA12	0.56	0.10	0.04	0.14	0.85	0.06	0.29	0.04	0.24	0.10	0.52	0.05
SA23	0.47	0.06	0.13	0.03	0.63	0.03	0.15	0.07	0.12	0.05	0.34	0.03
SA20	0.43	0.04	0.13	0.01	0.51	0.04	0.08	0.01	0.07	0.03	0.30	0.04
SA24	0.57	0.05	0.09	0.05	0.80	0.04	0.23	0.03	0.21	0.05	0.48	0.03
SA39	0.53	0.10	0.08	0.05	0.73	0.03	0.20	0.11	0.24	0.07	0.45	0.08

* Units in pmol/min/cell number

Table D14: Coupling efficiency, spare respiratory capacity (%) and BHI for Plates 3A and 3B at week 3

Subject	Plate 3A – Week 3						Plate 3B – Week 3					
	Coupling Efficiency (%)		Spare respiratory capacity (%)		BHI		Coupling Efficiency (%)		Spare respiratory capacity (%)		BHI	
	Value	SD	Value	SD	Value	SD	Value	SD	Value	SD	Value	SD
HC1	77.5	2.5	147.6	4.7	0.849	0.286	73.3	1.7	131.4	7.2	0.577	0.070
HC2	80.1	2.3	148.3	9.8	0.780	0.273	84.9	3.9	158.6	17.9	0.710	0.131
HC3	74.9	5.9	102.8	11.6	-0.16	0.232	67.7	5.9	105.9	14.6	-0.14	0.103
HC4	79.9	1.9	129.3	6.7	0.703	0.147	87.7	8.2	149.6	17.0	0.747	0.128
HC5	80.2	4.5	136.0	5.4	0.739	0.271	75.6	3.7	120.4	13.1	0.466	0.059
HC6	78.1	4.3	142.8	3.2	0.732	0.208	87.6	6.6	151.7	14.1	0.934	0.317
HC7	84.5	3.0	131.1	14.8	0.705	0.169	84.5	7.9	148.0	16.3	1.068	0.725
SA16	75.5	2.5	124.4	5.3	0.431	0.200	83.2	3.1	128.9	14.4	0.384	0.192
SA31	78.9	2.4	128.2	4.5	0.677	0.101	87.3	5.5	140.3	18.0	0.849	0.161
SA35	79.5	3.6	122.2	7.1	0.640	0.310	78.6	2.3	126.5	6.7	0.559	0.244
SA7	79.8	4.7	137.7	5.6	0.698	0.093	77.1	3.6	128.5	6.8	0.693	0.137
SA9	80.1	2.1	127.6	13.1	0.661	0.255	89.9	17.0	128.8	12.2	0.767	0.579
SA12	79.3	3.4	149.4	6.9	1.070	0.455	98.3	31.8	156.1	22.6	0.826	0.092
SA23	73.5	4.4	142.9	7.6	0.526	0.216	72.8	4.1	135.1	21.4	0.600	0.488
SA20	76.5	7.9	128.9	12.5	0.596	0.095	69.4	2.8	119.2	3.2	0.439	0.153
SA24	81.7	4.0	150.7	11.6	0.946	0.159	84.6	6.9	140.1	7.8	0.814	0.258
SA39	79.5	2.8	143.1	10.2	0.752	0.176	85.7	7.3	144.0	30.2	0.714	0.419

WEEK 6

Table D15: Non-normalized bioenergetics results for Plate 3A at week 6

Subject	Basal respiration*		Proton leak*		Maximal respiration*		Spare respiratory capacity*		Non-mitochondrial respiration*		ATP production*	
	Value	SD	Value	SD	Value	SD	Value	SD	Value	SD	Value	SD
HC1	45.2	2.5	14.6	1.8	62.4	5.5	17.3	3.4	13.9	1.8	30.6	3.3
HC2	39.7	1.7	9.3	2.1	65.5	6.2	25.8	5.2	15.8	1.6	30.4	2.9
HC3	48.1	2.0	17.0	2.3	50.5	2.4	2.4	2.9	13.3	3.1	31.1	2.4
HC4	47.3	1.2	11.9	1.6	67.7	3.0	20.4	4.1	17.0	1.2	35.4	1.9
HC5	44.8	3.6	12.7	0.8	56.8	2.4	11.9	2.2	13.5	1.1	32.1	3.5
HC6	39.4	3.6	11.0	1.6	56.3	4.1	16.9	5.7	14.8	2.4	28.4	2.5
HC7	58.6	2.5	14.4	1.1	80.0	2.7	21.5	1.6	18.5	3.9	44.1	1.4
SA16	32.7	2.2	11.2	1.6	39.9	1.4	7.2	2.1	10.9	2.2	21.4	1.7
SA31	68.5	3.2	15.1	1.8	108.7	6.4	40.2	6.3	18.6	2.0	53.5	2.6
SA35	41.5	1.3	12.2	1.2	55.2	2.7	13.7	1.7	12.5	0.9	29.3	1.7
SA7	48.8	2.0	13.9	1.0	70.0	3.9	21.3	4.5	14.8	2.9	34.8	2.9
SA9	42.8	7.3	10.7	4.2	63.3	3.0	20.5	5.9	13.2	1.3	32.1	3.2
SA12	59.7	4.9	14.8	1.7	84.5	3.8	24.8	2.4	12.8	2.7	44.9	4.8
SA23	42.2	1.8	12.7	0.6	57.5	2.7	15.3	2.2	12.7	1.2	29.6	1.5
SA20	40.3	3.3	13.0	1.1	57.9	5.5	17.6	2.6	12.4	1.8	27.3	2.9
SA24	44.3	4.1	11.5	3.0	67.2	5.4	22.9	4.9	12.8	4.4	32.8	2.9
SA39	37.5	4.5	11.3	2.1	59.3	4.8	21.9	6.7	15.9	3.4	26.2	3.7

* Units in pmol/min

Table D15N: Normalized bioenergetics results for Plate 3A at week 6

Subject	Basal respiration*		Proton leak*		Maximal respiration*		Spare respiratory capacity*		Non-mitochondrial respiration*		ATP production*	
	Value	SD	Value	SD	Value	SD	Value	SD	Value	SD	Value	SD
HC1	0.68	0.04	0.22	0.02	0.95	0.05	0.26	0.04	0.21	0.04	0.46	0.05
HC2	0.69	0.05	0.16	0.03	1.13	0.08	0.44	0.07	0.27	0.03	0.53	0.07
HC3	0.78	0.04	0.27	0.04	0.82	0.04	0.04	0.05	0.22	0.05	0.50	0.04
HC4	0.79	0.03	0.20	0.03	1.13	0.04	0.34	0.06	0.28	0.02	0.59	0.04
HC5	0.76	0.04	0.22	0.01	0.96	0.04	0.20	0.04	0.23	0.02	0.54	0.04
HC6	0.66	0.04	0.19	0.03	0.95	0.06	0.29	0.10	0.25	0.05	0.48	0.03
HC7	0.99	0.11	0.24	0.04	1.35	0.13	0.36	0.03	0.31	0.05	0.74	0.08
SA16	0.60	0.06	0.21	0.04	0.73	0.05	0.13	0.04	0.20	0.04	0.39	0.03
SA31	1.36	0.08	0.30	0.03	2.16	0.12	0.80	0.11	0.37	0.05	1.06	0.07
SA35	0.70	0.01	0.21	0.02	0.93	0.03	0.23	0.03	0.21	0.02	0.49	0.02
SA7	0.93	0.11	0.26	0.00	1.33	0.12	0.40	0.07	0.28	0.06	0.67	0.11
SA9	0.70	0.13	0.18	0.07	1.04	0.08	0.34	0.10	0.22	0.02	0.53	0.07
SA12	1.00	0.07	0.25	0.02	1.41	0.06	0.42	0.05	0.22	0.05	0.75	0.08
SA23	0.87	0.09	0.26	0.05	1.19	0.13	0.32	0.05	0.26	0.04	0.61	0.05
SA20	0.67	0.06	0.22	0.02	0.96	0.10	0.29	0.04	0.21	0.03	0.45	0.05
SA24	0.75	0.03	0.19	0.05	1.14	0.08	0.39	0.09	0.22	0.08	0.55	0.03
SA39	0.63	0.10	0.19	0.04	1.00	0.11	0.37	0.11	0.27	0.05	0.44	0.08

* Units in pmol/min/cell number

Table D16: Coupling efficiency, spare respiratory capacity (%) and BHI for Plate 3A at week 6

Subject	Coupling Efficiency (%)		Spare respiratory capacity (%)		BHI	
	Value	SD	Value	SD	Value	SD
HC1	67.6	4.8	138.1	5.7	0.413	0.113
HC2	76.5	5.4	164.8	11.7	0.737	0.132
HC3	64.7	4.5	105.2	6.1	-0.384	0.362
HC4	74.8	3.3	143.4	9.6	0.547	0.137
HC5	71.4	2.3	127.1	6.4	0.339	0.059
HC6	72.1	2.5	144.1	17.2	0.448	0.248
HC7	75.4	0.9	136.7	3.4	0.559	0.088
SA16	65.7	4.0	122.4	7.7	0.095	0.129
SA31	78.0	2.2	158.8	10.2	0.884	0.105
SA35	70.6	3.1	133.0	3.8	0.420	0.126
SA7	71.3	3.0	143.9	10.2	0.556	0.180
SA9	76.3	7.4	152.6	29.5	0.717	0.358
SA12	75.1	2.9	142.0	6.5	0.776	0.104
SA23	70.0	1.2	136.2	5.6	0.447	0.067
SA20	67.6	2.5	143.6	4.6	0.473	0.112
SA24	74.3	5.4	152.2	13.4	0.741	0.312
SA39	69.7	4.3	161.0	25.6	0.486	0.347

APPENDIX E: Bioenergetics Statistics

Table E1: Tukey's HSD post-hoc test for the comparison between the subject groups of each bioenergetic parameter.

Bioenergetics parameters	Group 1	Group 2	Mean difference (Group 1 – Group 2)	SEM	p
Basal respiration	Haplogroup U ME patients (N = 56)	Non-U haplogroup ME patients (N = 60)	-0.1048	0.0397	**0.043***
	Haplogroup U ME patients (N = 56)	Healthy controls (N = 49)	0.0104	0.0418	0.995
	Non-U haplogroup ME patients (N = 60)	Healthy controls (N = 49)	0.1153	0.0411	**0.028***
	ME patients (N = 116)	Healthy controls (N = 49)	0.0647	0.0364	0.287
Proton leak	Haplogroup U ME patients (N = 56)	Non-U haplogroup ME patients (N = 60)	-0.0159	0.0128	0.602
	Haplogroup U ME patients (N = 56)	Healthy controls (N = 49)	-0.0035	0.0135	0.994
	Non-U haplogroup ME patients (N = 60)	Healthy controls (N = 49)	0.0123	0.0133	0.789
	ME patients (N = 116)	Healthy controls (N = 49)	0.0047	0.0117	0.979
Maximal respiration	Haplogroup U ME patients (N = 56)	Non-U haplogroup ME patients (N = 60)	-0.1447	0.0498	**0.021***
	Haplogroup U ME patients (N = 56)	Healthy controls (N = 49)	0.0742	0.0524	0.491
	Non-U haplogroup ME patients (N = 60)	Healthy controls (N = 49)	0.2189	0.0516	**0.0002***
	ME patients (N = 116)	Healthy controls (N = 49)	0.1490	0.0457	**0.007***
Spare respiratory capacity	Haplogroup U ME patients (N = 56)	Non-U haplogroup ME patients (N = 60)	-0.0398	0.0231	0.314
	Haplogroup U ME patients (N = 56)	Healthy controls (N = 49)	0.0619	0.0243	0.056
	Non-U haplogroup ME patients (N = 60)	Healthy controls (N = 49)	0.1017	0.0240	**0.0002***
	ME patients (N = 116)	Healthy controls (N = 49)	0.0825	0.0212	**0.001***
Non-mitochondrial respiration	Haplogroup U ME patients (N = 56)	Non-U haplogroup ME patients (N = 60)	-0.0154	0.0245	0.922
	Haplogroup U ME patients (N = 56)	Healthy controls (N = 49)	0.0684	0.0258	**0.042***
	Non-U haplogroup ME patients (N = 60)	Healthy controls (N = 49)	0.0839	0.0254	**0.006***
	ME patients (N = 116)	Healthy controls (N = 49)	0.0764	0.0225	**0.004***

Table E1 continued…

Bioenergetics parameters	Group 1	Group 2	Mean difference (Group 1 – Group 2)	SEM	p
ATP production	Haplogroup U ME patients (N = 56)	Non-U haplogroup ME patients (N = 60)	-0.0784	0.0279	**0.027***
	Haplogroup U ME patients (N = 56)	Healthy controls (N = 49)	0.0266	0.0294	0.803
	Non-U haplogroup ME patients (N = 60)	Healthy controls (N = 49)	0.1049	0.0289	**0.002***
	ME patients (N = 116)	Healthy controls (N = 49)	0.0671	0.0256	**0.045***
Coupling efficiency	Haplogroup U ME patients (N = 56)	Non-U haplogroup ME patients (N = 60)	4.9861	20.7351	0.995
	Haplogroup U ME patients (N = 56)	Healthy controls (N = 49)	-3.8924	21.8297	0.998
	Non-U haplogroup ME patients (N = 60)	Healthy controls (N = 49)	-8.8784	21.4875	0.976
	ME patients (N = 116)	Healthy controls (N = 49)	-6.4714	19.0135	0.986
Percentage spare respiratory capacity	Haplogroup U ME patients (N = 56)	Non-U haplogroup ME patients (N = 60)	-26.3125	27.3858	0.772
	Haplogroup U ME patients (N = 56)	Healthy controls (N = 49)	-33.9158	28.8316	0.642
	Non-U haplogroup ME patients (N = 60)	Healthy controls (N = 49)	-7.6033	28.3796	0.993
	ME patients (N = 116)	Healthy controls (N = 49)	-20.3059	25.1120	0.850
BHI	Haplogroup U ME patients (N = 56)	Non-U haplogroup ME patients (N = 60)	-0.0112	0.0509	0.996
	Haplogroup U ME patients (N = 56)	Healthy controls (N = 49)	0.0589	0.0536	0.690
	Non-U haplogroup ME patients (N = 60)	Healthy controls (N = 49)	0.0701	0.0527	0.545
	ME patients (N = 116)	Healthy controls (N = 49)	0.0647	0.0467	0.509

* Indicates significant p-values of <0.05. SEM = standard error of the mean.

APPENDIX F: Language certificate

EDITING EXCELLENCE
084 365 4320
editingexcellencepotch@gmail.com

This is to certify that the dissertation submitted in partial fulfilment of the degree,
Magister Scientiae** in **Biochemistry
of
Hayley van Dyk
has been edited by
Valerie Viljoen, Editing Excellence.

The complete dissertation has been edited and includes the following:
Chapter 1 - Introduction
Chapter 2 – Literature study
Chapter 3 – Methods and materials
Chapter 4 – Results and discussion
Chapter 5 – Conclusion
Appendix A – E.

Date: 25 November 2015